AIX-MARSEILLE UNIVERSITE

EDSVS-ED62
IBDM-UMR 7288

DOCTORAL THESIS
To obtain the title of PhD in Neurosciences
Of the Aix-Marseille University

Theodora Velona

Insights into the generation of diversity in neocortical projection neurons.

PlexinD1 controls the correct laminar positioning of neurons with heterotopic transcallosal projections.

Defended on December 19, 2018

Thesis Supervisors

Dr Fanny Mann   IBDM, Marseille, France

Prof Sophie Chauvet   IBDM, Marseille, France

Jury members:

Dr Xavier NICOL	Institut de la Vision, CNRS, Paris, France	Reviewer
Dr. Michèle STUDER	iBV;Université de Nice Sophia Antipolis, France	Reviewer
Dr Emilie PACARY	Neurocentre Magendie - INSERM U1215, France	Examiner
Dr. Fanny MANN	IBDM, Marseille, France	Supervisor

Résumé

Les neurones à projection callosale (CPN) sont une sous-population de neurones néocorticaux qui relient les hémisphères cérébraux par le corps calleux, la plus grande commissure chez les mammifères non placentaires. Les CPNs varient dans leur position laminaire, identité moléculaire, morphologie somatodendritique et cibles axonales. La plupart des CPNs projettent de façon homotopique dans le cortex controlatéral, et certains CPNs projettent vers des régions corticales ou sous-corticales (ex. striatum) non homologues. Les mécanismes régissant le développement de ces CPNs à projection hétérotopique sont actuellement inconnus. Ici, j'ai étudié le récepteur PlexinD1 comme marqueur potentiel des CPNs à projections hétérotopiques. J'ai trouvé que PlexinD1 est exprimé au cours du développement et maintenu dans le cerveau adulte, où il est localisé dans les couches 4 et 5A. Les neurones positifs à PlexinD1 expriment le facteur de transcription Satb2 qui définit les CPNs. Le traçage axonal rétrograde a montré que les CPNs à projection hétérotopique du cortex moteur et somatosensoriel sont spécifiquement localisés dans la couche 5A et expriment PlexinD1. L'ablation génétique de PlexinD1 ou de son ligand Sema3E provoque un mauvais positionnement des CPNs à projection hétérotopique dans les couches corticales supérieures, alors que la surexpression de PlexinD1 dans les neurones des couches supérieures entraîne un mauvais positionnement des cellules dans les couches corticales profondes. Ces résultats indiquent que la signalisation PlexinD1 contrôle la position laminaire des CPNs à projection hétérotopique en régulant leur migration radiale pendant le développement néocortical.

Abstract

Callosal projection neurons (CPN) represent a subpopulation of neocortical neurons that interconnect the two brain hemispheres through the corpus callosum, the largest commissural tract in non-placental mammals. CPNs exhibit diversity in terms of laminar position in the neocortex, molecular identity, somatodendritic morphology and axonal targeting. For example, most CPNs send homotopic axonal projections to homologous areas of the contralateral cortex, while subgroups of CPNs send heterotopic projections to non-homologous cortical or subcortical (eg. striatum) regions. The mechanisms governing the development of heterotopically projecting CPNs are currently unknown. To address this question, I studied the axon guidance receptor PlexinD1 as a potential marker of CPNs with heterotopic projections. I found that PlexinD1 is expressed in the developing cortical plate and is maintained in the adult brain, where it mainly localized to layer 4 and 5A. PlexinD1-positive neurons were found to express the transcription factor Satb2 that define CPNs. Retrograde axonal tracing showed that heterotopically projecting CPNs in the motor and somatosensory cortex are specifically localized to layer 5A and express PlexinD1. Genetic ablation of PlexinD1 or its Sema3E ligand in the cortex caused mispositionning of heterotopically projecting CPNs in upper cortical layers, whereas overexpression of PlexinD1 in upper layer neurons resulted in misplacement of the cells in deep cortical layers. Together, these results indicate that PlexinD1 signalling controls the laminar position of heterotopically projecting CPNs by regulating their radial migration during neocortical development.

Acknowledgements

First and foremost, I would like to express my gratitude to my two thesis supervisors, Dr Fanny Mann and Professor Sophie Chauvet; without their guidance and support this work would have been impossible.

Thank you, Fanny for offering me the opportunity to conduct my thesis in your team and be a part of its dynamic scientific environment, which helped me evolve, both technically and intellectually and set the basis for my scientific autonomy. You provided me with all the necessary scientific input and guidance, as well as material infrastructure for a successful PhD. Throughout my thesis you were a persistent source of valuable advice, always available to help in any issue. Your rigorous approach towards the scientific questions inspired me to pay more attention to the details and to question everything. Certainly, our discussions will be a point of reference in my future way of thinking not only in science but also in life.

Heartfelt thanks go to Sophie, who invested herself into helping me initiate this project as well as complete it. Thank you, Sophie, for being always available to discuss with me and provide input on my results, you advice always helped me advance. I really appreciate your active efforts to create occasions for team bonding.

I would like to thank all the members of the jury, Dr Xavier Nicol and Dr Michèle Studer who accepted to be reviewers, for correcting and evaluating my thesis. Thank you to Dr Emilie Pacary, who accepted to be examinator of my thesis.

My sincere thanks to our collaborators, Pascal Salin, who conducted the Rabies Virus experiments and to Marta Nieto and Carlos Garcia Briz, who performed IUE experiments, providing me with valuable preliminary functional data.

I would like to acknowledge the contribution of old and new members of the team to my thesis.

Thank you to Jeremy and Erik for kindly helping me with my first steps as a PhD, for the stimulating scientific discussions in the lab and all the fun activities we shared out of the lab. Special thanks to Melanie for all the technical help and support, and for being so determined to keep the lab we work a healthy place. I know I will be grateful in the future.

From the new members of the team I would like to say special thanks to Anais for her invaluable help with technical issues and methodological approaches. She is always eager to provide a solution in both work-related and everyday life issues and I appreciate that. Thanks to Mike,

Micaela, Chloe for their psychological support throughout the challenging period of thesis writing and for the fruitful discussions that we had on technical issues.

This thesis would not have been possible without the help and support from my friends here in Marseille. Thank you, Marianna, Lexi, Marwa, for being there for me all along this journey.

Finally, I would like to thank my family, and especially my mother and my sister, who were my restless supporting team in difficult times and the proudest people in the world, in my slightest achievement. This PhD is dedicated to you.

Table of Contents

List of abbreviations

AC: anterior commissure

AgCC: agenesis of the corpus callosum

CC: Corpus Callosum

cCStrP: crossed-corticostriatal projections

cCStrPN: crossed-corticostriatal projection neurons

CFuPN: corticofugal projection neurons

CP: cortical plate

CPNs: Callosal projection neurons

CR: Cajal-Retzius

CST: corticospinal tract

CThPN: corticothalamic projection neurons

DCC: Deleted in Colorectal Cancer

DTI: Diffusion Tensor Imaging

FA: fast adapting

Fezf2: Fez Family Zinc Finger 2

FG : Fluorogold

fMRI: functional Magnetic Resonance Imaging

GP : globus pallidus

GPe: external globus pallidus

GPi: internal globus pallidus

SNr: substantia nigra pars reticulata

GW: glial wedge

HDAC1: Histone Deacetylase 1

HRP : horseradish peroxidase

IG: indusium griseum

Ins/PRh: Insular/Perirhinal

ISH: *In situ* hybridization

IUE*: in utero* electroporation

IZ: intermediate zone

LKB1: Liver kinase B1

Lmo4: LIM Domain Only Protein 4

M1: Primary motor area

MAP6: microtubule-associated protein 6

MAR: Matrix Attachment Regions

MNs: motor neurons

MSNs: medium spiny neurons

MTA2: Metastasis-associated protein 2

Ngn2: Neurogenin 2

Npn1: Neuropilin1

NUAK1: NUAK Family Kinase 1

NuRD: Nucleosome Remodeling Deacetylase

OB: olfactory bulb

PB: Probst bundles

PCL: Pyramidal cell layer

PGCs: periglomerular cells

PMC: premotor cortex

PN: projection neuron

PT: pyramidal tract

PV : Parvalbumin

RG: radial glia

Robo1/2: Roundabout homolog 1/2

S1: primary somatosensory area

SA: slowly adapting

SA-d: Slow adapting with initial doublet spikes

Satb2: Special AT-rich sequence-binding protein 2

SCPN: subcerebral projection neurons

SVZ : subventricular zone

Unc5c: uncoordinated-5 netrin receptor C

VEGFR2: vascular endothelial growth factor receptor type 2

VZ: ventricular zone

WGA-HRP: Wheat Germ Agglutinin-horseradish peroxidase

Wnt5a : Wingless 5a

Table of Illustrations

Figures

Tables

1 INTRODUCTION

Overview of the thesis

The neurons that connect the cortices of the two brain hemispheres (callosal projection neurons or CPNs) are distinguished into subpopulations defined by their final targets, dendritic morphology, synaptic properties and axon branching patterns. How molecular heterogeneity accounts for these aspects of diversity and what is the role of the different molecules expressed by CPN subpopulations in the development of subpopulation-specific characteristics remain elusive.

During my thesis, I addressed this question by exploring the role of a membrane axon guidance receptor, PlexinD1, in the development of a subpopulation of layer 5A CPNs, which send axonal projections to asymmetric regions (heterotopic projections) in the contralateral telencephalon. To achieve this, I first described the characteristics that are specific for PlexinD1-expressing CPNs. Secondly, I focused on elucidating the role of PlexinD1 in the development of these neurons, by using *in vivo* gain and loss of function approaches.

1.1 The Corpus Callosum

1.1.1 Evolution of the Corpus Callosum

Animals with bilateral symmetry have lateralized functions, which are preferentially processed by the left or the right side of their body. To integrate the outcome of this processing and create a unified behaviour, they need connections which transfer information between the two sides of the body. These connections, in both invertebrates and vertebrates are called commissures. All vertebrates share common commissures which connect conserved structures of the brain, such as the anterior commissure (AC), which can be found with variations in all vertebrate species, connecting principally olfactory recipient structures and subpallial elements, structures conserved in all vertebrate species. However, the appearance of the neocortex in mammals, a structure specialised for sensory processing, voluntary control of motor functions and cognitive functions, such as attentional control, reasoning and problem solving, led to the implementation of two different strategies in order to achieve the bilateral connection of the neocortex. In non-placental mammals, the two neocortices were reciprocally connected by

axons projecting through the already existing AC, following either the external capsule and/or the internal capsule. This route allows the connection of the two neocortices, but as this structure is located dorsally in the brain, it takes long for the information to arrive to the other side, passing through the ventrally located AC. In placental mammals on the other hand the appearance of the Corpus Callosum (CC), an axonal tract located relatively dorsally in the telencephalon allows faster integration of information between the two sides (Figure 1.1).
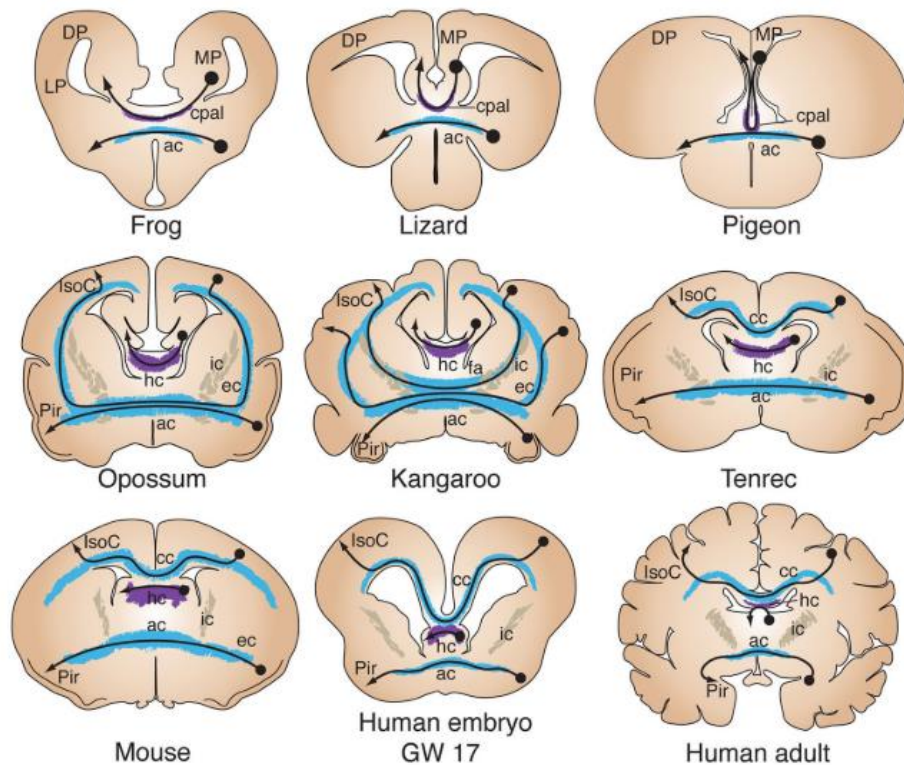
Figure 1.1 Evolution of commissures in vertebrates

Vertebrates share a basic organisation of commissures connecting regions conserved through evolution. The pallial commissure (cpal) and hippocampal commissure (hc) connect medial structures of the pallium, while the anterior commissure (ac) connects structures receiving olfactory input. In non-placental mammals, exchange of information between the two neocortices is ensured by the ac. In the opossum neurons from dorsal neocortical or isocortical (IsoC) regions reach the ac through the external capsule (ec), while in the kangaroo they take a shorter route through the internal capsule (ic), thus forming the fasciculus aberrans (fa). Finally, placental mammals developed a dorsal structure, the corpus callosum (cc), which is adapted for quick interhemispheric transfer. Adapted from Suárez et al., 2014.

In this group, the AC is limited to its initial role, which is to connect olfactory recipient structures and subpallial regions but also the pyriform cortex, a lateral cortical area. The CC tends to get larger in species with a high neocortex/pyriform ratio (Aboitiz and Montiel, 2003; Suárez et al., 2014a). In humans, the CC is the largest axonal tract in the brain. Because of its

considerable size and clinical relevance (see 1.1.2) the study of the properties, functions and development of the CC is important in order to have a better understanding of the pathologies in which it is implicated.

1.1.2 Functions of the Corpus Callosum

Insights on the functions of the corpus callosum in the human brain come from two categories of patients lacking a CC. The first category comprises adults that had to undergo callosotomy, in order to avoid the expansion of epileptic seizures in the late 60's and 70's. The second category are patients who fail to form the entirety or part of the CC, due to problems occurring during embryonic or early postnatal stages and affect the development of the CC.

Early studies examining the general neurological condition of callosotomised patients supported that these patients did not show any obvious neuropsychological defects (Akelaitis, 1944; Trescher and Ford, 1937). However, the implementation of a battery of elegant cognitive tests by Michael Gazzaniga, Roger Sperry and their colleagues on a group of patients who had previously undergone callosotomy revealed that these patients had lost the ability to transfer sensory information from one side of the cortex to the other (Gazzaniga, 2005), and that they presented defects in bimanual coordination (Zaidel and Sperry, 1977), a phenotype belonging to the family of disconnection syndromes, which involve neurological symptoms occurring after ablation of axonal tracts in the brain (Catani and Ffytche, 2005) . During these tests, the investigators would provide visual or tactile information to one side of the body and would subject the patients to cognitive tests for specific functions (Figure 1.2). Callosotomised patients were unable to make use of the information received if the function tested was lateralised to the opposite hemisphere. The most pronounced lateralized function lies in the production of speech, which in most people is executed by the dominant left hemisphere. When a split brain patient was given a visual stimulus perceived only by the right hemisphere, they would not be able to talk about it, as the "talking" left hemisphere had not perceived this stimulus, being no longer connected with the right hemisphere, but they would be perfectly able to sketch it with their left hand, which was dominated by the "non-talking" but "stimulus-receiving" left hemisphere. This type of experiments revealed a series of other functions which are lateralised either in the right or the left hemisphere of the brain (Gazzaniga, 2000). With regards to motor functions, lack of interhemispheric connections does not seem to affect the ability of moving the two hands at the same time, or the ability to execute simple motor commands, but it can seriously affect the

speed of movements, and even the quality of movements, especially when it comes to tasks requiring rapid bilateral co-ordination or execution of newly learned tasks (Zaidel and Sperry, 1977). Cognitive tasks requiring quick co-ordination such as attention (Dimond, 1976; Ellenberg and Sperry, 1979) and short-term memory (Zaidel and Sperry, 1977) were also affected after callosotomy. Alexithymia, the inability to talk about one's emotions, is a characteristic outcome observed after callosotomy, which is the result of the disconnection between two functions lateralised in opposite hemispheres, the speech (left) and processing of emotions (right) (Hoppe and Bogen, 1977).
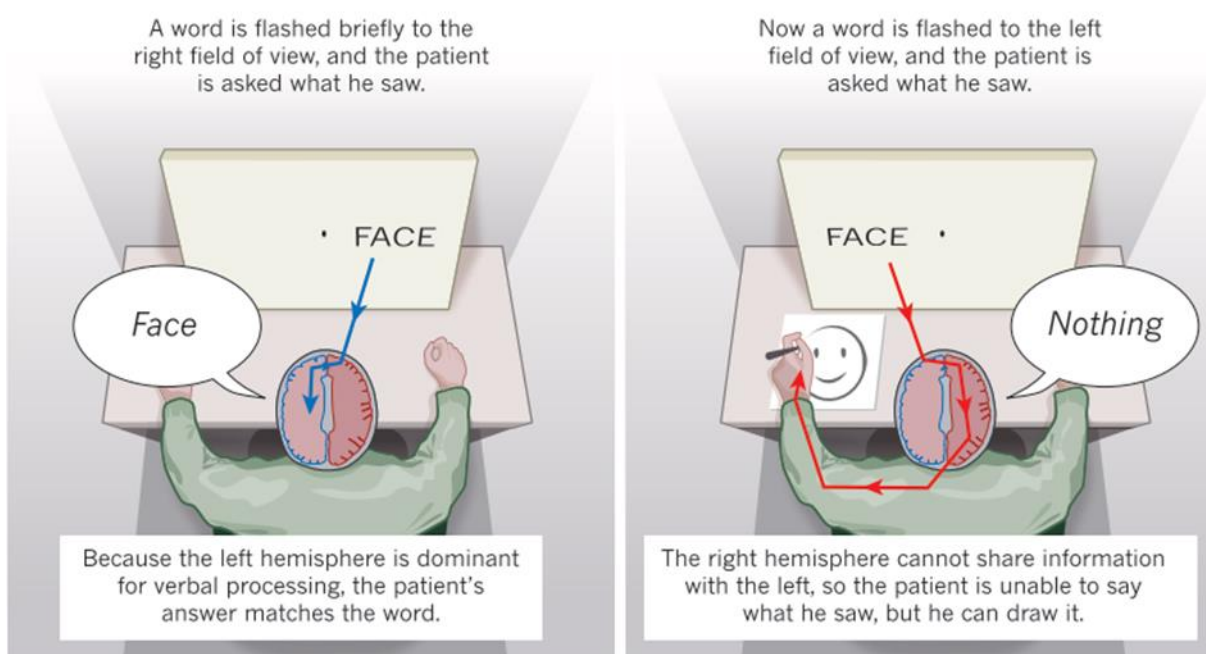
Figure 1.2 Experimental setup allowing to detect lateralised functions in split-brain patients
Adapted from Wolman, 2012.

Lack of intercortical connection may also occur through a developmental failure to form a CC, referred to as agenesis of the corpus callosum (AgCC). AgCC is a developmental defect with high prevalence (1:4000 births) (Guillem et al., 2003; Yeh et al., 2004), which has been observed in about 3-5% (Bodensteiner et al., 1994; Jeret et al., 1985) of patients with neurodevelopmental disorders.

Patients with AgCC exhibit a disconnection syndrome which is milder than in split-brain patients (Brown and Paul, 2000; Jeeves et al., 1988). For example, while primary visual information is not transferred to the contralateral hemisphere, they are still able to compare

between familiar visual stimuli received by the two hemispheres, which split brain patients cannot do. This difference may be a result of increased plasticity in the juvenile acallosal brain, which might allow misrouted axons to find alternative ways to the contralateral side and thus transfer information through pathways not involving the CC. This hypothesis is supported by the fact that interhemispheric transfer of information is relatively increased in patients that were callosotomised as infants, compared to patients who underwent the surgery in teenage or adult age (Lassonde et al., 1991). One pathway that may serve as alternative route is the AC, which has been found to be enlarged in certain AgCC patients. (Hetts et al., 2006a; Brown and Paul, 2000) and its enlargement has been linked to better interhemispheric transfer (Tovar-Moll et al. 2014).

Despite the milder disconnection phenotype of AgCC patients, developmental lack of a CC still results in cognitive defects related to the incapability to process quickly complicated information from the two hemispheres. Defects exhibited very often by AgCC patients are impairments in abstract reasoning (Brown and Sainsbury, 2000; David et al., 1993), problem solving (Aalto et al., 2002; Fischer et al., 1992; Imamura et al., 1994), generalization (Solursh et al., 1965) categorization of items. Furthermore children with AgCC may present defects in social integration and self-evaluation, which are autism related phenotypes. (Badaruddin et al., 2007; Stickles et al., 2002)

AgCC is distinguished into complete AgCC, where the CC fails to develop completely, partial agenesis or hypogenesis, in which only part in the rostrocaudal axis is missing, or hypoplasia of the CC, which results into a thinner tract (Edwards et al., 2014; Hetts et al., 2006; Paul et al., 2007) (Figure 1.3). AgCC has been linked to a large variety of neurodevelopmental outcomes, from seemingly unaffected cognitive functions, to autism and severe mental retardation. Studies until now failed to provide a clear correlation between the type of AgCC and the developmental outcome suggesting that other factors may contribute to the phenotype. Brain malformations which often accompany AgCC, such as colpocephaly, (Mori K, 1992), Probst bundles (PB) (En Ezit et al., 2015; Tovar-Moll et al., 2007), sigmoid bundles and impaired pyramidal tract decussation, could be responsible for the variety in behavioural defects. Such a correlation is not thoroughly investigated, however Diffusion Tensor Imaging (DTI)-tractography on patients with AgCC and analysis of their phenotypes have provided some first insights. Tovar-Moll et al. (2007) studied 11 patients with different types of AgCC and compared the paths followed by the remnant fibers with the normal pattern in 10 control individuals. In the control brain, callosal projections follow a topographic distribution according to which, fibers that leave one

hemisphere side-by-side, remain together in the contralateral hemisphere. This, in the case of callosal fibers has as a result that fibers passing from the genu (rostral part of the CC) connect the frontal cortices, while fibers passing from the splenium connect occipital cortices. DTI-tractography showed that in cases of hypogenesis or hypoplasia, the topography of the fibers is generally maintained, however 4 patients with partial AgCC exhibited the so-called "sigmoid bundle" which is a tract connecting aberrantly asymmetric (heterotopic) areas of the two cortices. In this study, the function of the sigmoid bundle was suggested to be harmful as the patients with a sigmoid bundle exhibited the most severe symptoms, which included moderate mental retardation and motor deficits. PBs on the other hand, which are longitudinal fibers running along the rostrocaudal axis as a result of their failure to cross the brain midline, were linked with more or less severe phenotypes and were present in most of the patients, suggesting a rather compensatory than harmful function of these projections.

In conclusion, split-brain and AgCC patients present defects in processes requiring rapid transfer of information between the two hemispheres, such as executive functions and social skills, validating the CC as a structure indispensable for the execution of higher cognitive functions. However, whereas the disconnection syndrome present in patients with callosotomy is overall not heterogeneous, the developmental outcome of AgCC patients is highly variable and to the moment unpredictable, impeding an accurate prognosis and proper medical guidance of mothers expecting babies with AgCC. This variety of phenotypes probably reflects disruption of distinct steps of the development of the CC, which result into diverse connectivity patterns. The CC is composed of axonal fibers sent bilaterally by specific neurons residing in the two neocortices. The knowledge of the mechanisms governing the different developmental steps that these neurons go through could provide valuable insight into the nature and the causes of structural malformations in the CC that lead to different phenotypes.
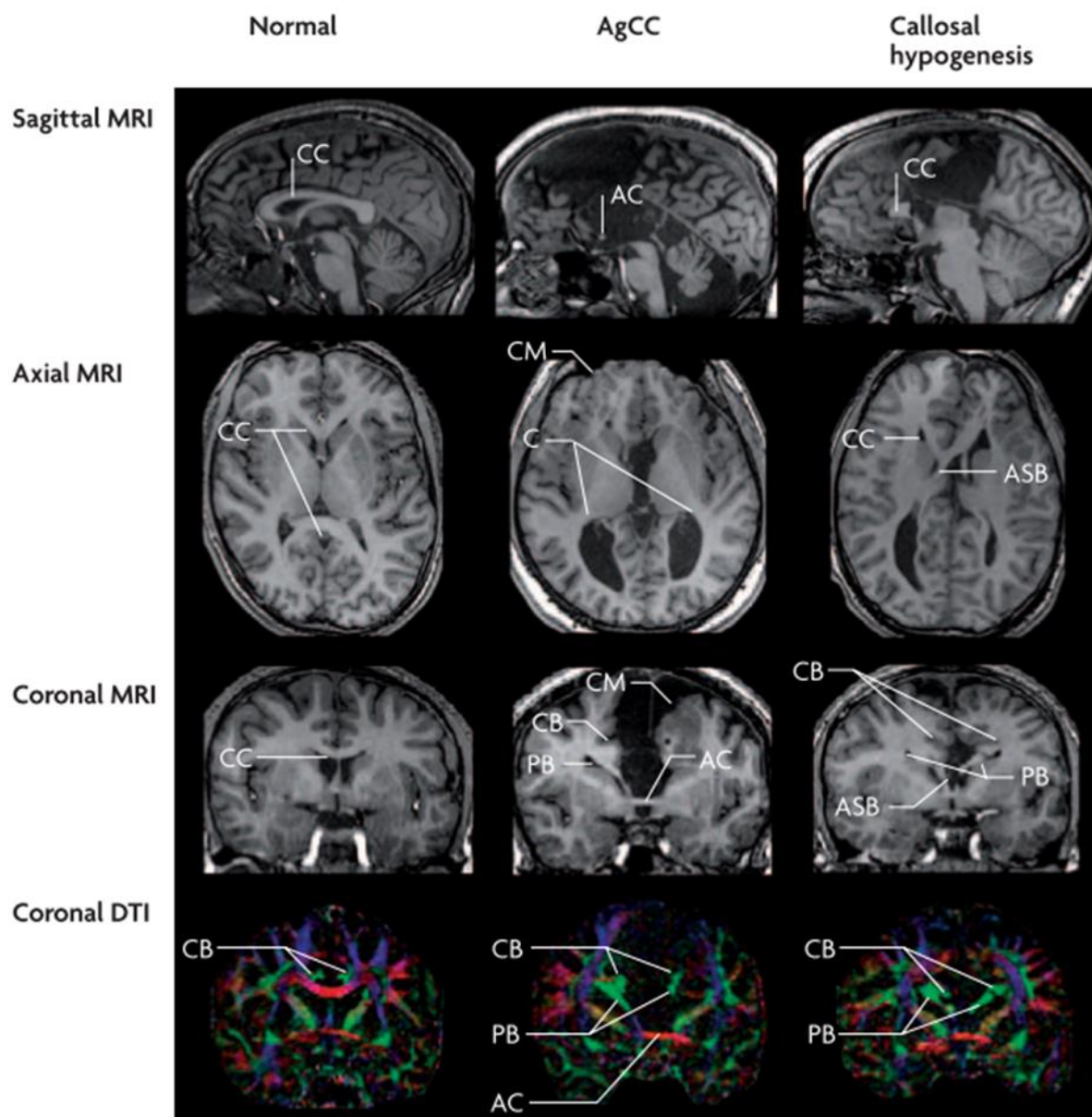
Figure 1.3 Neuroanatomical findings in AgCC. Magnetic Resonance Imaging (MRI) and diffusion tensor imaging (DTI) uncover the neuroanatomical characteristics of AgCC and callosal hypogenesis

The upper three rows come from structural T1-weighted MRI in a healthy male adult volunteer and two patients, one with AgCC and one with callosal hypogenesis. The DTI images encode fiber orientation in white matter tracts as follows: fiber pathways with predominantly left–right orientation are displayed as red, anteroposterior orientation as green, and craniocaudal orientation as purple. Apart from the colpocephaly and Probst bundles observed in both types of patients, callosal hypogenesis may also be concurrent with a heterotopic projection connecting aberrantly asymmetrical regions of the cortex, called sigmoid bundle. AC, anterior commissure; ASB, anterior sigmoid bundle; C, colpocephaly; CB, cingulum bundle; CC, corpus callosum; CM, cortical malformation; PB, Probst bundle. Adapted from Paul et al., 2007.

1.1.3 The Callosal Projection Neurons (CPNs) in the mammalian neocortex

The neocortex is a structure of the brain responsible for sensory motor processing and cognition. These functions require the recruitment of specialised neurons forming precise connections. The neocortex is composed primarily of two groups of neurons, the excitatory pyramidal projection neurons (PNs) and the inhibitory, locally projecting interneurons. The two neuronal types are born in the neurogenic niches of the dorsal and ventral telencephalon (Gorski et al., 2002; Wichterle et al., 2001) respectively. Excitatory neurons are the most abundant (70%) neuronal type in the cortex.

The mammalian neocortex is comprised of 6 cytoarchitectonically distinct layers. PNs, which make up the majority of its neuronal populations reside in these layers. PNs are heterogeneous in many aspects, but the principal characteristic that distinguishes them is the pathway that their axons follow to reach their principal targets, or else their hodology. There are three hodological types of PNs in the neocortex. Two of them, characterised collectively as corticofugal projection neurons (CFuPNs), project to targets outside of the cortex. The first group of CFuPNs includes corticothalamic PNs (CThPNs), which project to the thalamic nuclei, and the second features the subcerebral PNs (SCPNs), which project to the pons and/or the spinal cord. The third type of cortical PNs are the commissural-callosal PNs (CPNs), which project through the CC to telencephalic (cortical and striatal) targets in the contralateral hemisphere. (Lodato et al., 2015; Molyneaux et al., 2007) (Figure 1.4). In this study, we focus on the CPNs, the neurons whose fibers make up the CC.

a Commissural; callosal projection neurons

- Callosal neurons (layers II/III, V, VI)
- Callosal neurons with ipsilateral frontal projections (layer V)
- Callosal neurons with striatal projections (layer Va)

b Corticofugal; corticothalamic neurons

- Corticothalamic neurons (layer VI)

c Corticofugal; subcerebral projection neurons

- Corticotectal neurons (layer V)
- Corticopontine neurons (layer V)
- Corticospinal motor neurons (layer V)

Figure 1.4 Major subtypes of projection neurons within the neocortex

a) Callosal PNs are neurons located in all cortical layers and project through the CC to targets inside the contralateral telencephalon (cortex and Striatum). They may send only one projection to the contralateral cortex (black) but also a collateral branch ipsilaterally or contralaterally. b) Corticothalamic PNs reside in layer 6 and project to the ipsilateral thalamus. c) SCPNs are located in layer 5 and send projections to innervate areas outside of the telencephalon, such as the superior colliculus (Corticotectal), the pons (Corticopontine) and the spinal cord (Corticospinal). Adapted from Molyneaux et al., 2007.

1.1.4 Development of the CC

The formation of precise callosal connections between the two hemispheres is achieved through a series of tightly regulated developmental steps (Figure 1.5). Callosal neurons are born in the neurogenic niches of the dorsal telencephalon and migrate towards the cortical plate (CP). During migration, they start expressing the genetic program that specifies callosal fate against alternative fates. As a consequence of fate specification, all callosal neurons extend a process towards the medial part of the brain, which will subsequently cross the midline. However, following midline crossing, callosal axons extending from different subpopulations of CPNs follow diverse trajectories to invade their final targets. Inside their respective final targets, callosal processes form axonal branches and select their post-synaptic partners. At the same time, the different callosal subpopulations acquire their distinct Somato-dendritic morphologies and integrate into the local networks. The following chapter will provide an overview of the current knowledge on the molecular mechanisms regulating the steps of callosal neuron development, with a focus on the mechanisms differentiating between distinct callosal subpopulations.
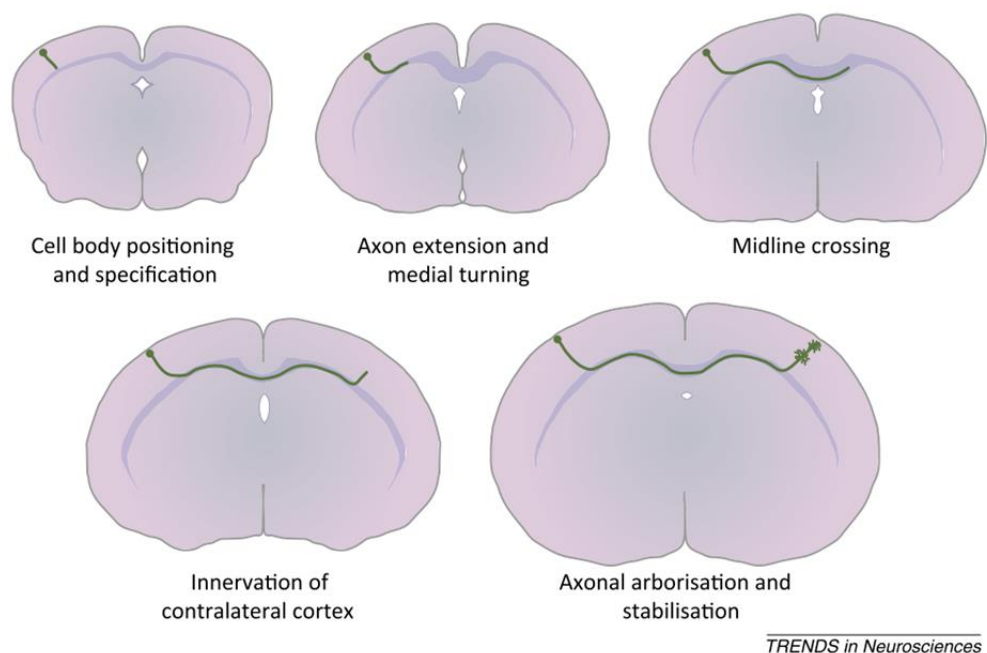
Figure 1.5 Developmental steps of the CC

CPNs migrate to establish their cell body position inside the cortex and go through fate specification at the same time. Fate specification leads to the extension of an axon towards the midline. After the axon crosses the midline, it leaves the white matter and invades its contralateral target area. Finally, the axon innervates this area and forms elaborate terminal branches. Adapted from Fenlon and Richards (2015).

1.1.4.1 Birth and fate specification of CPNs

1.1.4.1.1 Birth of CPNs

Pyramidal neurons are born in neurogenic niches of the pallium located in the surface of the lateral ventricles, the ventricular zone (VZ) and subventricular zone (SVZ) throughout corticogenesis and their date of birth determines their laminar position (Figure 1.6). PNs that are born early during neurogenesis sit in the deep cortical layers whereas PNs born in later stages of neurogenesis migrate past the early born ones and populate more superficial layers. In particular, birth of neurons residing in layer 6 peaks around E12.5, layer 5 at E13.5, layer 4 at E14.5 and layer 2/3 neurons are born around E15.5 (Figure 1.6). CFuPNs belong to early born neurons, with CThPNs being restricted in layer 6 and SCPNs in layer 5. On the other hand, CPNs are born throughout all cortical neurogenesis, with most of them taking up layers 2/3 and 5. As a consequence, early born CPNs are generated alongside with the other two types of PNs. The specific genetic programs that ensure fate specification of CPNs against alternative corticofugal fates have been the subject of a series of studies during the last decade.
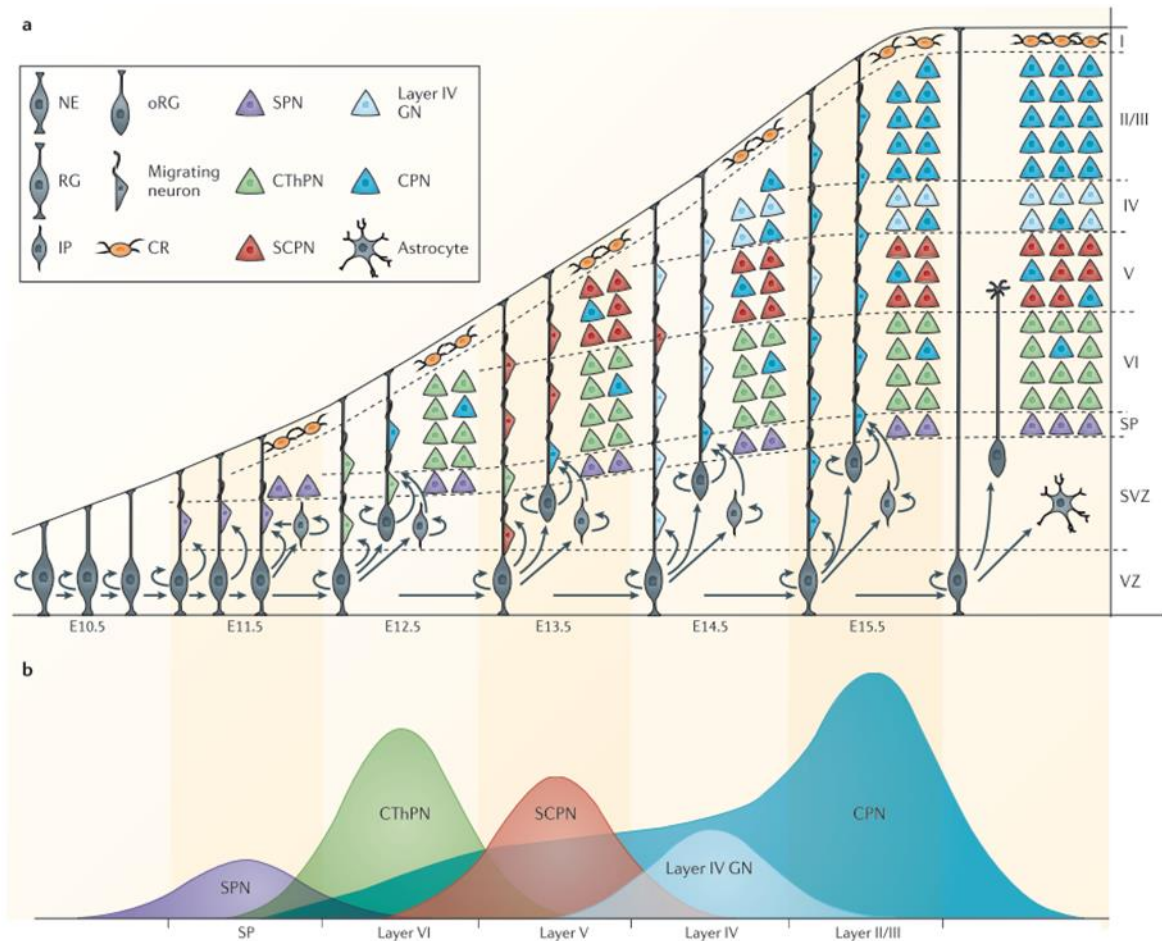
Figure 1.6 Birth, migration and cell body positioning of neocortical PNs

a) At E11.5, radial glia (RG) cells in the VZ produce both layer 6 neurons and intermediate progenitors (IPs) and outer RG (oRG) which will comprise the SVZ, a neurogenic zone. After neurogenesis, radial glia cells continue to divide and they produce glial cells (astrocytes and oligodendrocytes). b) Neocortical PNs are born in sequential waves starting from the ones that will occupy deeper and finishing by the ones that will occupy the most superficial layers. Thus, layer 6 CThPNs present a peak of birth at E12.5, layer 5 SCPNs around E13.5, layer 4 granular neurons (GNs) at E14.5. CPNs can be located in all cortical layers with the highest density in layers 2/3, so they are born throughout neurogenesis with a peak around E15.5. Adapted from Greig et al., 2013.

1.1.4.1.2   Fate specification of CPNs

A series of studies has dissected the mechanisms of fate determination of the different PN types. According to these studies, a group of major transcription factors are responsible for the acquisition of CPN, CThPN or SCPN identity, either by repressing alternative fates or by regulating the expression of downstream effectors. For example, in layer 5, where SCPN coexist with CPN, SCPN identity is maintained by the repression of the transcription factor Satb2 (Special AT-rich sequence-binding protein 2), which is considered as the major transcription

factor important for CPN specification (see below), by the transcription factor Fezf2 (Fez Family Zinc Finger 2). This repression de-represses Ctip2, a transcription factor known to be necessary and sufficient for SCPN specification (Arlotta et al., 2005), but Fezf2 was shown to act also independently to promote SCPN identity acquisition (Chen et al., 2008a). Another example of alternative fate repression can be found in layer 6, where suppression of Fezf2 expression by Tbr1 allows neurons to acquire a CThPN, but not a SCPN, identity (McKenna et al., 2011).

A similar mechanism was proposed to guide fate specification of CPNs. Two important studies published in 2008 attributed Satb2 a key role in driving the specification of callosal neurons against the SCPN fate by repressing the expression of Ctip2 (Alcamo et al., 2008; Britanova et al., 2008). The two studies used two different knockout lines to characterise the Satb2-expressing population of cortical neurons and the effects of its absence in the brain. In these lines, reporter genes, such as cre recombinase (Britanova et al., 2008) or lacZ (Alcamo et al., 2008) were inserted in the Satb2 locus, leading to a failure to produce a functional Satb2 protein, but at the same time allowing to monitor the neurons in which Satb2 is ablated. In both cases, Satb2 defective neurons failed to project through the CC, but in turn they sent aberrant projections towards the internal capsule and cerebral peduncles, a pathway normally followed by corticofugal axons towards subcortical and subcerebral targets. In the absence of Satb2, at E18.5, several molecules expressed specifically in CPNs were downregulated whereas the expression of SCPN markers, such as Ctip2, which is normally restricted in deep layers, was expanded to include upper layer neurons.

These results suggested that Satb2 could function as a repressor for Ctip2. Indeed, *in vitro* and *ex vivo* overexpression of Satb2 resulted in downregulation of Ctip2 and impaired the development of the corticospinal tract which suggested that Satb2 antagonises Ctip2 expression and in this way, impairs the formation of corticospinal projections. In silico search for Matrix Attachment Regions (MAR) and chromatin immunoprecipitation for chromatin state markers revealed several sequences targeted by Satb2 upstream of the Ctip2 locus, which Satb2 is necessary and sufficient to keep active by recruiting the members of the Nucleosome Remodeling Deacetylase (NuRD) chromatin remodelling complex Histone Deacetylase 1 (HDAC1) and Metastasis-associated protein (MTA2). Another piece to this puzzle was added by Baranek et al. (2012) who showed that Ski, a transcriptional co-repressor, is also recruited by Satb2 and is in turn important for the recruitment of HDAC1 in the NuRD complex. (Figure 1.7).
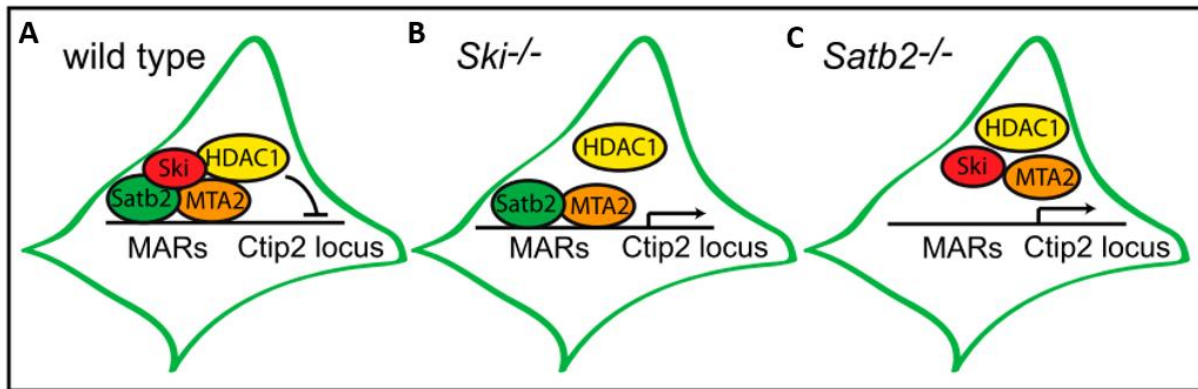
Figure 1.7 Satb2 inhibits Ctip2 expression by recruiting elements of the NuRD chromatin remodelling complex

A) Satb2 binds in Matrix Attachment Regions (MATs) upstream of the Ctip2 locus and binds directly with the NuRD elements Ski and MTA2. Ski then binds directly to HDAC1 thus completing the formation of a complex that inhibits Ctip2 expression. (B,C) In absence of either Satb2 or Ski, the complex fails to assemble and the Ctip2 locus is free to be translated. (Adapted from Baranek et al., 2012).

Overall these studies suggested a mechanism by which Satb2 allows neurons expressing it to be specified as callosal neurons by repressing the alternative SCPN fate. However, things are more complicated than that, as a later study by (Leone et al., 2015) showed that this mechanism is only true for deep layer neurons and not for upper layer CPNs. Indeed, in conditional Satb2 mutants, fluorescent latex microspheres injected inside tracts followed by SCPNs failed to label any upper layer neurons, indicating that Ctip2 de-repression was not sufficient to induce extension of subcortical projections by Satb2 defective upper layer neurons, even though these neurons exhibited electrophysiological properties normally present only in SCPNs.

Altogether, these results indicated that Satb2 is not sufficient to generate callosal projections in all cortical layers, and that the outcome of its action depends on the type of the neurons it is expressed in. Neurons from different layers are born in different timepoints and acquire different genetic programs, which modify the actions of Satb2. For example, deep layer CPNs are born together and share common progenitors with SCPNs and thus retain genetic programs that induce subcortical projection in absence of Satb2. On the other hand, upper layer CPNs keep part of the deep layer genetic programs but not all. For example, in absence of Satb2, Fezf2 a transcription factor sufficient to induce the formation of subcortical projections is overexpressed by deep layer Satb2 defective neurons but not by upper layers and could be one of the explanations for this difference. On the other hand, Ski, an element of the Satb2-

related repressing complex is expressed in the upper layer CPNs in a higher percentage than in the deep layers and may equally contribute to their inability to project subcortically even in absence of Satb2.

Apart from the cell type, Satb2 functions also rely on time point of expression. Indeed, data coming from two recent studies illustrate that Satb2 expression is not sufficient to initiate a CPN-specific program in deep layer neurons when it is not expressed at the correct time point but earlier or later than that. In turn, Satb2 expression at these time points is still important in these neurons, but for different functions.

Early in corticogenesis, at E13.5, Satb2-expressing neurons in deep layers also co-express Ctip2, while from E14 onwards, Satb2 is downregulated in these neurons, as the expression of the two molecules becomes mutually exclusive. This early transient Satb2 expression was shown to be necessary for the normal formation of the corticospinal tract (CST) (Leone et al., 2015). Indeed, in absence of Satb2, neurons expressing a knockout Fezf2 knockin alkaline phosphatase allele which labels deep layer SCPNs, failed to send projections past the cerebral peduncle into the spinal cord, while in the control mouse they were visible throughout the entirety of the corticospinal tract. Ablation of Satb2 using the BAC transgenic line Rbp4-cre which targets layer 5 neurons and is expressed from E16 onwards, did not result in this phenotype, suggesting that it is early and not late expression of Satb2 which is responsible for the CST formation in these neurons. So, early expression of Satb2 in deep layer neurons acts on the refinement of their subcortical projections rather than on callosal identity specification.

In later stages, from E16 onwards, a subgroup of layer 5 neurons start to co-express Satb2 and Ctip2 (C/S+) and in postnatal stages this population increases progressively until P21 in both the frontal/motor (F/M) cortex and S1 (Harb et al., 2016). Retrograde tracing followed by immunohistochemistry revealed that the C/S+ neurons in the postnatal brain do not acquire dual subcerebral and callosal projections, but instead they are divided into a purely callosal population and a purely subcerebral (but not corticospinal) population. The co-expression of Ctip2 and Satb2 was shown to become possible through the timely overexpression of the transcription factor LIM Domain Only Protein 4 (Lmo4), which antagonises Satb2 for binding Hdac1, thus cancelling the Satb2-mediated repression of Ctip2. However, de-repression of Ctip2 in these layer 5 neurons at the specific time point was not sufficient to induce the formation of of subcerebral projections.

Overall these studies reveal that Satb2-mediated de-repression of Ctip2 is a mechanism leading to CPN fate-specification, only in a specific neuronal population and only in a particular window of time and that in any other context it has different functions, such as refinement of final targets and morphological or electrophysiological properties.

Apart from time and cell type-specific, a recent study suggested that Satb2 fuctions are also species-specific (Nomura et al., 2018). Indeed, Satb2 is still present in areas homologous to the mammalian pallial region of vertebrates that do not possess a CC, such as the gecko dorsal cortex and the chick hyperpallium apicale. Ctip2 and Satb2 are colocalised to a high extent during embryonic development in these species. While all the components of the NuRD complex are present in C/S+ neurons in both the chicken and the reptilian pallium, and the Ctip2 locus possesses a MAR in the chick, which is able to interact with Satb2, in the presence of Satb2 the transcriptional activity of the chick MAR region is increased, thus not only allowing but in fact promoting Satb2/Ctip2 co-expression. Strikingly, while single Satb2-positive neurons do not exist in the gecko, only Ctip2-positive but not C/S+ neurons project to the contralateral pallium, perhaps through another commissure, whereas both Ctip2-positive and C/S+ neurons project to the ipsilateral septum. These data indicate that in different species the same transcriptional program can be interpreted differently, giving rise to species-specific projection outcomes.

1.1.4.2 Turning towards the midline

CPN fate specification is followed by the extension of an axonal projection towards the midline. Certain CPN populations send directly a medially oriented tangential projection while their cell body is still in the intermediate zone (IZ), which is maintained, as they migrate radially into the CP (Hatanaka and Yamauchi, 2013). On the other hand, CPNs located in the dorsal and dorsolateral cortex send an axon which initially bifurcates into two branches, one towards the midline and a second into the internal capsule (Garcez et al., 2007), which is eventually pruned by P11. The decision to bifurcate was shown to depend on the cell environment and not on cell intrinsic mechanisms. This was shown through slice overlay experiments, in which dissociated neurons derived from the lateral or medial cortex were placed on homologous (lateral to lateral or medial to medial) or heterologous (lateral to medial or medial to lateral) cortical areas in brain slices. Neurons derived from the medial cortex bifurcated less when placed in the medial and more when placed in the lateral cortex, while bifurcation in laterally derived neurons

decreased when placed into medial cortex as opposed to when they would be placed to the homologous lateral cortex.

The mechanisms governing the decision of CPNs to project medially, either directly or through bifurcation and eventual pruning, are not fully understood. In neurons residing in layer 2/3 the decision could be governed by the proneural factor Neurogenin 2 (Ngn2). This factor was shown to promote the formation of callosal projections (Hand and Polleux, 2011), as its silencing caused the increase of lateral projections, while at the same time decreasing medial projections sent from defective layer 2/3 neurons. Axon guidance cues could also be implicated in this decision. In layer 5 neurons, the decision to project medially to the CC and not laterally to the internal capsule was shown to be guided by the Netrin1 receptor uncoordinated 5C (Unc5C) (Srivatsa et al., 2014). Gain and loss of function experiments indicated that Satb2 promotes the expression of Unc5C and represses Deleted in Colorectal Cancer (DCC) in CPNs. At the same time, Netrin1, a repulsive cue for Unc5c-positive axons, is expressed in the basal ganglia and not in the midline. Absence of Netrin1 caused a group of deep layer Satb2 neurons to mis-project to the internal capsule. Importantly, callosal projections from GFP-electroporated deep layer CPNs were shown to be repelled by Netrin1 ectopically secreted in the midline by coated beads suggesting that Netrin1 expression in the basal ganglia and absence in the midline causes Unc5C-positive axons from deep layer Satb2$^+$ neurons to be repelled by basal ganglia Netrin1 and thus project towards the midline.

1.1.4.3 Midline crossing

Growth of axons through the CC is achieved through permissive signals that attract them towards the midline and repulsive signals that keep them restrained inside the CC or eventually drive them away from the midline. Such signalling molecules are secreted by three transient structures composed of guidepost cells, located close to or directly at the midline. The first two types, the indusium griseum (IG) and glial wedge (GW), are composed of glial cells and secrete repulsive guidance molecules (Figure 1.8). The IG is located in the ventromedial part of the cingulate cortex, dorsally of the CC, whereas the GW is located in the dorsolateral septum, ventrally to the CC. Together they channel callosal axons through the midline and prevent them from projecting to structures located dorsally or ventrally of the CC. The third type of guidepost structure is called the subcallosal sling and constitutes a corridor made up of neuronal cells, GABAergic and glutamatergic, through which the callosal axons grow.
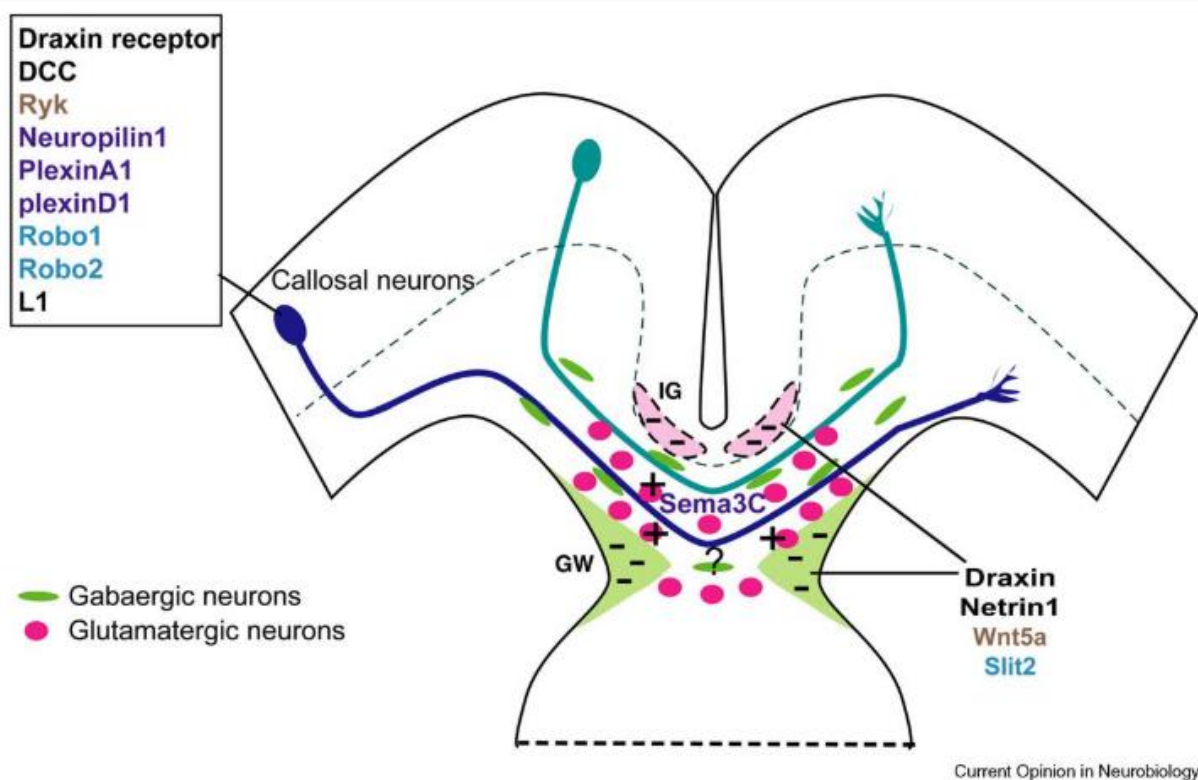
Figure 1.8 Guidepost cells and axon guidance molecules guiding midline crossing

Schematic of a mouse brain coronal section at the level of the midline, summarizing the ligands secreted by guidepost cells anf the receptors expressed by crossing axons. The GW and IG secrete repulsive axon guidance molecules such as Draxin, Netrin1, Wnt5a and Slit2, while the neurons of the subcallosal sling secrete attractants. Glutamatergic neurons in this structure secrete Sema3C, whereas the attractant secretes by the GABAergic population is unknown. Ephrins. Adapted from Chédotal A, 2010.

Both the glutamatergic and GABAergic populations of the subcallosal sling secrete attractants for the developing callosal axons. The only attractant identified until now is Sema3C, an attractive ligand of Neuropilin1 (Npn1), which is expressed by Calretinin-positive glutamatergic neurons in the lateral CC, but also by the cells of the IZ of the cingulate cortex. Pioneer callosal axons sent by neurons of the cingulate cortex express Npn1 while crossing the midline at E15-E17. In absence of Npn1/Semaphorin interaction, axons from the cingulate cortex are misrouted and cross the GW to project into the septum or form Probst bundles (Gu et al., 2005; Piper et al., 2009). In Sema3C mutants there is partial to complete AgCC and Probst bundles, suggesting that Sema3C/Npn1 signalling is important for midline crossing (Niquille et al., 2009, 2013)

Upon midline crossing, axons exit the midline. For this, axons need to switch on repulsion to guidance molecules secreted in the midline. Different studies have indicated molecules which repel callosal axons after midline crossing. Wingless 5a (Wnt5a) is a molecule

expressed by the IG and the GW, starting from E16. Ryk, a chemorepulsive receptor of Wnt5a is expressed by callosal axons while they cross the midline. In the absence of Ryk, post-crossing axons fail to escape the midline and to enter the contralateral white matter. These results suggested a role for Wnt5a/Ryk repulsive signalling in the exit of post-crossing axons from the midline. Whereas Wnt5a is expressed in both sides of the brain from E16 to E18, only post-crossing behaviour seems to be affected by its presence. Co-cultures of explants derived from E16, E17 and E18 cortex with agarose blocks expressing Wnt5a showed that only E18 and not E16 or E17 cortical neurons were repelled by Wnt5a. This suggested that whereas pre-crossing neurons are insensitive to repulsion caused by Wnt5a, post-crossing neurons become sensitive, probably by upregulating Ryk at the correct timepoint (Keeble et al., 2006). A later study showed that Wnt/Ryk dependent guidance of post-crossing axons away from the midline requires promotion of repulsion and outgrowth mediated by calcium signalling (Hutchins et al., 2011).

Another chemorepellent secreted by glial guidepost cells in the IG and GW is Slit2. Callosal axons, which express the two Slit receptors Roundabout homolog 1/2 (Robo1/2), are repelled by these structures in vivo and in vitro (Shu and Richards, 2001). Complete Robo1 knockout mice exhibit among other defects dysgenesis of the CC. Callosal axons from Robo1-defective or Slit2-defective cortex fail to cross the midline and project into the septum (Andrews et al., 2006; Bagri et al., 2002). Slit2 was proposed to control only post-crossing guidance of callosal axons. According to this model, axons are not repelled by Slit2 before, but only after crossing the midline. DCC downregulation was shown to be important for this sensitivity to repulsion of the axons by Slit2. Through a series of cocultures of cingulate cortex explants with sources of ligands, it was shown that in the absence of DCC, Robo1-mediated Slit2 signalling is repulsive, whereas in presence of DCC, through interaction of its intracellular domain P3 with the intracellular domain CC1 of Robo, the repulsive signal of Slit2 is attenuated. According to this mechanism, DCC-expressing pre-crossing pioneer axons can approach the midline, as increasing levels of Netrin result in attenuated repulsion from the midline. Later in development, post-crossing axons, which have downregulated DCC, exit the midline through Robo/Slit2 repulsion (Figure 1.9) (Fothergill et al., 2014).
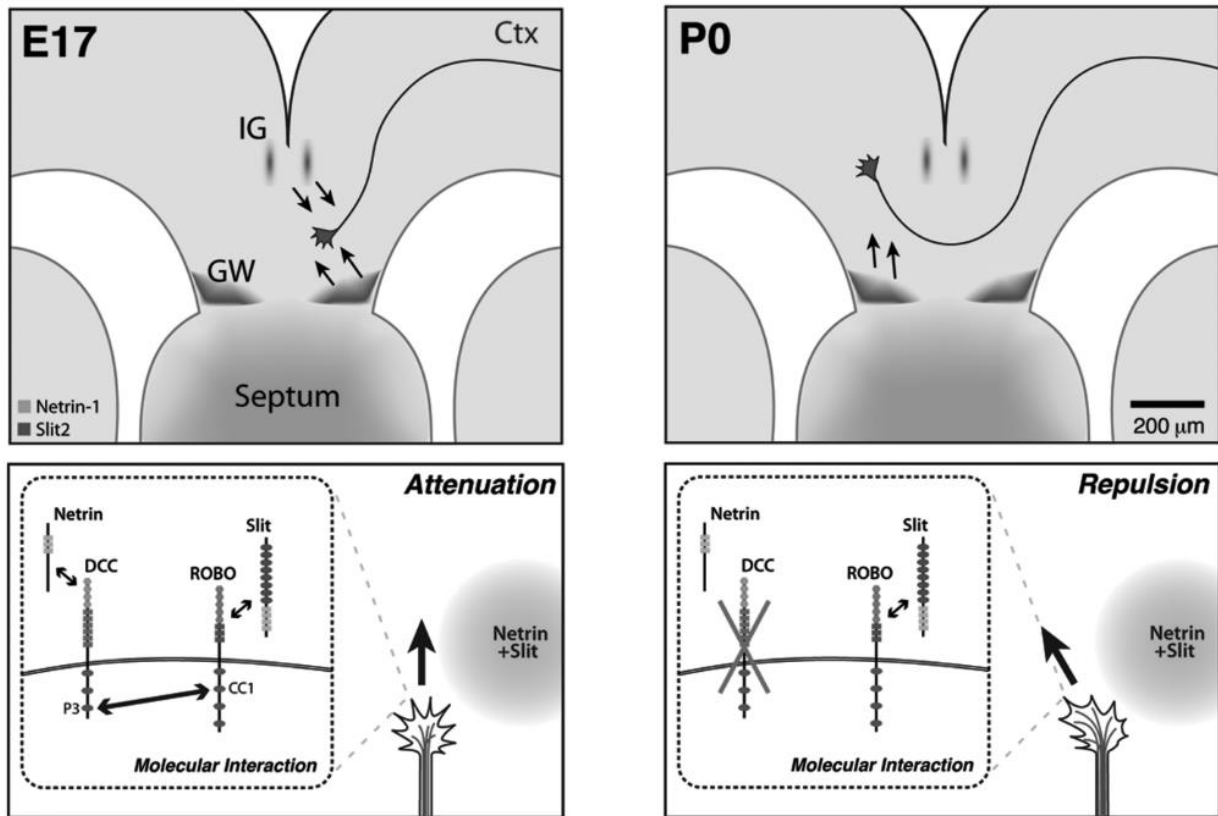
Figure 1.9 Repulsion of postcrossing axons away from the midline is mediated by repulsion from Slit2 triggered by DCC downregulation

Schematic representation illustrating callosal axons as they cross the midline at E17 (pre-crossing) and P0 (post-crossing) in mouse. At E17, DCC is expressed by callosal axons together with ROBO. In response to Netrin1 which increases as the axons approach the midline, the intracellular P3 domain of DCC interacs with CC1 domain of ROBO, thus attenuating Slit2 induced repulsion. Thus axons can be chaneled into the midline (arrows). At P0, while axons enter the contralateral hemisphere, DCC downregulation allows Slit2-mediated repulsion. Adapted from Fothergill et al., 2014.

After having crossed and exited the midline, callosal axons need to navigate into an environment which is a mirror replication to the one that attracted them towards the midline in the pre-crossing stage. To avoid being attracted again towards the midline by Sema3C, post-crossing axons which still express Npn1, need to become insensitive to this attractant. EphrinB1, an axon guidance molecule upregulated in post crossing Npn1^{+} axons extending from the frontal cortex, was shown to abolish Sema3C/Npn1 attractive response (Miré et al., 2018). Indeed, neurons harvested from E15.5 (pre-crossing stage) neocortex elongated their axons in presence of Sema3C whereas this elongation was not observed by the same neurons in presence of full length or extracellular domain of EphrinB1. On the other hand, axons from neurons derived from E18.5 (post-crossing stage) neocortex were insensitive to Sema3C signalling, and conditional deletion of *Efnb1* in cortical neurons restored axonal response to

Sema3C. Overall, these results showed that EphrinB1 is necessary and sufficient to silence Sema3C/Npn1 attractive activity in post-crossing callosal axons, by interacting with Npn1 (Figure 1.10).
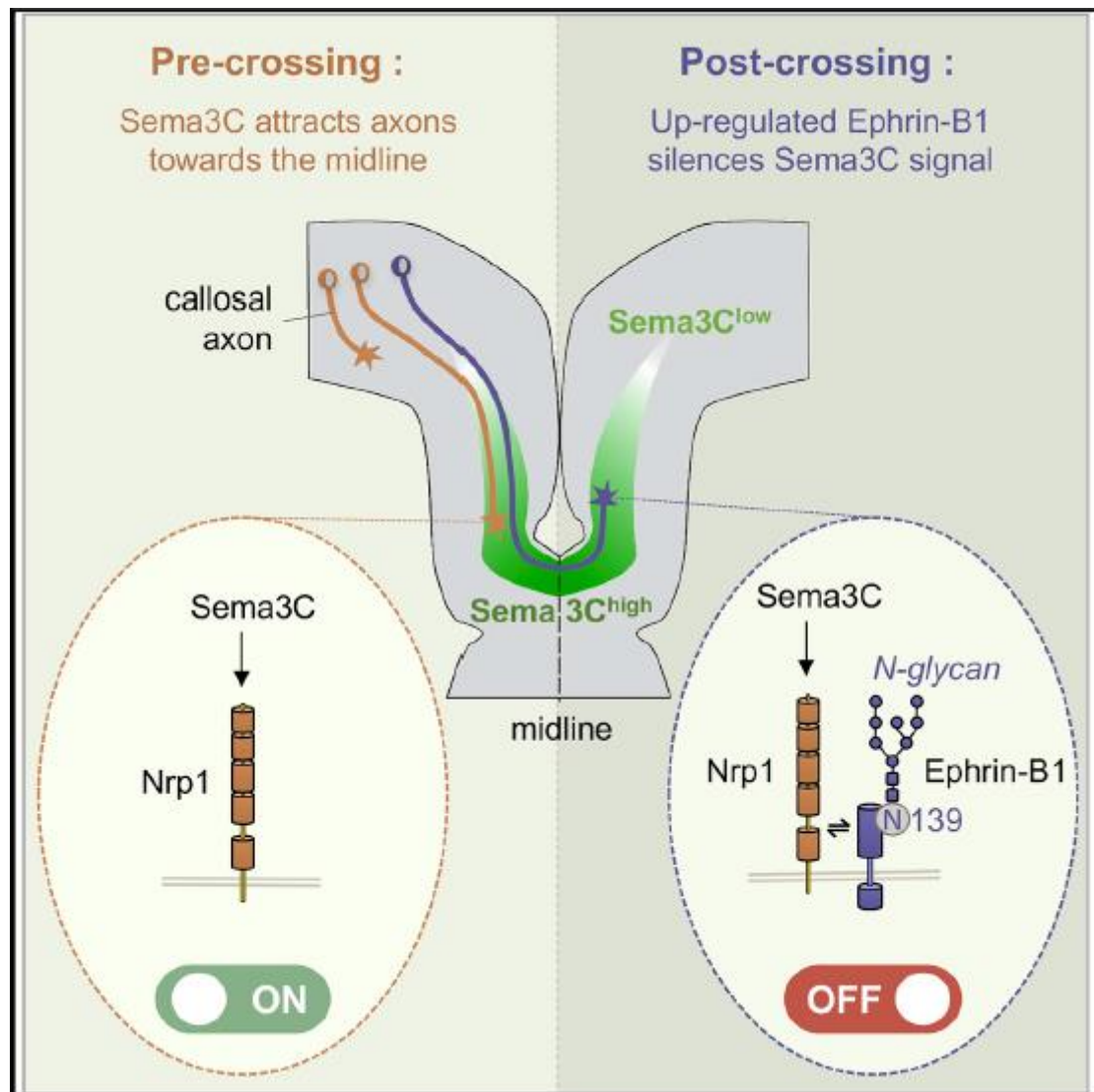
Figure 1.10 Schematic representation of the mechanism that switches off Sema3C/Npn1 attractive signalling in post-crossing callosal axons

Sema3C is secreted by neuronal guidepost cells inside the midline thus creating a gradient that is stronger as the axons approach the midline. At pre-crossing stages, Sema3C/Npn1 signalling attracts callosal axons into the midline. After midline crossing, Npn1^{+} neurons need to switch off attraction to Sema3C in order to navigate against its gradient. This switching-off is mediated by EphrinB1 which is upregulated in post-crossing axons and interacts with Npn1. Ephrin-B1-mediated silencing of Sema3C/Npn1 attractive signalling requires N-glycosylation of its extracellular domain. Adapted from Miré et al., 2018.

1.1.4.4 Targeting and branching

Midline crossing and post-crossing guidance are followed by a period in which callosal axons invade their final targets in the contralateral cortex. The topographic positioning of axons inside the CC has been shown to determine the correct targeting of axonal projections into cortical areas symmetric (homotopic) to their cell of origin. Callosal axons originating from medial (motor) or lateral (somatosensory) cortical areas are segregated inside the CC in a topographic manner, which is maintained until the invasion to their final targets in the homotopic contralateral cortical area. Carbocyanine dye (DiI, DiO) injections as well as sequential *in utero* electroporation (IUE) of reporter genes of different colour showed that CPNs located medially send axons through the dorsal part of the CC whereas laterally located CPNs project through the ventral part of the CC (Nishikimi et al., 2003; Zhou et al., 2013). Subsequently, axons passing through the dorsal CC turn to invade the cortex medially, while axons projecting through the ventral CC target lateral cortical areas. Sema3A/Npn1 signalling was shown to be important for the maintenance of the dorso-ventral segregation of axons in the CC. Indeed, disruption of Npn1/Sema3A signalling through shRNA electroporation or in complete knockout mice, leads to aberrant overlap of axons derived from medially and laterally residing CPNs inside the CC. This effect can be both cell autonomous and non-autonomous, as disruption of Sema3A/Npn1 in one hemisphere is capable of disrupting topography of axons deriving from the opposite cortex. Interestingly, upon loss of dorso-ventral topography in the CC, post-crossing axons invade final mediolateral targets, as mandated by their aberrant position in the CC, indicating that it is the position of the axon in the CC and not the location of the cell body that leads the axon to invade a homotopic cortical target. This mechanism of final targeting facilitates the correct invasion into homotopic targets and minimises the number of axons which, in the normal brain project aberrantly from the primary somatosensory area (S1) to the primary motor area (M1) early in development and are normally pruned until P30. Indeed, when topography in the CC is disrupted, pruning mechanisms are not sufficient to eliminate completely these aberrant heterotopic projections. This mechanism has been shown to govern homotopic targeting in layer 2/3 CPNs, however it is not known whether this is also the case for CPNs residing in layer 5.

Axon guidance mechanisms governing targeting, invasion and maintenance of contralateral innervation in the different cortical areas have been shown to depend upon neuronal activity. Transcriptional regulation of intrinsic activity patterns in early stages of

cortical invasion has been shown to be critical for the maintenance of contralateral innervation in layer 2/3 CPNs. The transcription factor Cux1 was shown to regulate this process (Rodríguez-Tornos et al., 2016). In the absence of Cux1, axons develop normally until P8, when they initiate the invasion of the contralateral cortex, but upon this point they fail to innervate the cortex and as a result they are retracted. This leads to absence of axons in the contralateral somatosensory and insular areas and reduction of axons in the contralateral white matter at P16, whereas ipsilateral axonal branches remain intact. Cux1 exerts developmental control over contralateral connectivity by changing the intrinsic activation properties of CPNs. Disruption of excitability through overexpression of the inward-rectifier potassium-ion channel Kir2.1, led to partial rescue of the axonal loss in absence of Cux1. Examination of cell membrane properties and parameters describing the firing pattern in Cux1-deficient neurons revealed that Cux1 is important for the acquisition of a transient state of strong firing adaptation and weak excitability that CPNs normally pass between P10-P12, before they increase progressively their spiking rates and become less adapting, while at the same time acquiring their mature firing patterns at P16. In absence of Cux1, CPNs increase their excitability and present weak adaptation as early as P10-P12, while they exhibit abnormal firing patterns at P16, indicating that they did not mature properly. In vitro experiments showed that Cux1 controls the electric maturation of CPNs during this phase by upregulating the expression of genes encoding for Kv1, a voltage gated potassium channel. In vivo knockdown of Kv1 severely disrupted callosal connectivity, whereas overexpression of Kv1 resulted in a rescue of the axonal loss caused by Cux1 knockdown, while at the same time rescuing the transient physiological characteristics at P10-P12 and leading to the acquisition of proper mature firing patterns by CPNs until P16.

Callosal neurons in layers 2/3 of the S1 send axonal projections that invade and branch extensively inside the contralateral S1/S2 border and Insular/Perirhinal (Ins/PRh) borders and more sparsely into the homotopic S1. While Cux1-induced regulation of electric maturation is important for the establishment of all three types of S1-derived contralateral projections, innervation of the S1/S2 border was shown to be dependent also upon interhemispheric balance of intrinsic and input-mediated activity (Suárez et al., 2014b). Indeed, ablation of sensory input by whisker cauterisation either in the ipsilateral or contralateral cortex, caused failure of contralateral axonal invasion in the S1/S2 by P10, which was sustained in the adult mouse. Furthermore, inactivation of intrinsic activity in CPNs, by electroporating the inward rectifying channel Kir2.1, also disturbed axonal invasion in the S1/S2. On the other hand, bilateral sensory input deprivation as well as bilateral Kir2.1-mediated inactivation, both rescued contralateral

S1/S2 invasion, suggesting that this process requires a balance in activity inter-hemispherically, rather than a specific global level of activity. However, general balanced interhemispheric activity is not sufficient to allow the invasion of S1/S2, as input has to be received from symmetrically placed whiskers, as indicated by bilateral cauterisation of the same number of asymmetrically positioned whiskers which ended in disruption of contralateral S1/S2 projections. Interestingly, both uni- and bi- lateral manipulations of intrinsic and input-mediated activity did not affect the invasion of axonal projections in the S1 and the Ins/PRh border, suggesting that balanced interhemispheric activity is not necessary for the innervation of these areas.

After target innervation, callosal axons form branches inside their final targets. The maintenance of these branches and the establishment of functional synapses is a process requiring high availability of energy in the axon terminals. The local maintenance of mitochondria in the axon terminals has been shown to ensure the formation and maintenance of axonal branches by CPNs both in the ipsilateral and contralateral cortex (Courchet et al., 2013). Liver kinase B1 (LKB1), a Ser/Thr kinase has been shown to regulate this process through the phosphorylation of its downstream target NUAK Family Kinase 1 (NUAK1). Both ipsilateral and contralateral axonal branching is reduced after either conditional ablation of LKB1 or knockdown of NUAK1 target kinase, whose expression is stabilised through phosphorylation by LKB1 in layer 2/3 CPNs in the S1. Both proteins are sufficient to promote axonal branching and in vitro rescue experiments revealed that NUAK1 acts downstream of LKB1 to mediate this action. Promotion of branching by NKB1/NUAK1 was shown to require immobilisation of mitochondria along the axons. In *Nkb1* and *Nuak1* defective cortical neurons, the percentage of motile/non-motile mitochondria increased, together with their velocity and maximum distance covered, while overexpression of *Nkb1* and *Nuak1* led to the opposite results, suggesting that NKB1/NUAK1 promote mitochondrial immobilisation. Syntaphilin, a mitochondria-related protein which promotes mitochondria immobilisation in vitro, was shown to be necessary for axon branching both in vitro and in vivo. Overexpression of syntaphilin rescued the loss of axonal branching in LKB1-defective neurons in vitro, thus suggesting that LKB1 effect on branching requires mitochondrial immobilisation, possibly in a syntaphilin-dependent way. Finally, through in vitro loss- and gain-of-function of LKB1/NUAK1 in neurons expressing markers for nascent presynaptic puncta it was demonstrated that the kinases promote specifically the dwelling of mitochondria on these cellular compartments, indicating

that maybe immobilised mitochondria promote branching through synaptic stabilisation, by unknown mechanisms, possibly involving ATP production.

Fate specification and midline crossing are the developmental steps followed by all CPNs and distinguish them from the other two types of PNs. However, the steps following midline crossing, such as target selection and refinement of axonal and dendritic processes shape characteristics that distinguish CPN subpopulations according to their final targets, dendritic morphology and electrophysiological properties. The next chapter describes the different aspects of heterogeneity among CPNs that are shaped by late steps in CPN development.

1.1.5 Diversity within callosal neurons

CPNs are distinguished from the other two PN types based on the general pathway that their axons follow, after they have entered the white matter. However, within the CPN population there is a remarkable heterogeneity of subtypes, which are distinguished by their different connectivity patterns, Somato-dendritic morphologies, electrophysiological properties and molecular identities. The developmental mechanisms shaping these characteristics are not completely understood. This study asked how the different types of connectivity within CPNs are created throughout development and whether morphology and molecular identity can be correlated with distinct connectivity patterns. Herein I provide an overview of the different aspects of diversity within the CPNs.

1.1.5.1 Axonal Connectivity

All CPNs send axon terminals in areas symmetric (homotopic) to the location of their cell body (Caviness, 1975). However, subgroups among CPNs of different areas, in addition to their homotopic projections, send a collateral branch to other ipsilateral regions (Cauller et al., 1998; Mitchell and Macklis, 2005) and/or heterotopic regions in the contralateral hemisphere. Contralateral heterotopic projections can be either short-range or long-range. Long-range heterotopic projections are sent into distant cortical areas from the area of origin or to subcortical areas, whereas short-range cortico-cortical heterotopic projections are sent to an

adjacent secondary cortical area, or to the border between a primary and a secondary area. Examples of the three types of heterotopic projections have been described in several mammalian species including human. Efforts to describe the distribution of callosal targets with regards to their area of origin date back to the 1970's. Early studies, using targeted lesions in the cortex or CC and Wheat Germ Agglutinin-horseradish peroxidase (WGA-HRP) or tritiated amino-acids to label anterogradely callosal fibers and horseradish peroxidase (HRP) injections to label the cell bodies of origin in the contralateral cortex provided the first detailed maps of callosal connectivity in rodents and other mammals. The development of fluorescent retrograde and anterograde tracers as well as layer-specific labelling of callosal fibers by IUE of plasmids encoding for reporter genes allowed for a more sophisticated characterisation of these neurons and their projections. Data on the precise connectivity in humans come from post-mortem lesions and subsequent visualisation of axon terminal degradation as well as post-mortem microdissection, or *in vivo* functional Magnetic Resonance Imaging (fMRI) followed by DTI-tractography. Tables 1-1, 1-2 and 1-3 summarise the studies describing heterotopic projections of the three types (short range, cortico-cortical long-range and cortico-subcortical long-range) in non-human primates, rodents, cats and humans. Here I discuss the main characteristics of each category separately, with a focus on the long-range heterotopic projections described in the mouse, which is the model organism used in this study (Figure 1.11).

Homotopic projections
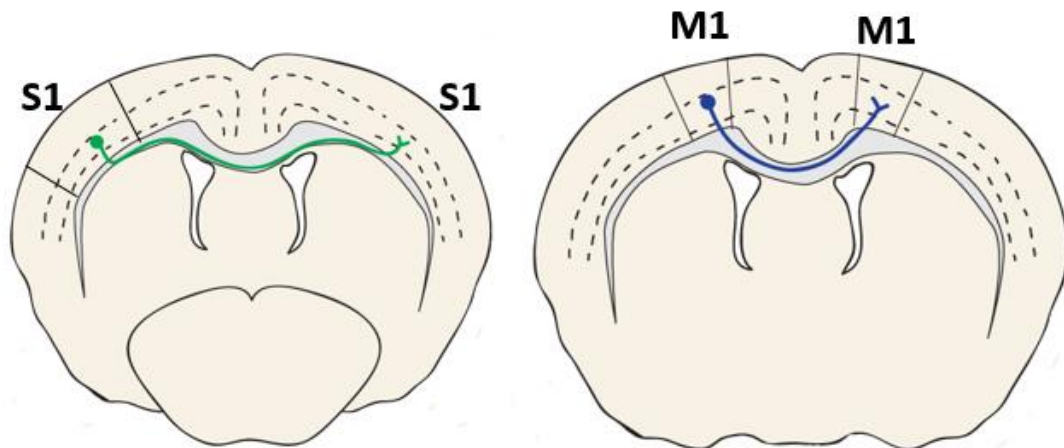
Heterotopic projections
(Long-range)
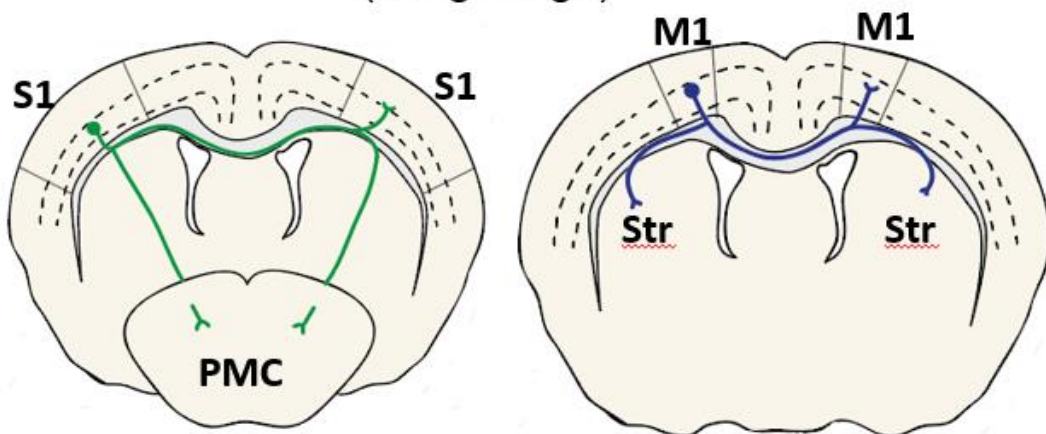
Figure 1.11 Two types of long-range heterotopic projections documented in mice

Except for the homotopic projections, CPNs in the S1 may send projections to the contralateral premotor cortex (PMC) while CPNs located in the M1 may send a projection to the contralateral striatum (Str). Both types may additionally send a projection to the ipsilateral heterotopic area.

1.1.5.1.1   Short-range heterotopic callosal projections

Short-range projections from primary to secondary sensory areas have been documented in all species reviewed here (Table 1-1). The most commonly identified projections of this type are reciprocal connections between primary and secondary areas in the somatosensory and visual cortex, but projections between primary and secondary auditory cortices have also been documented in cats. Motor and frontal cortex can also send reciprocal projections with their

equivalent secondary areas in primates. In the human brain, short range heterotopic projections were shown to exist in the healthy human brain by a recent post-mortem study using a novel microdissection approach (De Benedictis et al., 2016). In this study, the medial frontal cortex is shown to be connected with both the homotopic medial and the heterotopic contralateral frontal cortex. In the mouse, anterograde approaches have revealed the existence of short-range heterotopic projections sent from the M1 and the S1 into their respective medially and laterally located secondary areas. The layers of origin of short-range heterotopic projections vary from species to species. For example, connections from primary to secondary visual cortices in primates originate from layers 2/3 and 4, and in the cat from layer 2/3. On the other hand, in rats the same type of connections is sent by cells residing mainly in layer 5. In the mouse, S1>S1/S2 projections are formed by layer 2/3 electroporated cells, by it is possible that also deep layer CPNs contribute to these projections.

Table 1.1 Summary of studies reporting short range cortico-cortical projections in different mammalian species

Area abbreviations: V1: Primary Visual Cortex, V2,V3: Secondary visual cortex, PM: Premotor area, SMA: Supplementary Motor Area, CMA: Cingulate Motor Area, AI: Primary auditory area, AAF: Anterior Auditory Field, VPAF: Ventro-Posterior Auditory Field, PMLS: Postero-medial lateral suprasylvian visual area. Tracer abbreviations: HRP: Horseradish Peroxydase, WGA: Wheat Germ Agglutinin, FB: Fast Blue, DY: Diamidino-Yellow, BDA: Biotinylated Dextran Amine, CTB: Cholera Toxin Unit B, AAV: Adeno-associated Virus, FG: Fluorogold, DT: Diffusion Tractography

Species	Area of origin	Layer of origin	Targeted area	Tracing method	Reference
Cynomolgus Monkey (*Macaca fascicularis*)	Border of primary to secondary (V1/V2)	Layer 3	Primary Visual (V1) Secondary Visual (V3, V2)	Retrograde HRP Anterograde HRP-WGA	(Kennedy et al., 1986)
Squirrel monkey (*Saimiri sciureus*)	Primary visual (V1)	-	Secondary Visual	Anterograde Electrophysiological recordings	(Boyd et al., 1971)
Callithrix Jacchus	Primary Visual (V1 or 17)	Layers 3 (deep), 4 (upper)	Secondary visual (19DM, MT)	Anterograde HRP-WGA	(Spatz Birgit Kunz and Steffen, 1987)
Cynomolgus Monkey (*Macaca fascicularis*)	Primary Motor M1 Secondary Motor (PM areas, pre-SMA , SMA-proper and CMA.	-	Adjacent secondary motor (PMd-c and PMv-c)	Retrograde Fast Blue (FB), Diamidino-Yellow (DY)	(Boussaoud et al., 2005)
Cat	Primary auditory (AI) Secondary auditory (AAF) Secondary auditory (VPAF)	2/3 (rarely 5,6)	Secondary auditory (AAF) Primary auditory (AI) Adjacent secondary auditory (PAF)	WGA-HRP	(Rouiller et al., 1991)

Species	Area of origin	Layer of origin	Targeted area	Tracing method	Reference
	Secondary visual (PMLS)	Layers 3(deep), 6	Primary Visual (17/18)	**Retrograde** DY, FB	(Segraves and Innocenti, 1985)
	Primary Visual (17 or 18)		**Secondary Visual (21)**	**Anterograde** Lesion	(Sanides, 1978)
Rat	**Primary Visual** (17-lateral and medial)	**Layer 5**	**Secondary Visual** (18a, 18b)	**Anterograde** Tritiated amino-acids	(Miller and Vogt, 1984)
	Secondary Visual (18a, 18b)		**Primary Visual** (17-lateral and medial)	**Retrograde** WGA-HRP	
	S1	-	S2	**Anterograde** Tritiated amino-acids	(Wise and Jones, 1976)
	Primary Somatosensory (Forepaw of S1)	**Layer 5**	**Secondary Somatosensory** (Perigranular and disgranular cortex)	**Anterograde** BDA **Retrograde** CTB	(Decosta-Fortune et al., 2015)
Mouse	**Primary Somatosensory** (S1)	Layer 2/3 (5 not excluded)	**Border of Primary to Secondary Somatosensory** (S1/S2)	**Anterograde** IUE	(Suárez et al., 2014b)
	Lateral and medial adjacent areas	Layers 2/3, 4, 5, 6	**Primary Somatosensory** (S1) **Primary Motor** (M1)	**Anterograde** BDA, EYFP-expressing AAV **Retrograde** FG	(Chovsepian et al., 2017)
Human	**Medial/lateral frontal cortex**	-	**Medial/lateral frontal cortex**	**Imaging** Microdissection/DTI	(De Benedictis et al., 2016)

Most of the long-range cortico-cortical connections that are documented in the literature are sent to areas of the frontal cortex and specifically the secondary motor areas (Table 1-2). The areas of origin can be sensory areas, such as auditory and visual, but the most commonly reported is the somatosensory area, primary or secondary. In the mouse, a study by Mitchell and Macklis (2005) revealed the existence of long range cortico-cortical heterotopic projections extended from S1 to the contralateral premotor cortex (PMC). Retrograde tracing with Fluorogold (FG) revealed the existence of a small callosal population in layer 5 of sensory-motor cortex, projecting heterotopically to the contralateral premotor cortex. The study found that a majority (69.5%) of these neurons send also a second projection to the ipsilateral PMC. As a substantial fraction among frontally projecting neurons also send a homotopic callosal projection, it is highly likely that the homotopically (S1>S1) and heterotopically (S1>PMC) projecting callosal populations in this layer overlap. However, the study did not directly address this question. In addition, the pathway followed by S1>PMC projections to reach their final target as well as their developmental course are largely unknown.

Table 1.2 Summary of studies reporting long-range cortico-cortical heterotopic callosal projections in different mammalian species

Area Abbreviations: S1: Primary Somatosensory Cortex, V1: Primary Visual Cortex, PMC: Premotor Cortex, Ins/PRh: Insular Cortex/Perirhinal area. Tracer Abbreviations: FE: Fluoroemerald, FB: Fast Blue, DY: Diamidino Yellow, CTB: Cholera toxin B subunit.

Species	Area of origin	Layer of origin	Targeted area	Tracing method	Reference
Squirrel monkey (*Saimiri sciureus*)	**Somatosensory** (Postcentral forelimb, hindlimb, and trunk areas of S1)	-	**Frontal/Motor**	**Anterograde** Suction lesion	(Boyd et al., 1971)
Cynomolgus Monkey (*Macaca fascicularis*)	**Parietal, motor, insular, temporal areas**	-	**Frontal/Motor** (Dorsal and ventral premotor areas)	**Retrograde** FE, FB, DY, CTB	(Lanz et al., 2017)
Squirrel monkey	**Primary visual (V1)**	**-**	**Frontal /Motor** (areas 4,6)	**Anterograde** Electrophysiological recordings	(Boyd et al., 1971)
Mouse	**Somatosensory** (S1)	5A	**Frontal** PMC	**Retrograde** DiI	(Mitchell and Macklis, 2005)
Mouse	**Somatosensory** (S1)	2/3	**Lateral** Ins/PRh	**Anterograde** IUE	(Suárez et al., 2014b)
Human	**Visual** (Right inferior temporal cortex)	-	**Frontal** (Broca's area)	**Anterograde** Lesion	(Di Virgilio and Clarke, 1997)

A subpopulation of CPNs residing in the motor cortex, in addition to their homotopic projections to the contralateral M1, send also a sub-cortical collateral to the contralateral Striatum. Cells producing this projection type have been long known as crossed-corticostriatal projection neurons (cCStrPNs). CPNs projecting to the contralateral Striatum have been described in the monkey and the cat (Jones et al., 1977; Royce, 1982), but also in the rat (Wilson, 1987) and the mouse (Sohur et al., 2014). cCStrPNs have been described also in the human brain. Through a post-mortem microdissection approach (De Benedictis et al., 2016) revealed the existence of cCStrPNs in the healthy human brain, as both the medial and lateral frontal cortices project to the contralateral putamen and caudate nucleus, which are areas belonging to the striatum.

Cell bodies of cCStrPNs are restricted in rostral areas of the cortex and in rodents they are found in frontal, premotor and motor areas of the cortex (Table 1-3). However in the rat, CTB injections from the somatosensory (caudal) striatum were able to label a small group of neurons in the layer 5 of the contralateral somatosensory cortex (Wright et al., 2001). In all species cCStrPNs are located principally in layer 5 except in the cat, in which they are also detected in layers 2/3 and 6 (Royce, 1982). In rats, they are located mostly in the superficial part of layer 5 and deep layer 3, whereas in mice they extend from deep layer 3 to upper layer 6.

In both the rat and the mouse, cCStrPNs were shown to send a collateral branch inside the ipsilateral Striatum and the contralateral cortex (Sohur et al., 2014; Wilson, 1986). Specifically, in the mouse, placement of multiple tracers in the two striata and the contralateral cortex in the same P15 brain, revealed the existence of different of cCStrPN types, among which, a group sends a collateral branch to the ipsilateral Striatum, a second projects to the contralateral cortex and a third projects to both (Sohur et al., 2014). However, due to the probable inability of tracers to label all projections in an area, we cannot rule out the possibility that all cCStrPNs project to both striata and the contralateral homotopic cortex.

Layer 5 SCPNs also send a collateral branch in the ipsilateral Striatum and are referred to as pyramidal tract (PT) corticostriatal (CStr) neurons. Even though they both give input from the cortex in the Striatum, cCStrPNs and PT-CStr neurons are completely different in terms of connectivity and functions. The two pathways have been suggested to project differentially to striatal medium spiny neurons of the direct pathway striatal neurons projecting to the internal

globus pallidus and substantia nigra pars reticulata (GPi-SNr) and to the indirect pathway neurons that project to the external globus pallidus (GPe). In particular, a higher percentage of cCStrPNs project to the direct pathway neurons, whereas PT-CStr neurons project preferentially to the indirect pathway neurons in the rat Striatum (Deng et al., 2015). While PT-CStr projections transmit a copy of motor commands given to the spinal cord, cCStrPNs transmit information about motor planning (Bauswein et al., 1989; Beloozerova et al., 2003; Turner and DeLong, 2000) and sensory inputs.

The development and molecular identity of cCStrPNs in mice, was described by Sohur et al (2014). In the mouse, projections from cCStrPNs invade the contralateral Striatum between P3 and P4 (Sohur et al., 2014). Invasion in the ipsilateral Striatum happens also at the same timepoint, which precedes the timepoint of callosal invasion into the contralateral cortex (Mizuno et al., 2007; Wang et al., 2007), which happens at around P5. At this stage, projections to the contralateral Striatum arise from all cortical areas. However, until P15, cCStrPNs are restricted in the motor cortex, probably after massive pruning of the striatal collaterals of callosal neurons or cell death in other (non-motor) cortical areas. From P15 on, the rostro-caudal distribution of cCStrPNs in the cortex resembles the distribution in the adult brain.

Table 1.3 Summary of studies reporting long-range cCStr projections in different mammalian species.

Area abbreviations: M1: Primary Motor Cortex, PM: Premotor area, AGm: Agranular medial area. Tracer abbreviations: HRP: Horseradish Peroxydase, WGA: Wheat Germ Agglutinin, BDA: Biotinylated Dextran Amine, DT: Diffusion Tractography, (RDA)3k: tetramethylrhodamine-dextran amine

Species	Area of origin	Layer of origin	Targeted area	Tracing method	Reference
Cynomolgus Monkey (*Macaca fascicularis*)	**Motor** (M1)	**Layer 5**	**Striatum** (Caudate putamen)	**Anterograde and Retrograde** BDA injections	(Parent and Parent, 2006)
	Motor (Area 4)	-	**Striatum** (Caudate putamen)	**Anterograde** Radioactively labelled proteins	(Künzle, 1975)
Squirrel Monkey (*Saimiri sciureus*)	**Frontal/Motor** (Areas 4, 6, 8)	**Layer 5** (upper)	**Striatum** (Caudate Putamen and head of n caudatus)	**Anterograde** Tritiated amino-acids **Retrograde** HRP	(Jones et al., 1977)
Rhesus Monkey (*Macaca mulatta*)	**Frontal/Motor** (SMA, PS)	-	**Striatum** (Caudate Putamen and n caudatus)	**Anterograde** WGA-HRP	(McGuire et al., 1991)
Cynomolgus Monkey (Macaca fascicularis	**Frontal/Motor** (Prefrontal, PM, M1)	-	**Striatum** (Putamen and n caudatus)	**Anterograde** BDA **Imaging** DT	(Innocenti et al., 2017)
Cat	**Frontal/Motor** (Areas 4,6)	**Layers 2, 3, 5, 6**	**Striatum** (Caudate nucleus)	**Retrograde** HRP	(Royce, 1982)
Rat	**Frontal/Motor** (AGm)	-	**Striatum** (Dorsolateral caudate putamen)	**Anterograde** Orthodromic electrical stimulation	(Wilson, 1986)
	Frontal/Motor (AGm)	**Layers 3** (deep)**,5**	**Striatum**	**Retrograde** Antidromic stimulation WGA_HRP	(Wilson, 1987)
	Motor/ Somatosensory (M1, S1)	**Layers 3,5** (upper)	**Striatum**	**Retrograde** (RDA)3k	(Reiner A., 2003)
	Frontal/Motor/ Somatosensory	-	**Striatum** (Caudate Nucleus and Putamen)	**Anterograde** Lesion	(Carman et al., 1965)

Species	Area of origin	Layer of origin	Targeted area	Tracing method	Reference
	Frontal (Medial agranular and anterior cingulate)	**Layers 3** (deep)**, 5**	**Striatum**	**Retrograde** CTB-555	(Morishima and Kawaguchi, 2006)
	Motor (M1 forepaw and whiskers)	-	**Striatum**	**Anterograde** Fluoro-ruby (FR) Alexa-fluoro (AF) BDA	(Alloway et al., 2009)
Mouse	**Motor** (M1)	**Layers 3** (deep), **5, 6** (upper)	**Striatum**	**Retrograde** CTB-555	(Sohur et al., 2014)
Human	**Frontal Cortex**	-	**Striatum** Caudate nucleus	**Imaging** Microdissection-DT	(De Benedictis et al., 2016)
	Frontal /Motor (Premotor, SMA and M1) **Parietal and Temporal** (Language Processing Areas)	-	**Striatum** (Putamen and n caudatus)	**Imaging** MRI+DT	(Innocenti et al., 2017)

1.1.5.2 Somato-dentritic morphology

A second level of diversity among callosal subpopulations lies in their dendritic morphology. A series of studies have tried to characterise the somato-dendritic morphologies of layer 5 pyramidal neurons and many among these studies not only revealed the existence of morphological subtypes among the CPNs, but also examined the possibility that connectivity and morphology are correlated. From these studies, we retrieve valuable insight to the question of whether heterotopically projecting neurons have also unique morphologies.

Morphologies of layer 5 CPNs have been well studied with the view to compare with other types located in this layer (SCPN and CThPN) (Larsen et al., 2008; Oswald et al., 2013), and these studies have revealed the existence of CPN subtypes with different dendritic morphologies. In particular, a study by Larsen and Callaway (2006) described the heterogeneity of pyramidal morphologies in the somatosensory cortex, revealed through biocytin filling. Pyramidal neurons of layer 5 have diverse somato-dendritic morphologies, based on which, they are classified into three subtypes, namely the tall tufted, tall simple and short pyramidal neurons. Tall tufted neurons have large cell bodies and an apical dendrite which extends until layer 1 and forms an extensive tuft in layer 2. Their ipsilateral axons branch mostly in deep layers. Tall simple neurons also extend their apical tuft to the layer 1, but it is a smaller and simpler tuft expanding at the more superficial part of layer 2 and their cell body is smaller and more elongated than that of tall tufted pyramidal neurons. Short layer 5 neurons have a small cell body and do not maintain a tuft, as their apical dendrite does not extend past layer 2. Both tall simple and short neurons have extensive ipsilateral axonal arborisations in superficial layers. Injections of a recombinant monosynaptic GFP-expressing rabies virus in the contralateral S1, superior colliculus and the thalamus performed by the same team (Larsen et al., 2008) correlated these three morphological types of layer 5 pyramidal neurons with their long-range connectivity. Neurons projecting to the thalamus or the brainstem where found to be tall tufted, while homotopically projecting callosal neurons fell into both, tall simple and short, morphologically types. A more elaborate study of the ipsilateral axonal branching of these two types revealed that tall simple expand their axonal branches to adjacent columns, whereas short pyramidal neurons restrict their axonal arborisations inside a single column. This finding prompts to question whether one of these two morphological types would correlate with CPNs projecting heterotopically to the contralateral PMC. This question until now has not been addressed. However, Oswald et al (2013) provided a first answer to the general question of

whether morphological types correlate with heterotopically versus homotopically projecting types. This work conducted a morphological and electrophysiological characterisation of the different projection types of layer 5 pyramidal neurons in the M1. In this context, they distinguished neurons with callosal projections into the contralateral cortex (crossed corticocortical-cCCPN) from neurons projecting through the CC to the contralateral Striatum (cCStrPN), by differentially labelling them with CTB injections in the M1 or Striatum respectively. Sholl analysis showed no difference in dendritic complexity between the two populations, and principal component analysis considering morphological and electrophysiological characteristics, managed to put the two populations into two clusters, with the most predictive parameters for distinction between them, being not morphological but electrophysiological characteristics, such as the amplitude and the rise rate of the action potential. As expected, the cluster analysis showed an overlap between cCCPNs and cCStrPNs, explained perhaps by the extension of collaterals by some among the cCStrPNs into the contralateral M1. In the rat frontal cortex things are more complicated than a mere categorisation in two subtypes. Whereas all CPN of the layer 5 have a tuft reaching layer 1, neurons are categorised along a continuous distribution, in which the distance of tuft origin from the pia correlates with laminar position of the soma (Otsuka and Kawaguchi, 2011). Whether different interhemispheric connectivity patterns correlate with part of this morphological spectrum it is currently unknown. Another study by Kim et al (2015), using a combination of transgenic BAC cre-expressing lines and a recombined AAV expressing GFP in a cre-dependent way, identified and characterised morphologically and electrophysiologically two distinct populations of layer 5 neurons with cortico-cortical projections in the primary visual cortex (V1). The first population was visible in the Tlx3-cre mouse and the second in the Efr3a-cre line. The two populations are distinct, both in terms of morphology and electrophysiology. Efra3 cell bodies are oval shaped whereas Tlx3 cell bodies maintain a pyramidal shape. Tlx3-positive neurons project to ipsilateral secondary visual areas (V2, V2ML and V2MM) and contralaterally to the V1. Interestingly, Tlx3-positive neuron-derived projections were also visible in the striatum. On the other hand, Efr3a positive neurons in layer 5, either project to only adjacent visual areas like Tlx3 or belong to local pyramids projecting only inside the V1. In this case we see a differentiation of two different connectivity types among CPNs, with different morphologies. Examination of transgenic BAC cre-expressing lines under the promoters of CPN-specific genes expressed in layer 5, could provide further information on the relation between connectivity and morphology within the CPNs.

1.1.5.3 Electrophysiology

Diversity of morphologies and axonal connectivity within CPNs in layer 5 suggests the existence of different electrophysiological types which correspond to the differential computations and outputs that occur as a result of the morphology. Otsuka and Kawaguchi (2011) defined three electrophysiologically distinct CPN subtypes in layer 5 of the rat frontal cortex. Based on the adaptation rate of their firing response to current-pulse injection, they were categorised into fast adapting (FA), slowly adapting (SA), and slowly adapting with an initial spike doublet SA-d types. This study revealed a correlation between morphology and electrophysiology, as these physiological types were linked with different morphological characteristics. In particular, the apical tufts of FA type neurons bifurcated exclusively inside layer 1, while the tuft of some among the SA type neurons bifurcated deeper, in layers 2/3. However, SA type neurons exhibited a smaller length of the apical shaft than the FA type (Otsuka and Kawaguchi, 2011).

Correlations between electrophysiological types and axonal connectivity patterns have also been described. Indeed, CPNs in the frontal cortex sending an ipsilateral collateral either to the S1 or to the Striatum were identified mostly as FA, whereas the ones without a collateral were identified as SA (Morishima and Kawaguchi, 2006). Except for the adaptation pattern, other electrophysiological properties can distinguish between axonal connectivity types in layer 5 CPN. Such properties may be the action potential (AP) amplitude and the sag percentage. In the M1, layer 5 CPN projecting homotopically to the contralateral M1 exhibit a higher AP amplitude than cCStrPN (Oswald et al., 2013), while in the visual cortex, Efra3-positive neurons projecting locally to the adjacent secondary areas, exhibit a higher sag percentage than Tlx3-positive neurons which are callosal and corticostriatal,

Overall, these studies reveal the vast complexity of CPNs. This diversity is being shaped by the existence of not only different connectivity types but also of neuronal types with different morphologies and physiological properties. Whether this diversity is reflected on molecular identities of CPN subpopulations is currently unknown.

1.1.5.4   Molecular diversity

Callosal neurons are a remarkably heterogeneous population, comprising neurons with diverse molecular identities. CPNs residing in different cortical layers express layer-specific genes and the expression of these genes may vary according to the developmental stage. The molecular diversity within CPNs was revealed in the context of a series of studies having as main goal to identify genes differentially expressed in the three main PN categories, SCPNs, CThPNs and CPNs at different stages of development (Arlotta et al., 2005; Galazo et al., 2016; Molyneaux et al., 2009). In these studies, authors labelled each of these populations through retrograde tracing with different fluorescent markers injected in their final targets. After dissociation of the cortex and purification through FACS sorting, genes differentially expressed in the three PN types were extracted by hybridization on a microarray probe set. One of these studies (Molyneaux et al., 2009) focused on genes expressed specifically by CPNs. In this work, CPNs were labelled through retrograde tracing by injecting green fluorescent microspheres in the contralateral somatomotor cortex and SCPNs and CThPN through injections of Cholera toxin unit B conjugated with the fluorophore Alexa 555 in the pons and thalamus respectively. This approach provided a list of genes expressed specifically in CPNs, as opposed to SCPNs and CThPNs. The 40 most interesting, biologically relevant genes belonged to three categories: transcription factors, signalling molecules and axon guidance molecules.

In situ hybridization (ISH) for the most intensely differentially expressed genes at P14 revealed that apart from the genes, like Satb2, which are expressed by CPNs in all layers, several CPN-specific genes were restricted in populations residing in specific layers or sublayers. The expression patterns of 20 genes among them are indicated in Figure 1.12. This figure illustrates that among the CPN specific genes, there are genes expressed in all layers (*Lpl, Satb2*), but also there are genes restricted in upper layers or only layer 2/3 (*Tmtc4, Cux2*), deep layers (*Tcrb*) and finally there are genes whose expression pattern sub-parcellates the canonical layers. For example, *Frmd4b* and *Epha3* are expressed in upper layer 2/3 whereas *Nectin3* and *Chn2* take up the deeper part of layer 2/3. Accordingly, layer 5 is divided by the expression of genes like *Tcrb*, which is expressed in deep layer 5 (5B) and genes like *Gfra2* and *Plxnd1*, which present a narrow strip of expression in the superficial layer 5 (5A). As seen until now, different cortical layers and sub-layers host CPNs with different connectivity, morphologies and electrophysiological identities. For example, in the mouse, cortico-subcortical and long-range cortico-cortical heterotopically projecting CPNs are found mainly in layer 5 (cCStrPN) of the

motor cortex and 5A (S1>PMC) of the somatosensory cortex, but not in upper layers 2/3. Furthermore, in the rat somatosensory cortex, CPNs residing in different cortical depths exhibit different morphologies of the apical dendrite. How the different molecular identities of CPNs residing in different layers are correlated with their characteristics is poorly understood. A recent study (MacDonald et al., 2018) showed that *Cav1*, one of the CPN-specific genes expressed in upper layer 5 defined a CPN subpopulation that sends frontal projections to the ipsilateral PFC. Further work is necessary to describe the structural and functional characteristics of molecularly distinct CPN subpopulations, but also to shed light to the functions of the different genes-determinants of molecular subtypes in the development of subtype-specific characteristics.

In a first analysis, it is possible to form hypotheses on the function of these genes based on the temporal expression patterns of CPN-specific genes, provided by Molyneaux et al (2009). The temporal profile of expression of these genes was obtained by repeating the experimental process in four developmental stages: E18, P3, P6 and P14. Genes expressed in early developmental stages could be involved in early aspects of CPN development, like cell-fate specification, migration and initial axonal extension. Genes missing from the cortex at E18 but expressed highly from P3 (mid-stage of CPN development) onwards, may be involved in aspects of late differentiation, such as final target selection and innervation, and refinement of dendritic arborisations. Finally, genes expressed and maintained until adult stages could be important for maintenance of projections, and synaptic maturation or synaptic plasticity.
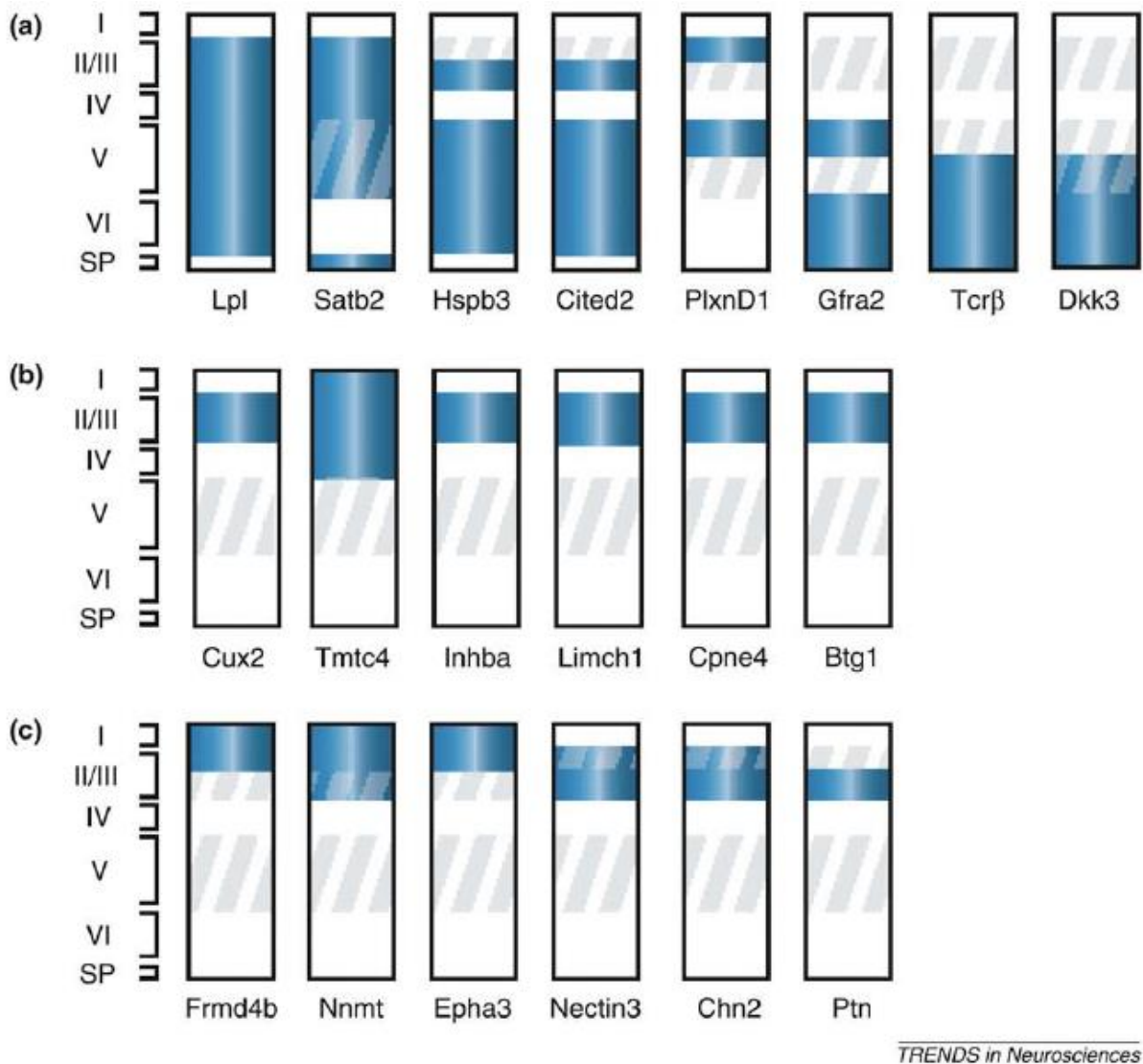
Figure 1.12 Layer-specific expression of genes expressed exclusively in CPNs reveals molecular heterogeneity in the CPN population

Schematic representation of expression patterns from twenty selected genes sorted out by Molyneaux et al (2009) as CPN-specific, expressed during early postnatal stages. Blue colour codes for intense expression, while oblique gray stripes code for sparse expression. a) Genes expressed in all layers or mostly in deep layers. B) Genes expressed only in upper layers and c) genes whose expression pattern divides superficial and deep layers 2/3 (II/III). Abbreviation: SP, subplate. Adapted from (Fame et al., 2011).

1.2 PlexinD1, a possible determinant of CPN heterogeneity

The goal of the present work is to study the development of long-range heterotopic projections, which are known to be sent by neurons residing mainly in layer 5. With the view to find mechanisms regulating the formation of heterotopic callosal connections in the mouse brain, we went through the literature in search for candidate genes, which could regulate aspects of CPN development. Among the CPN-specific genes sorted out by Molyneaux et al (2009), PlexinD1 an axon guidance receptor and Gfra2 a growth factor receptor presented interesting expression profiles, as they were both expressed in layer 5A, in which we find heterotopically projecting CPN in both motor and somatosensory cortex (Mitchell and Macklis, 2005; Sohur et al., 2014). It was proposed by this study that PlexinD1 and Gfra2 could be markers for CCStrPN. Retrograde tracing from the contralateral cortex and the spinal cord followed by ISH for *Plxnd1*, verified that it is expressed by CPNs and not by SCPNs, but whether CPNs with collaterals to the contralateral Striatum also express *Plxnd1* was not addressed in this study. During my thesis, I asked whether PlexinD1 is a marker of long range heterotopically projecting CPNs and what aspect of the development of these CPNs it could regulate. PlexinD1 was previously shown to be transiently expressed in the cortical plate from E13-E15, when it was downregulated, only to re-appear again in the cortical plate at E17.5, where its expression increases by P3 and is maintained until adult stages (Chauvet et al., 2007; Deck et al., 2013; Molyneaux et al., 2009; Watakabe et al., 2006). This expression timing leads to hypothesize that it could regulate late aspects of CPN development, such as final target innervation and branching, synaptogenesis and dendritic refinement. PlexinD1 has been implicated in various processes in the development of the nervous system, such as axon guidance, synaptogenesis but also cell migration. The next chapters review these functions.

1.2.1 Axon guidance

PlexinD1 is a transmembrane protein which belongs to a group of receptors for guidance molecules of the Semaphorin family (Yoshida, 2012) and it mediates the signalling of secreted class 3 Semaphorins, as well as for the transmembrane class 4 Semaphorine Sama4A. Most class 3 semaphorins do not bind directly their Plexin receptors, but instead they interact with Neuropilins (Npn1-2) to associate with Plexins A1-A4 or PlexinD1. PlexinD1 associated or not with Npn, was shown to bind in vitro Sema3C and Sema3A, while it can also bind directly

Sema4A (Gitler et al., 2004; Toyofuku et al., 2007). However, the main ligand of PlexinD1 in axon guidance is Sema3E, the only one among class 3 semaphorins that can bind directly PlexinD1. Sema3E has a bi-functional activity in axon guidance, as it may act either as a repulsive or attractive signal, depending on the composition of its receptor complex.

When PlexinD1 acts both as a receptor and as a signal transduction unit, Sema3E signalling pathway leads to repulsion. Repulsive Sema3E/PlexinD1 signalling requires the endocytosis of the receptor and its correct transport to recycling endosomes. Direct binding of Sema3E to PlexinD1 promotes endocytosis of the receptor and at the same time increases interaction of the intracellular domain of PlexinD1 with an adaptor protein, GIPC. This protein targets PlexinD1 from early Rab5-positive endosomes to recycling Rab4 and Rab11-positive endosomes, where it is coming in contact with active R-Ras and subsequently de-activates it through its intrinsic GAP activity. R-Ras inactivation leads to inactivation of the PI3K/Akt pathway. This cascade leads to the collapse of growth cones and repulsive axon guidance. Absence of GIPC causes mis-targeting of PlexinD1 into degrading Rab7-positive endosomes and prevents Sema3E-dependent growth cone collapse in vitro (Burk et al., 2017) (Figure 1.13).
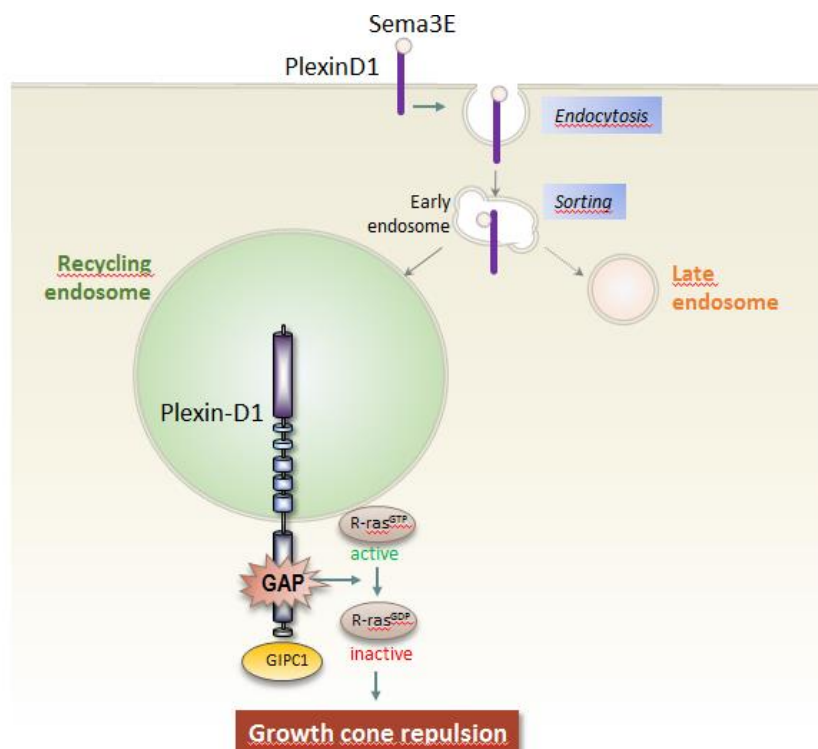
Figure 1.13 Repulsive Sema3E/PlexinD1 signalling

Repulsive Sema3E signalling is important for the development of many axon tracts in the brain, such as the anterior commissure (Burk et al., 2017), the striatonigral projections (Burk et al., 2017), the cortico-thalamic projections (Deck et al., 2013), the hippocampal projections (Mata et al., 2018), and proprioceptive projections (Fukuhara et al., 2013; Pecho-Vrieseling et al., 2009).

When PlexinD1 serves only as a ligand-binding subunit and interacts with other molecules for signal transduction, binding of Sema3E to PlexinD1 leads to attraction of growing axons. Attractive Sema3E signalling involves the co-receptors Npn1, the vascular endothelial growth factor receptor type 2 (VEGFR2) and the microtubule-associated protein 6 (MAP6), which functions as an adaptor protein, coupling VEGFR2 to activation of the downstream PI3K/Akt pathway (Figure 1.14). Attractive PlexinD1/Sema3E signalling was shown to be necessary for the formation of the subiculo-mammillary pathway (Bellon et al., 2010; Chauvet et al., 2007; Deloulme et al., 2015).
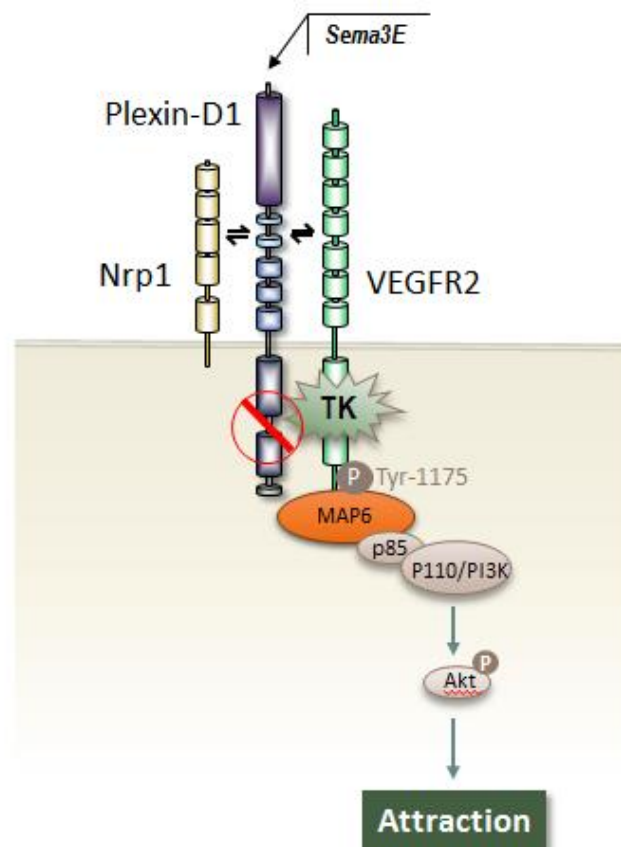
Figure 1.14 Attractive Sema3E/PlexinD1 signalling

PlexinD1 expression in CPNs suggests a potential function in the formation of callosal projections, which has not been yet investigated. The expression in the cortical plate peaks at a late stage (P3) in the development of the CC, so PlexinD1 may be implicated in the late aspects of the callosal projection development, which may involve target selection, invasion and branching. Expression in layer 5 suggests it might be expressed by heterotopically projecting callosal neurons and might contribute to the formation of heterotopic projections.

1.2.2 Synapse formation

PlexinD1/Sema3E signalling was found to promote synapse formation on direct pathway medium spiny neurons (MSNs) in the Striatum (Ding et al., 2012). PlexinD1 is highly expressed in the Striatum at early postnatal stages, from P0-P8 and is down-regulated from P14-P25. Ablation of PlexinD1 in direct pathway MSNs resulted in decrease in spine density on these neurons and a slight increase in dendrite complexity, probably counteracting for the spine loss. Absence of Sema3E resulted in the same phenotypes. Interestingly, ablation of PlexinD1 postnatally through stereotaxic injections of AAV-cre-mCherry in Plxnd1$^{f/f}$ mice, produced same phenotype as PlexinD1 cKO in early stages, indicating that PlexinD1 function might be sufficient to promote spine formation happening in postnatal stages.

PlexinD1 has also been shown to promote synaptogenesis to neocortical neurons in vitro (Wang et al., 2015). Primary cultures of neocortical neurons co-transfected with human *Plxnd1* cDNA and GFP-encoding vector before the initiation of synapse formation (5 DIV) were used for quantification of the apposition of pre- and post-synaptic markers on GFP-positive dendrites during synaptogenesis peak (14DIV) as a readout of synapses. In this system, levels of PlexinD1 expression correlated positively with spine density on the GFP-positive dendrites. In turn, absence of PlexinD1, caused by either transfection of Plxnd1 shRNA in wild type neocortical neuron cultures, or by transfection of cre-expressing vector in cultures of neocortical neurons derived from Plxnd1$^{fl/fl}$ mice, caused reduction in spine density. Furthermore, co-transfection of Plxnd1 cDNA together with cre rescued the phenotype suggesting that PlexinD1 specifically promotes synaptic formation on neocortical neurons in vitro. Further studies are necessary to determine whether PlexinD1 has a role in synapse formation of layer 5 CPNs in vivo.

1.2.3 Neuronal cell migration

Several studies have implicated Plexin in the regulation of neuronal migration, by exerting either a promoting or inhibitory effect.

PlexinD1/Sema3E signalling was shown to exert an inhibitory effect on tangential migration of Cajal-Retzius (CR) cells, through modulation of chemokine signalling (Bribián et al., 2014). CR cells are a transient neuronal population which appear in the marginal zone of the neocortex during corticogenesis and disappear during the first postnatal week. A group of CR cells are born mainly between E9.5-E12.5 in the cortical hem (CH) and migrate to occupy

the preplate and later the marginal zone of the cortex. In early corticogenesis, PlexinD1 is detected in the marginal zone of the developing neocortex and at P0 PlexinD1 expression is restricted in Calretinin and Reelin expressing CR cells. On the other hand, *Sema3e* mRNA at E12 is detected in lower layers of dorsomedial neocortical regions while its protein can also be detected in upper cortical layers.

A series of in vitro and ex vivo culture experiments revealed that Sema3E reduces the motility of CH-derived CR cells, but not their attraction to meningeal cells, which happens in control conditions. PlexinD1 is necessary for the Sema3E activity in CR migration, as in its absence, treatment of CH explants with Sema3E failed to decrease the number of migrating cells. The meninge-mediated chemoattraction on the other hand was not affected by ablation of PlexinD1, confirming that PlexinD1/Sema3E signalling does not act on chemoattraction. Meninges have been shown to attract CH-derived CR cells and to keep them in the marginal zone, by secreting the CXCL12 chemokine, which acts via the receptor CXCR4. CXCL12 was also shown to promote motility of these neurons, apart from its chemoattractive action. Inhibition of CR cell migration by Sema3E/PlexinD1 was shown to be mediated by modulation of CXCL12/CXCR4 downstream signalling. Indeed, Sema3E treatment of PlexinD1/CXCR4 co-transfected cells resulted in delayed CXCR12 mediated activation of ERK1/2 and increase in cofilin activation, actions requiring the PlexinD1 intracellular GTPase-activating protein (GAP) domain. This modulation of CXCL12/CXCR4 downstream pathway is important for CR migration in vivo. Indeed, in Plxnd1$^{-/-}$ mice, Reelin expressing CR cells over-migrate and manage to reach dorsolateral areas of the neocortex, while in the controls they are restricted to the medial cortex.

PlexinD1/Sema3E signalling in migrating neurons was shown to promote migration in granule cells (GCs) and periglomerular cells (PGCs) in the olfactory bulb (OB) (Sawada et al., 2018). OB interneurons are born postnatally in the VZ-SVZ of the lateral ventricles and after tangential migration through the rostral migratory stream they switch their migration mode to radial inside the OB. This process allows granule cells (GCs) to be finally located in the deep granule cell layer (GCL), whereas periglomerular cells (PGCs) are in the more superficial glomerular layer (GL). Filopodium-like lateral protrusion (FLP) is a specialised protrusion and is necessary for termination of the radial migration of interneurons in the correct OB layer. It is formed in the proximal part of the leading process and its appearance is correlated with resting and not migratory phase in vitro and is present in cells which reach their final destination and stop migrating in *ex vivo* cultured slices. PlexinD1 inhibits the extension of FLPs and PlexinD1

downregulation is necessary to permit the formation of FLP. Indeed, live imaging showed that FLP appearance was preceded by local PlexinD1 downregulation in the proximal leading process, and PlexinD1 overexpression lead to a decrease of FLPs. On the other hand, overexpression of Sema3E suppresses the appearance of FLP and this effect is mediated by R-Ras inhibition, as overexpression of an R-Ras form resistant to PlexinD1-mediated inactivation, abolished Sema3E-mediated inhibition of FLP.

Several Plexins, including PlexinD1, have been shown to regulate migration of cortical neurons. Radially migrating neurons first leave the VZ/SVZ and spend up to one day inside the intermediate zone (IZ) throughout which they display a multipolar morphology. In the moment of their passage from the IZ to the developing cortical plate, migrating neurons undergo a switch from the multipolar to a bipolar morphology. In the bipolar form, they migrate following the radial glial fibers using a fast-migratory type of movement which is called locomotion, and comprises three repetitive steps: extension of a leading process, nucleus translocation and withdrawal of the rear trailing process. Finally, neurons reaching the pial surface terminate the locomotion, detach from the RG fiber and undergo a terminal translocation and differentiation. (Azzarelli et al., 2015; Nadarajah and Parnavelas, 2002; Ohtaka-Maruyama and Okado, 2015)

PlexinD1 has been shown to promote radial migration of cortical neurons in the rat brain, probably by contributing to Npn1-dependent chemoattractive signalling of Sema3A (Chen et al., 2008b). Removal of Npn1 impedes radial migration of layer 2/3 cortical pyramidal neurons and it causes a mis-alignment of leading process of migrating neurons with the adjacent RG processes, indicating that Npn1 is necessary for the direction of these neurons towards the pia. Sema3A, a Npn1 ligand, is expressed by neurons in the upper cortical layers from E14 until early postnatal stages. Disruption of Sema3A gradient by external addition of Sema3A in cultured cortical slices hindered cell migration and caused misorientation of the leading process, suggesting that Sema3A signalling regulates the direction of radial migration of cortical neurons. Secretion of Sema3A from these cells creates a gradient of Sema3A protein in the cortex, which rises progressively from the deeper to the upper cortical layers, as shown through immunohistochemistry and Western Blot for Sema3A. In vitro experiments revealed that Sema3A is an attractant of migrating cortical neurons. Npn1 knockdown in dissociated neurons derived from the IZ abolished Sema3A-mediated attraction in vitro, suggesting that Npn1 is required to mediate Sema3A attractive signalling in migrating cortical neurons. PlexinD1 knockdown resulted in accumulation of neurons in lower CP layers, suggesting that it may promote cell migration by contributing to the attractive Sema3A/Npn1 signalling.

Plexins have been implicated also in radial migration of cortical pyramidal neurons through interaction with Rnd proteins, members of the Rho GTPase family. The small GTP-binding protein Rnd2 is expressed in newly born cortical neurons in the SVZ and IZ of the cortex during migration (Heng et al., 2008; Nakamura et al., 2005) whereas Rnd3 is expressed in the VZ and the CP (Pacary et al., 2011). The expression of these proteins is regulated by proneural factors. For instance, Rnd2 expression is induced by the proneural protein Neurogenin2. Rnd2 acts downstream of Neurogenin2, mediating its migration promoting effect (Heng et al., 2008). Ascl1, another proneural factor, promotes radial migration through Rnd3. Rnd3 and in part Rnd2 promote migration by inhibiting RhoA signalling. However, the two Rho-GTPases are localised in different subcellular compartments and regulate different phases of radial migration (Pacary et al., 2011). Rnd3 regulates locomotion, while Rnd2 is important for the multipolar-to-bipolar switch.

Apart from proneural proteins, axon guidance receptors also interact with Rnd proteins to regulate directional migratory behaviours. It has been proposed that PlexinB2 promotes migration in the rat cortex by antagonising p190RhoGAP for binding to Rnd3 (Azzarelli et al., 2014). In the rat embryo, PlexinB2 is expressed inside the VZ and SVZ, presenting a similar expression pattern as Rnd3. PlexinB2 silencing results in defective radial migration in the cortex, with shRNA-electroporated neurons accumulating in the IZ and the VZ/SVZ and neurons reaching the CP exhibiting a multipolar, rather than the normal bipolar morphological type. This phenotype was also caused by Rnd3 silencing. Simultaneous silencing of PlexinB2 and Rnd3 lead again to accumulation of neurons in the IZ and VZ/SVZ, similar to the result of silencing of each gene, but the neurons that reached the CP were distributed more superficially, suggesting that the two genes might antagonise each other for locomotion. (Azzarelli et al., 2014) showed that PlexinB2 increases RhoA activity, whereas Rnd3 decreases RhoA by interacting with the RhoA GTPase-activating protein p190RhoGAP. Antagonistic co-immunoprecipitation assay revealed that PlexinB2 competes with Rnd3 for binding to p190RoGAP. On the other hand, PlexinB2-dependent R-Ras inactivation was not shown to need Rnd3 activity. This result suggested that PlexinB2 promotes migration by maintaining high levels of RhoA. This is probably mediated by PlexinB2 binding with Rho-GEFs, as the phenotype could not be rescued by the co-electroporation of a PlexinB2 form that was unable to bind Rho-GEFs. Whether PlexinD1 regulates the migration of layer 5 CPNs has not been directly addressed.

In this study, we aimed to characterise the subpopulation of CPN expressing PlexinD1 in terms of molecular identity, projections, morphology and synaptic properties. We further examined the role of PlexinD1 in the development of these neurons. We report that absence of PlexinD1 causes the appearance of heterotopically projecting neurons in layers 2/3, while in the wild type context these neurons are found in layer 5A.

2 RESULTS

2.1 PlexinD1 expression in the developing and adult brain

To study the expression of PlexinD1 in the mouse neocortex, we used bacterial artificial chromosome (BAC) transgenic mice in which expression of the enhanced green fluorescent protein (eGFP) is under control of the *Plxnd1* promoter (hereafter referred to as *Plxnd1*-eGFP mice) (Bribián et al., 2014; Burk et al., 2017). The embryonic expression pattern of PlexinD1 (E12.5-E16.5) has been described previously (Bribián et al., 2014; Deck et al., 2013). Here we focus our analysis on later developmental stages (E18.5-P15) and adulthood. We found that eGFP is expressed from E18.5 to P7 in the marginal zone (MZ) of the cortex, where hem-derived Cajal-Retzius (CR) neurons have been reported to express PlexinD1 (Bribián et al., 2014) (Fig 2.1, panels A-C). Consistent with the transient nature of CR cells, such expression has disappeared from the MZ at P15 (Fig. 2.1, panel D). Neuronal expression of eGFP is also observed from E18.5 to P7 in the deep CP. This expression follows lateral-to-medial and anterior-to-posterior gradients, which reflect the gradients of neurogenesis (Fig 2.1, panels A and B). At P15, when laminar differentiation is completed, eGFP-positive neurons are found in the upper part of layer 5 (layer 5A) across all neocortical areas, including the primary sensory (S1) and motor (M1) areas (Fig 2.1, panels D-F). In addition, eGFP-positive cells are also found in layer 4 of S1 (Fig. 2.1, panel E) and labelling in layer 2/3 was sparse (S1) or nearly absent (M1) (Fig 2.1, panels E and F). This layer-specific expression pattern is maintained in the brain of adult mice (Fig 2.1, panel G) as previously reported (Watakabe et al., 2006).
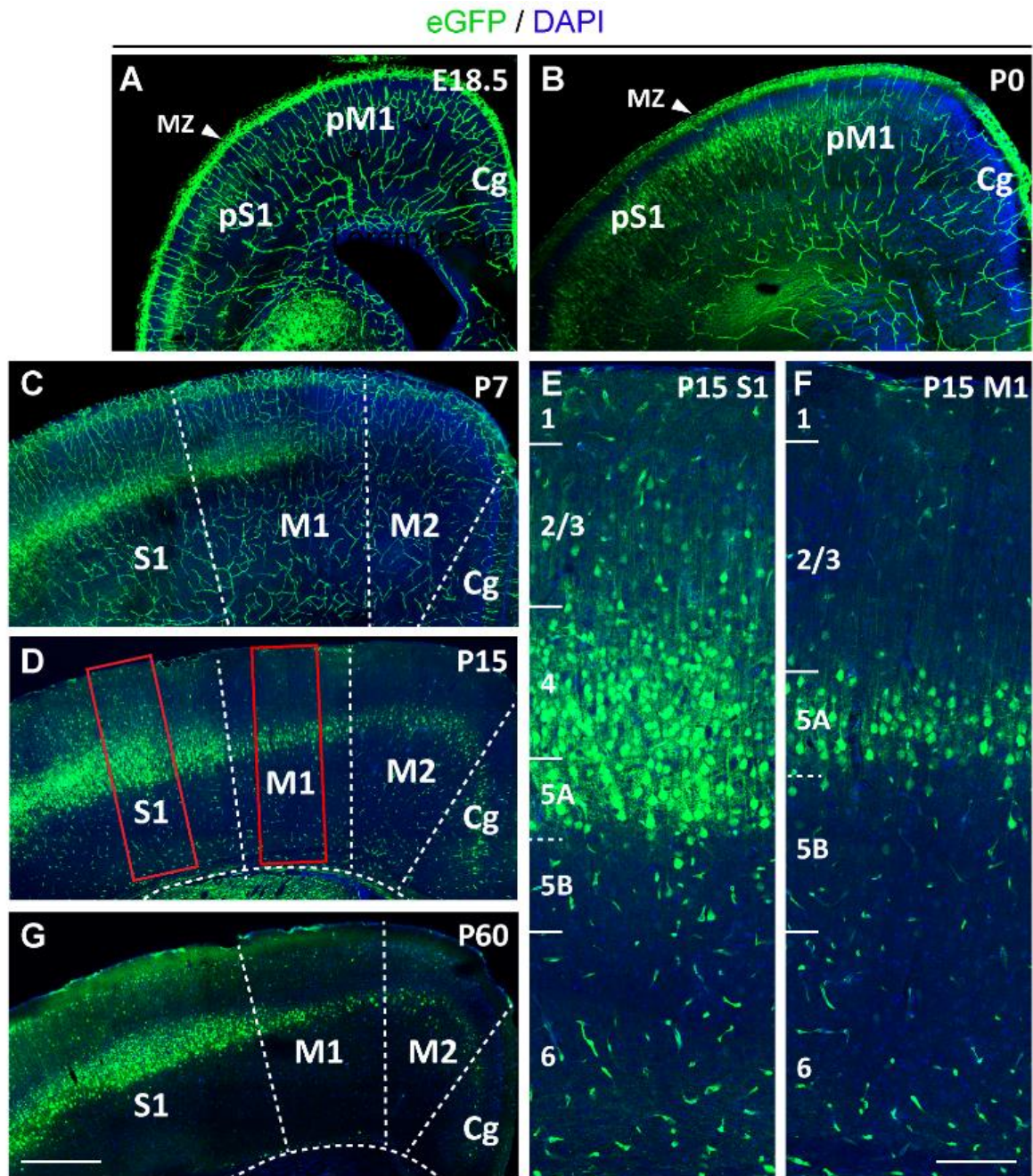
Figure 2.1 Distribution of eGFP in the Plxnd1-eGFP mouse neocortex

(A-D) Distribution of eGFP fluorescence in coronal sections of E18.5 (A), P0 (B), P7 (C) and P15 (D) Plxnd1-eGFP brains. (E-F) Enlargement of boxed areas in (D) showing the laminar distribution of eGFP⁺ neurons in somatosensory (E) and motor (F) areas at P15. Cortical layers were identified using DAPI stain. (G) Distribution of eGFP fluorescence in coronal sections of adult P60 Plxnd1-eGFP brain.

Cg: cingulate cortex, pM1: presumptive motor cortex, pS1: presumptive somatosensory cortex, M1: primary motor cortex; M2: secondary motor cortex, MZ: marginal zone, S1: primary somatosensory cortex.

Scale bars: 500 μm (A-D, G), 150 μm (E, F).

Next, we performed fluorescent in situ hybridization (FISH) of *Plxnd1* mRNA on the cortex of adult *Plxnd1*-eGFP mice. We found that the eGFP protein is expressed in 98.9% of *Plxnd1*^{+} cells in layers 5A and 4 and is absent in *Plxnd1*^{-} cells (layer 5A: n= 366 *Plxnd1*^{+}/GFP^{+} neurons, 4 *Plxnd1*^{+}/GFP^{-} neurons, 0 *Plxnd1*^{-}/GFP^{+} neurons; layer 4: n= 64 *Plxnd1*^{+}/GFP^{+} neurons, 1 *Plxnd1*^{+}/GFP^{-} neurons, 0 *Plxnd1*^{-}/GFP^{+} neurons, 2 sections, 1 mouse) (Fig 2.2). This indicates that the *Plxnd1*-eGFP mice faithfully recapitulate the endogenous expression of *Plxnd1* in these cortical layers. On the other hand, we found that eGFP does not reflect the complete expression pattern of *Plxnd1* in the upper layers 2/3, where eGFP is expressed in only 14 % of the *Plxnd1*^{+} cells (n=50 *Plxnd1*^{+}GFP^{+} neurons, 302 *Plxnd1*^{+}GFP^{-} neurons, 2 sections, 1 mouse) (Fig 2.2).
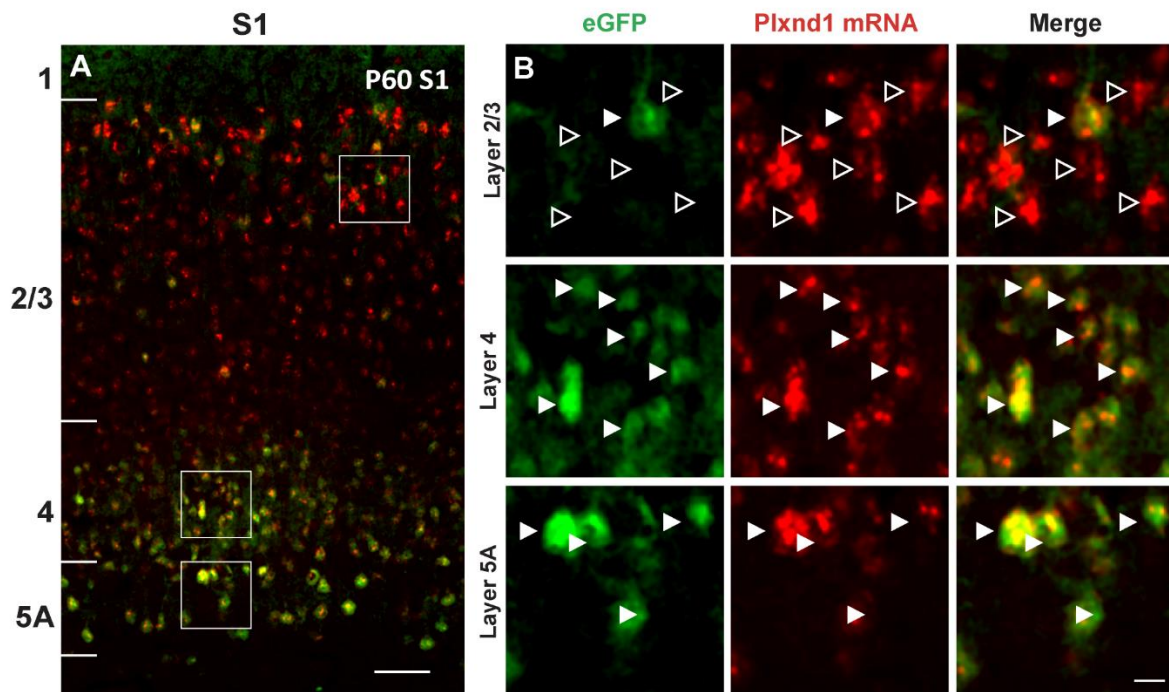
Figure 2.2 Plxnd1 mRNA expression in Plxnd1-eGFP mouse

(A) Plxnd1 mRNA expression detected by FISH in S1 area of P60 Plxnd1-eGFP brain. (B) Enlargement of the boxed areas in (A) showing co-localisation of eGFP with Plxnd1 signal.
Scale bar: 40 μm (A), 10 μm (B-D).

2.2 PlexinD1 is expressed by CPNs

PlexinD1 has been previously reported to be expressed by CPNs (Molyneaux et al., 2009). We confirmed this finding using makers for cortical projection neuron subtypes: Ctip2 defines subcortical projection neurons (Chen et al., 2008a), Satb2 defines callosal neurons

(Alcamo et al., 2008; Britanova et al., 2008; Leone et al., 2015), and Cux1 defines layer 2/3 CPNs (Rodríguez-Tornos et al., 2016). In the presumptive somatosensory cortex of *Plxnd1-*eGFP neonates, eGFP^{+} cells co-expressed the transcription factor Satb2, but not Ctip2 (Fig 2.3, panels A and B). In addition, the upper layer eGFP^{+} cells co-expressed Cux1 (Fig 2.3, panel C). The co-expression pattern of eGFP with Satb2 or Cux1 was maintained in the adult S1 cortex (Fig 2.3, panels D-F).
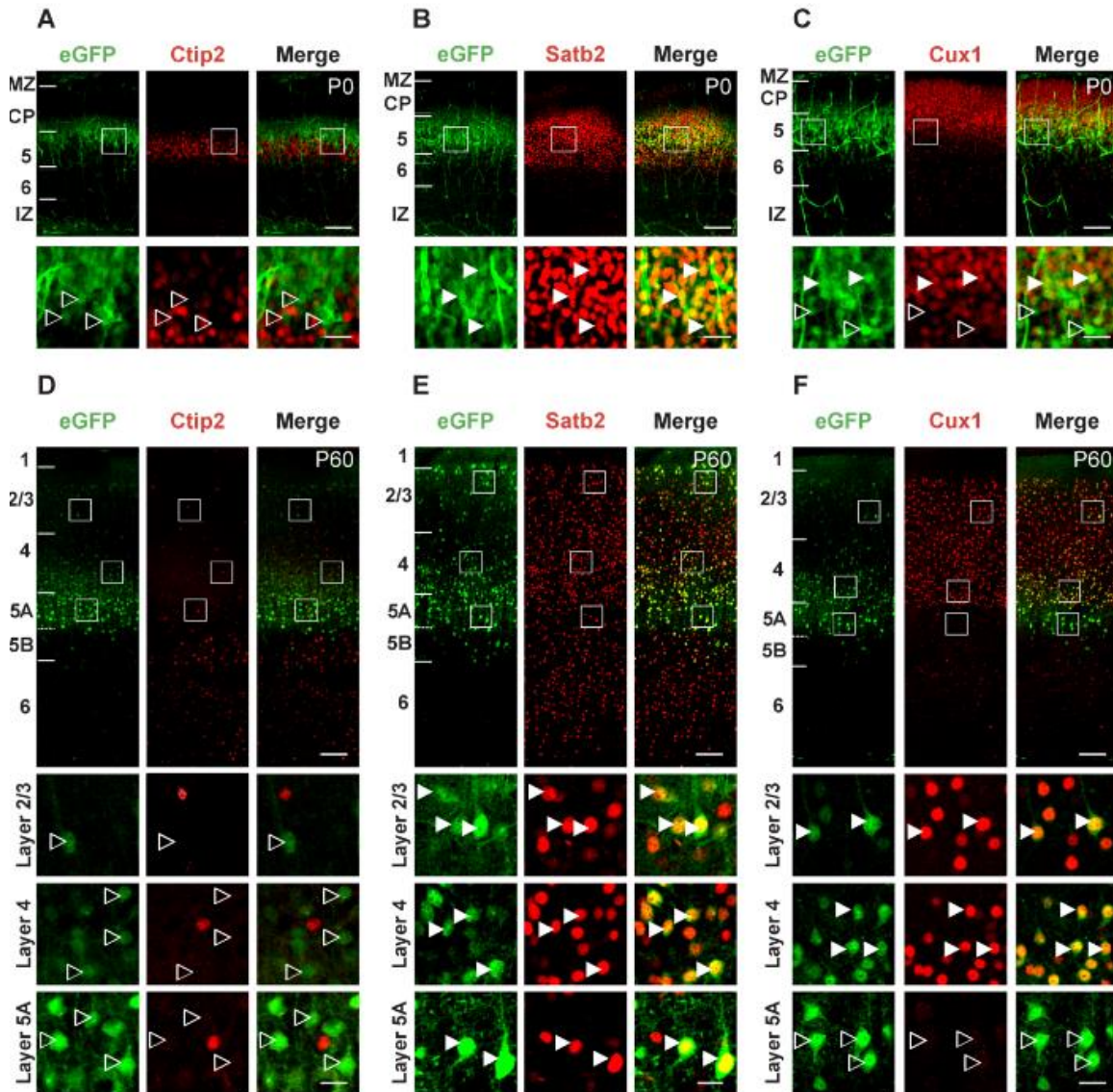
Figure 2.3 Molecular signature of eGFP+ neurons in S1

Double labelling of eGFP with Ctip2, Satb2 or Cux1 on sections through the S1 area of P0 (A-C) and P60 (D-F) Plxnd1-eGFP mice. The boxed areas are enlarged to show co-localization of eGFP with Satb2 or Cux1 (white arrow heads), but not with Ctip2 (empty arrow heads). MZ: marginal zone, CP: cortical plate, IZ: intermediate zone. Scale bars: 80 µm (A-C), 20 µm (enlarged panels in A-C), 40 µm (D-F), 10 µm (enlarged panels in D-F).

A similar co-location was observed for eGFP and Satb2 in the M1 cortex, with the few cells of layer 2/3 expressing eGFP also positive for Cux1 (Fig 2.4).
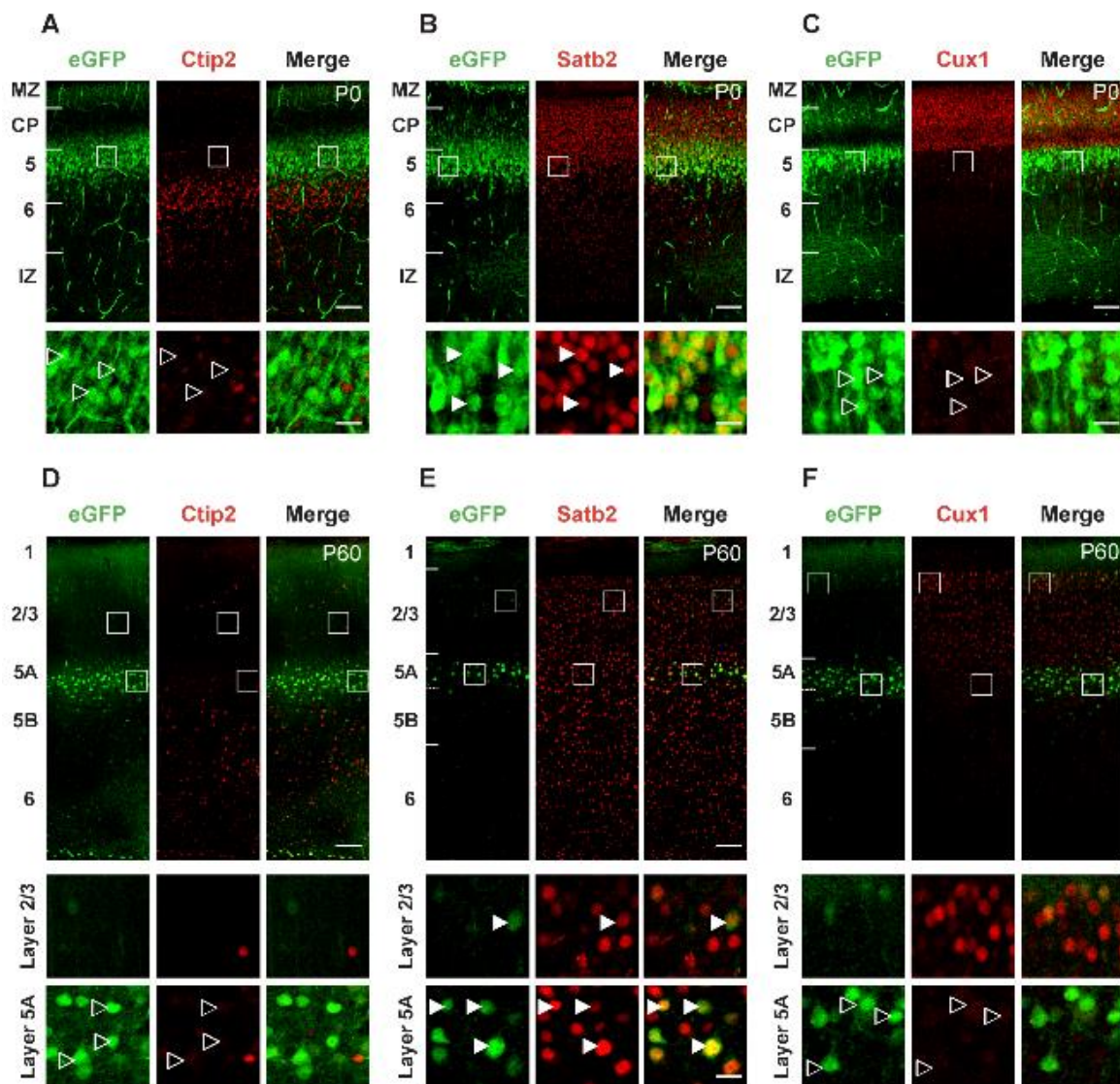
Figure 2.4 Molecular signature of eGFP+ neurons in M1

Double labelling of eGFP with Ctip2, Satb2 or Cux1 on sections through the M1 area of P0 (A-C) and P60 (D-F) Plxnd1-eGFP mice. The boxed areas are enlarged to show co-localization of eGFP with Satb2 or Cux1 (white arrow heads), but not with Ctip2 (empty arrow heads). MZ: marginal zone, CP: cortical plate, IZ: intermediate zone. Scale bars: 80 µm (A-C), 20 µm (enlarged panels in A-C), 40 µm (D-F), 10 µm (enlarged panels in D-F).

Callosal identity was further confirmed by analyzing the main output projection paths of the cortex. As expected, in P3 *Plxnd1*-eGFP brains, immunostaining for eGFP and PlexinD1 was observed in the corpus callosum, where expression is restricted to the ventral portion of the tract (Fig 2.5, panels A-C). We also found co-labelling of eGFP and PlexinD1 proteins in the internal capsule and midbrain cerebral peduncles, the pathway for SCPNs of layer 5 (Fig 2.5,

panels D-I). Indeed, retrograde labelling by injection of DiI in the cerebral peduncles back-labelled neurons in the layer 5 of the cortex. However, these neurons are located in the deepest part of the layer 5 (in layer 5B), just beneath eGFP-expressing layer 5A neurons (Fig 2.5, panels J and K). Back-labelled eGFP^{+} neurons were instead found in the striatum (Fig 2.5, panels L-O), indicating that the eGFP[+]/PlexinD1[+] fibers observed in the internal capsule and cerebral peduncles are part of the striatonigral tract (Burk et al., 2017).
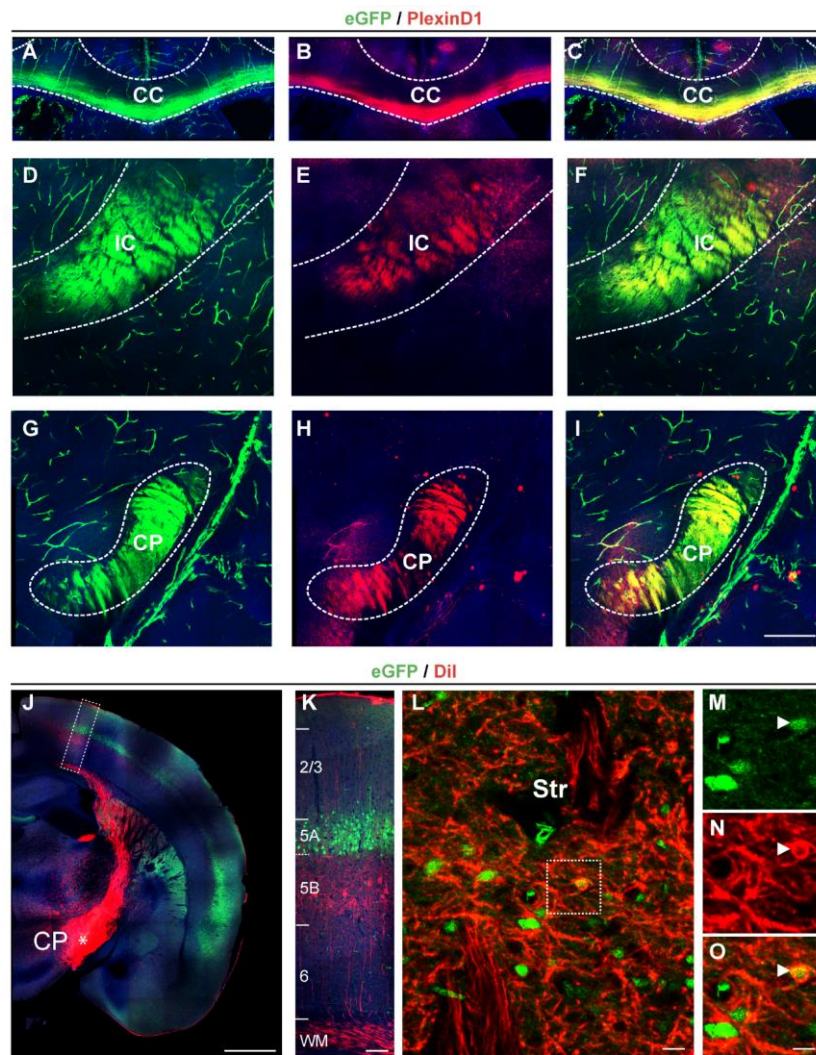
Figure 2.5 Axonal projections of eGFP+ neurons

(A-I) Double immunofluorescence staining with anti-eGFP and anti-PlexinD1 antibodies in P3 Plxnd1-eGFP brains revealed co-labelled axons in the ventral part of the corpus callosum (A-C), internal capsule (D-F) and cerebral peduncles (G-I). (J-K) Retrograde labelling of layer 5B cortical subcerebral projection neurons after DiI injection in the cerebral peduncle (*) of adult Plxnd1-eGFP mice. eGFP^{+} neurons are located more superficially in cortical layer 5A. (K) is an enlargement of the boxed area in (J) showing no overlap between DiI and eGFP staining. (L-O) Retrograde labelling of eGFP^{+} striatal neurons after DiI injection in the cerebral peduncle of adult Plxnd1-eGFP mice. (M-O) are enlargements of the boxed area in (L) showing double labelled DiI[+]/eGFP^{+} striatal neurons. CC: corpus callosum, CP: cerebral peduncle, IC: internal capsule, Str: Striatum. Scale bars: 100 μm (A-I), 500 μm (J), 100 μm (K), 20 μm (L), 10 μm (M-O).

Three-dimensional imaging of eGFP$^+$ and PlexinD1$^+$ tracts in cleared brains further confirmed expression in the corpus callosum and striatonigral tracts (Fig 2.6). Together these data indicate that PlexinD1 is specifically expressed in a subset of callosal neurons during cortical development and in the adult brain.
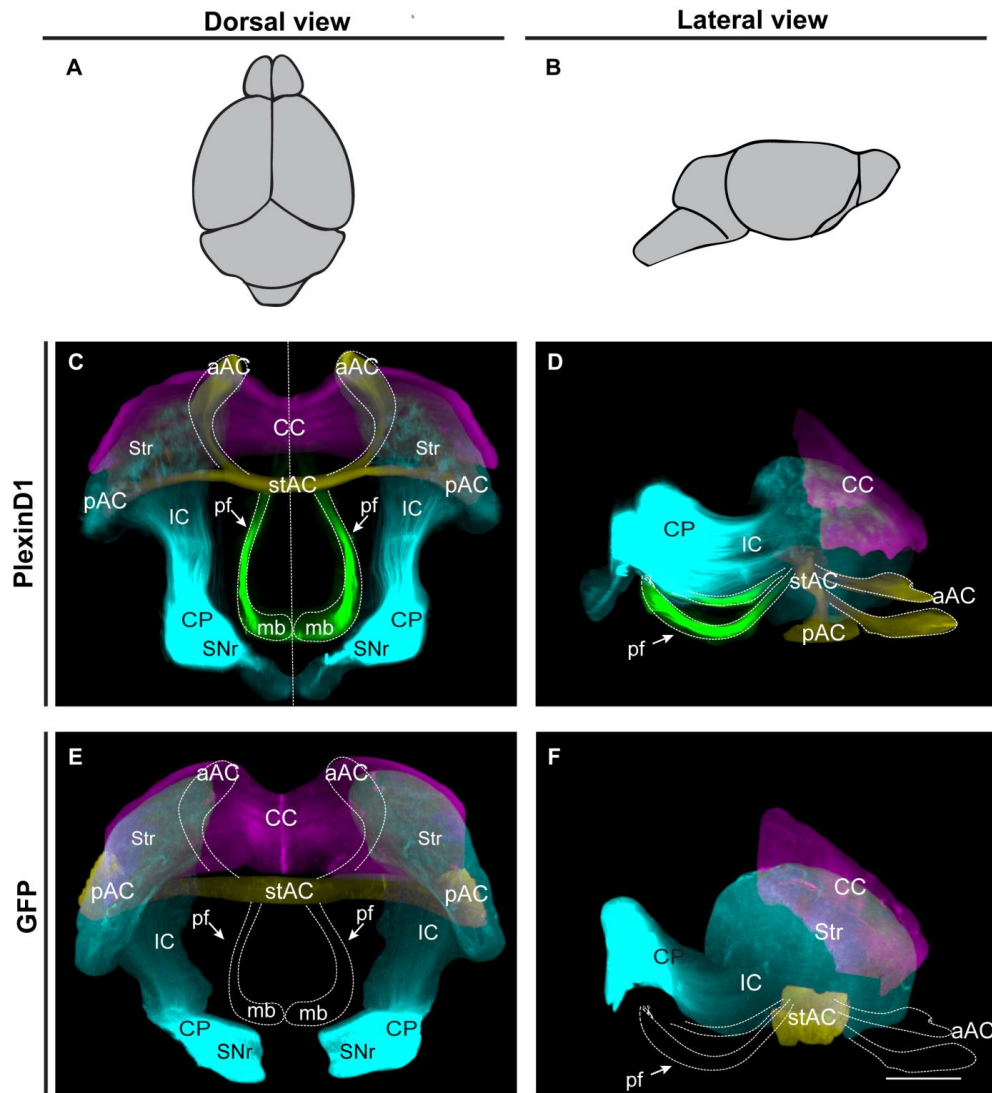
Figure 2.6 Three-dimensional imaging of PlexinD1+ and eGFP+ axon tracts

3D reconstructions of light-sheet microscopy images from cleared neonatal (P3) Plxnd1-eGFP mouse brains immunolabelled for PlexinD1 (C, D) and eGFP (E, F). (C, E) dorsal views (A) and (D, F) ventral views (B) of the immunolabelled brains. PlexinD1 labels axons in the corpus callosum (purple), striatonigral tract (blue), anterior commissure (yellow), and postcommissural fornix (green). eGFP partially recapitulates PlexinD1 expression and labels axons of the corpus callosum, striatonigral tract and posterior limb of the anterior commissure. CC: corpus callosum, , AC: anterior commissure, pf: post-commissural fornix, aAC: anterior limb of the anterior commissure, pAC: posterior limb of the anterior commissure, Str: striatum, IC: internal capsule, CP: cerebral peduncles, SNr: substantia nigra pars reticulata, mb: mammillary bodies. Scale bar: 1000 μm.

2.3   Somato-dendritic morphology of PlexinD1-expressing CPNs

Distinct somato-dendritic morphologies have been described among subclasses of layer 5 CPNs (Kim et al., 2015; Larsen et al., 2008). We therefore examined whether PlexinD1-positive and PlexinD1-negative CPNs sitting in layer 5A differ in their morphological features. CPNs were retrogradely labelled by injection of rabies virus (RV) into the contralateral M1 cortex of adult *Plxnd1*-eGFP mice. Immunofluorescence detection of the RV-infected neurons with a monoclonal antibody directed against the viral phosphoprotein 31G10 resulted in a Golgi-like staining of the entire neuron (Salin et al., 2008; Fig 2.7, panels A-G). Overall, there was no difference between soma size and shape and between number of basal dendrites of layer 5 GFP$^+$/RV$^+$ and GFP$^-$/RV$^+$ neurons (Fig 2.7, panels H-M). Since PlexinD1 expression is involved in synapse formation (Ding et al., 2012; Wang et al., 2015), we also analyzed the number and shape of dendritic spines, but no difference was found between GFP$^+$/RV$^+$ and GFP$^-$/RV$^+$ neurons (Fig 2.7, panels N-Q). Thus, the expression of PlexinD1 was not correlated with morphological differences.
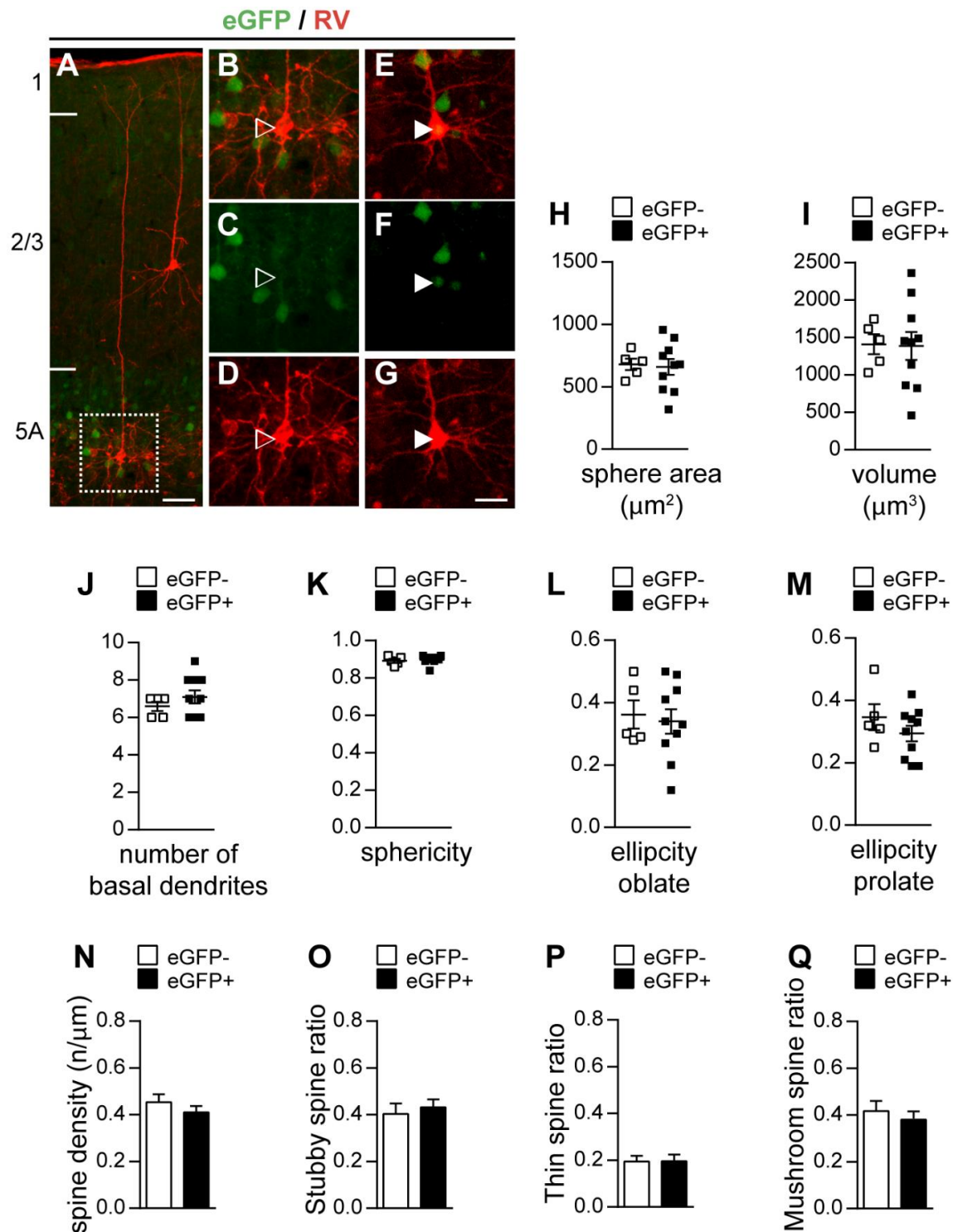
Figure 2.7 Somato-dendritic morphology of layer 5A callosal neurons

(A-G) Examples of eGFP- (A-D) and eGFP+ (E-G) RV-infected callosal neurons in layer 5A of M1 area of an adult Plxnd1-eGFP brain. (B-D) are enlargements of the boxed area in (A). (H-M) Comparisons of different morphological features between layer 5A eGFP- and eGFP+ neurons. n= 6 eGFP- neurons and n= 9 eGFP+ neurons. Data are mean +/- SEM. No statistical difference with the Mann-Whitney test. (N-Q) Comparisons of dendritic spine densities and shapes between layer 5A eGFP- and eGFP+ neurons. n= 14 eGFP- dendrites from 9 neurons and n=21 eGFP+ dendrites from 9 neurons. Data are mean +/- SEM. No statistical difference with the Mann-Whitney test. Scale bars: 40 µm (A), 10 µm (B-G).

2.4 PlexinD1 is expressed by heterotopically projecting CPNs

A large majority of CPNs interconnect symmetrical (homotopic) regions of both cortical hemispheres, but connections between non-homologous (heterotopic) regions have also been demonstrated, in most cases originating from layer 5 CPNs. Two types of long-range heterotopic callosal projections have been described in the mouse brain: a small proportion of layer 5 CPNs in the sensory-motor cortex have projection to the contralateral PMC (Mitchell and Macklis, 2005) and some layer 5 CPNs in motor and premotor cortices project to contralateral cortex and striatum (Sohur et al., 2014). The expression of PlexinD1 in layer 5A CPNs has suggested that they might represent heterotopically projecting neurons (Molyneaux et al., 2009).

To address this idea, we used a double retrograde labelling technique in adult *Plxnd1-eGFP* mice. In the first setting, we injected Alexa Fluor 647-conjugated Cholera Toxin B subunit (CTB-647) in the S1 cortex and Alexa Fluor 555-conjugated Cholera Toxin B subunit (CTB-555) in the PMC of the same hemisphere. This allowed us to back label simultaneously CPNs with homotopic (S1>S1) and heterotopic (S1>PMC) projections residing in the contralateral S1 cortex (Fig. 2.8, panel A). Consistent with the known distribution of CPNs, homotopically projecting callosal neurons (CTB-647^{+}) distributed across cortical layers 2/3 and 5 (Fig. 2.8, panel B). In layer 5A, 64 % of CTB-647^{+} neurons were eGFP[+] (n=569 CTB-647^{+}/eGFP^{+} neurons, 351 CTB-647^{+}/eGFP^{-} neurons, 12 sections, 2 mice; Fig 2.8, panel C). In contrast, heterotopically projecting neurons (CTB-555^{+}) were largely restricted to layer 5A and most of them were eGFP[+] (76%, n= 142 CTB-655^{+}/eGFP^{+} neurons, 42 CTB-555^{+}/eGFP^{-} neurons, 12 sections, 2 mice; Fig 2.8, panels D and E). These results suggest that layer 5A eGFP^{+} neurons might represent callosal neurons that send long-range dual projections to the homotopic region of the contralateral cortex and rostrally to the contralateral premotor cortex. Consistent with this idea, we found that the large majority of neurons double labelled for CTB-647 and CTB-555 were indeed eGFP^{+} neurons (96 %, n= 23 CTB-647^{+}/CTB-655^{+}/eGFP^{+} neurons, 2 CTB-64^{+}/CTB-555^{+}/eGFP^{-} neurons, 12 sections, 2 mice; Fig 2.8, panels F and G). Together, these data indicate that PlexinD1 is expressed by a large proportion of layer 5A CPNs that send long-range projections to heterotopic targets and/or dual projections to homotopic as well as heterotopic areas in the contralateral cortex.
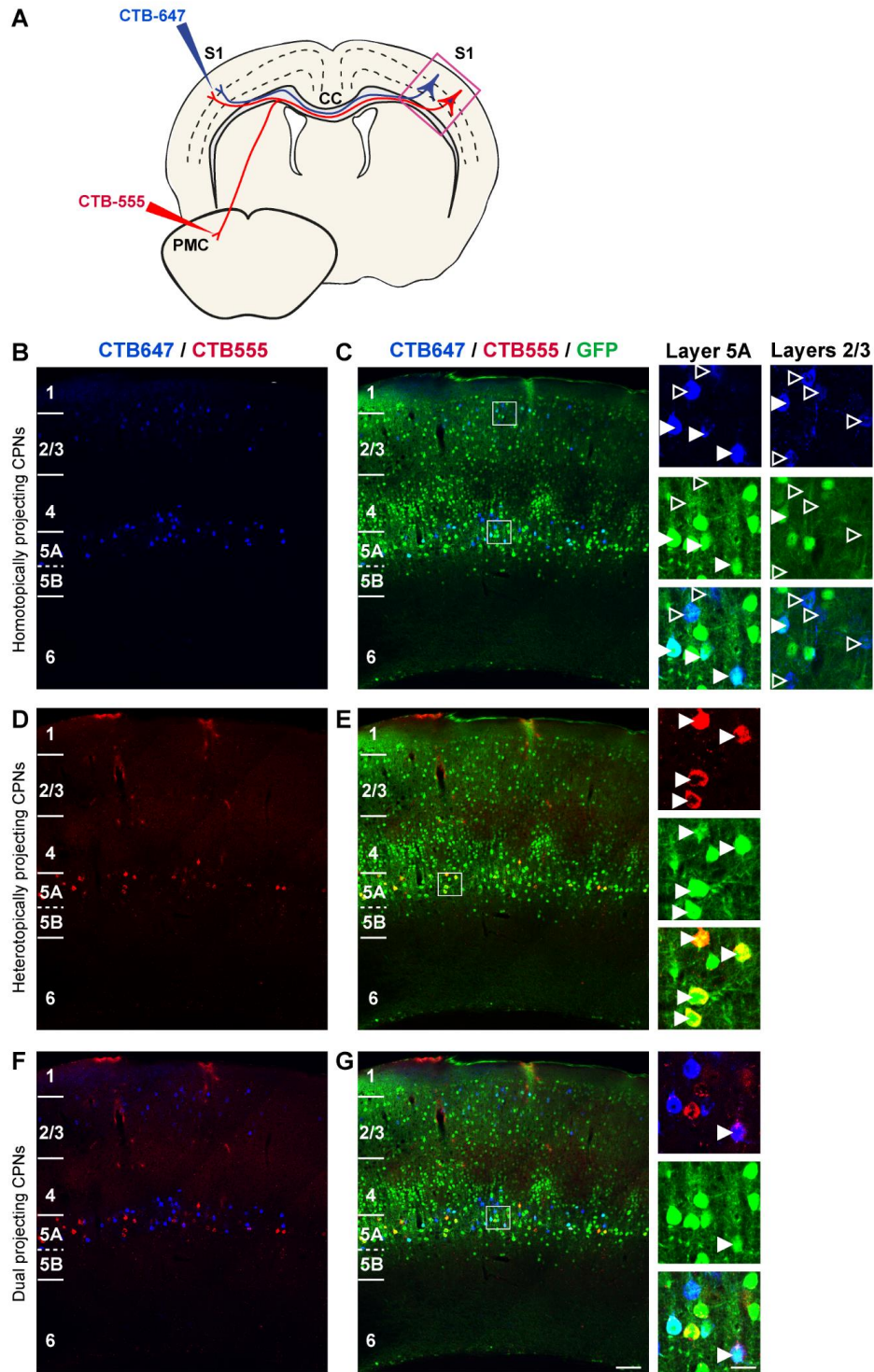
Figure 2.8 eGFP+ CPNs in S1 area send heterotopic projections to the contralateral PMC

(A) Schematic representation of dual retrograde labeling of homotopic (S1>S1) and heterotopic (S1>PMC) transcallosal projections with two CTB-conjugated fluorophores (CTB-647 and CTB-555) in the brain of adult Plxnd1-eGFP mice. (B-G) Visualization of eGFP⁺ CPNs in S1 cortex with retrograde labelling from contralateral S1 (CTB-647⁺) (B-C), from contralateral PMC (CTB-555⁺) (D-E) or from both regions (CTB-647⁺/CTB-555⁺) (F-G). The boxed areas are enlarged to show co-localization of CTB-conjugated fluorophores with eGFP (white arrow head) or absence of co-localisation (empty arrow head). Scale bars: 40 μm (B-G), 10 μm (enlarged panels).

In a second setting, CTB-647 and CTB-555 were injected in the M1 cortex and in the dorsolateral sector of the striatum, respectively. The distribution of homotopically (M1>M1) and heterotopically (M1>Str) projecting neurons was assessed in the contralateral M1 cortex (Fig. 2.9, panel A). Similar to results in the somatosensory cortex, homotopically projecting neurons were distributed in cortical layers 2/3 to 5, whereas heterotopically projecting neurons were principally located in layer 5A. Within layer 5A, 59 % of (homotopic) CTB-647$^+$ (n= 277 CTB-647$^+$/eGFP$^+$ neurons, 221 CTB-647$^+$/eGFP$^-$ neurons, 22 sections, 3 mice) and 57 % of (heterotopic) CTB-555$^+$ (n= 351 CTB-655$^+$/eGFP$^+$ neurons, 211 CTB-555$^+$/eGFP$^-$ neurons, 22 sections, 3 mice) neurons were eGFP$^+$ (Fig 2.9, panels B-E). In addition, eGFP$^+$ cells in layer 5A represent 69 % of double CTB-647/CTB-555 labelled neurons (n= 16 CTB-647$^+$/CTB-655$^+$/eGFP$^+$ neurons, 10 CTB-647$^+$/CTB-555$^+$/eGFP$^-$ neurons, 22 sections, 3 mice; Figs 2.9, panels F and G). These data indicate that PlexinD1 is expressed by CPN subpolulations that send transcallosal projections to the contralateral striatum and/or dual projections to contralateral cortex and striatum.
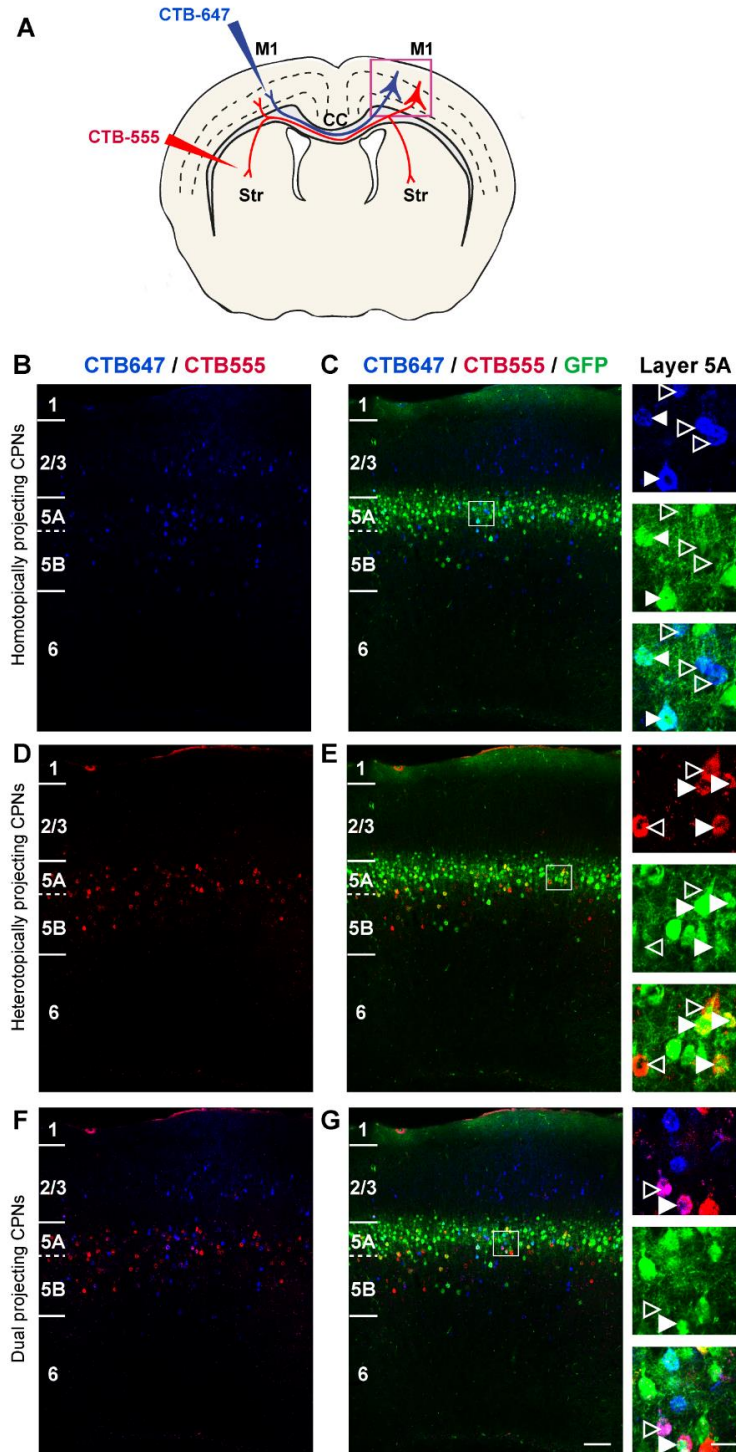
Figure 2.9 eGFP+ CPNs in M1 area send heterotopic projections to the contralateral striatum

(A) Schematic representation of dual retrograde labeling of homotopic (M1>M1) and heterotopic (M1>Str) transcallosal projections with two injections of CTB-conjugated fluorophores (CTB-647 and CTB-555) in the brain of adult Plxnd1-eGFP mice. (B-G) Visualization of eGFP⁺ CPNs in M1 cortex with retrograde labelling from contralateral M1 (CTB-647⁺) (B-C), from contralateral striatum (CTB-555⁺) (D-E) or from both regions (CTB-647⁺/CTB-555⁺) (F-G). The boxed areas are enlarged to show co-localization of CTB-conjugated fluorophores with eGFP (white arrow head) or absence of co-localisation (empty arrow head). Scale bars: 40 μm (B-G), 10 μm (enlarged panels).

2.5 PlexinD1 is required for laminar positioning of heterotopically projecting CPNs

PlexinD1 has been shown to exert a diverse range of physiological activities, including regulation of cell survival and migration, axon growth and guidance, and synapse formation (Oh and Gu, 2013). To evaluate the role of PlexinD1 in CPNs, we used conditional knockout mice that lack PlexinD1 in cortical glutamatergic neurons ($Plxnd1^{lox/-}$; $Emx1^{cre}$ mice). Expression patterns of the cortical layer markers $Cux1$ (layers 2-4) and $Er81$ (layer 5) were undistinguishable from control mice (Fig 2.10), suggesting normal cortical lamination in $Plxnd1$ conditional mutants.
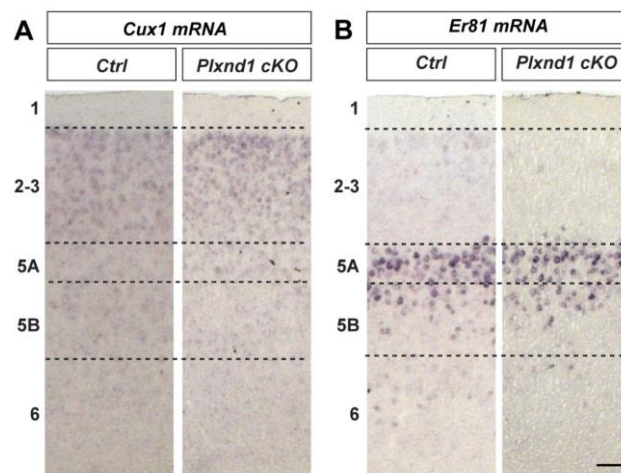
Figure 2.10 Laminar organization of the cortex of Plxnd1 mutant mice

ISH for the laminar markers Cux1 (A) and Er81 (B) in the motor cortex of adult Plxnd1$^{lox/-}$; Emx1^{cre} mutants was indistinguishable from control mice. Scale bar: 40 μm

Homotopically and heterotopically projecting CPNs in M1 were labelled selectively by contralateral injections of CTB-647 and CTB-555 in the motor cortex and dorsolateral striatum, respectively. The distribution of (homotopic) CTB-647$^+$ cells in the contralateral M1 of $Plxnd1^{lox/-}$;$Emx1^{cre}$ mice was similar to that in controls (control wild-type and $Plxnd1^{lox/+}$; $Emx1^{cre}$ mice were pooled together as there were no differences between these two groups) (Fig 2.11, panels A-D). Numerous cells were labelled retrogradely by CTB-555 in $Plxnd1^{lox/-}$; $Emx1^{cre}$ mice, indicating that heterotopic transcallosal projections are made independently of PlexinD1 expression. However, we noticed that CTB-555$^+$ and double CTB-647$^+$/CTB-555$^+$ neurons distributed differently across cortical layers in $Plxnd1^{lox/-}$; $Emx1^{cre}$ mice, with a

significantly higher proportion of heterotopically and/or dual projecting neurons in upper layer 2/3 as compared to controls (Fig 2.11, panels B, C, E and F).
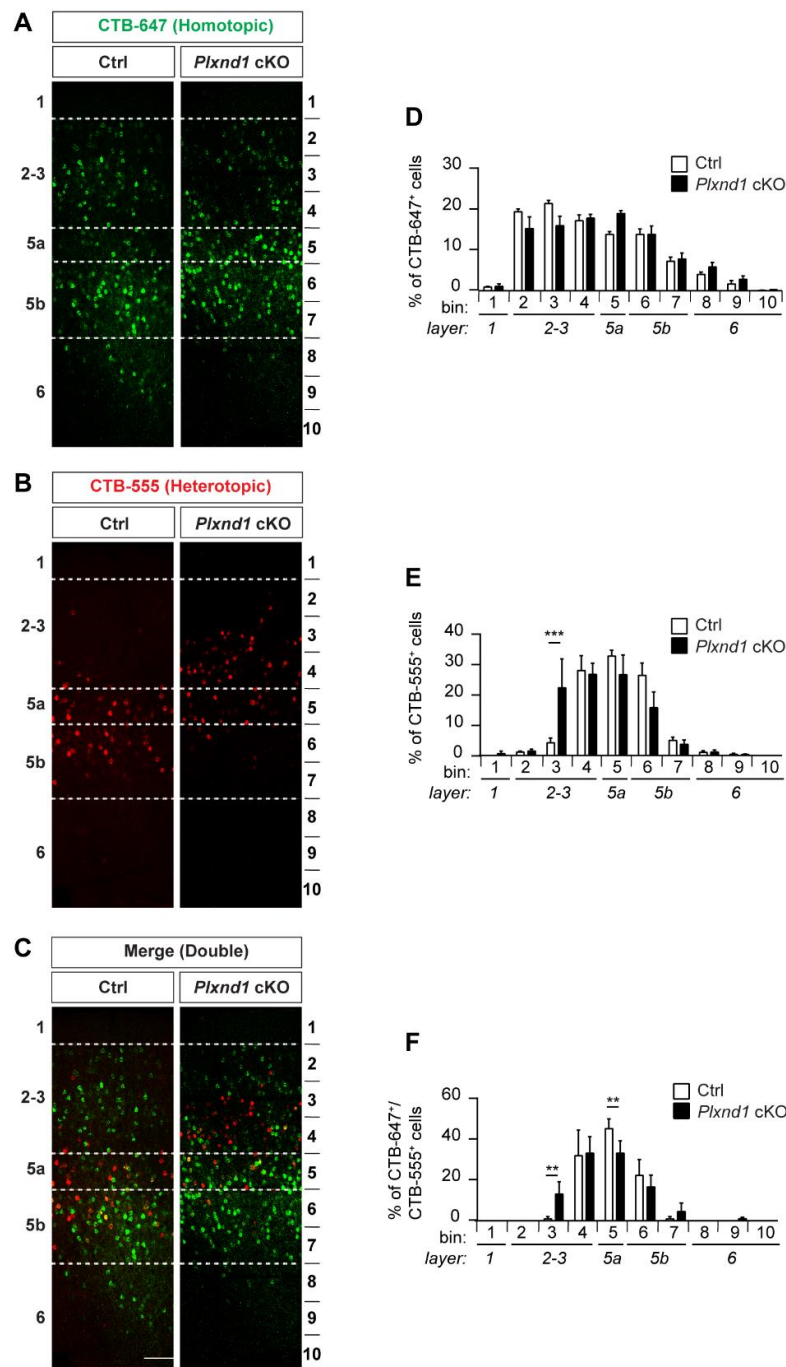
Figure 2.11 Mispositioning of heterotopically projecting CPNs in the cortex of Plxnd1 conditional mutant mice

*Adult Plxnd1$^{lox/−}$; Emx1^{cre} mice were subjected to dual injections of CTB-647 and CTB-555 in M1 and dorsolateral striatum, respectively. (A-C) Distribution of CPNs in M1 cortex with retrograde labelling from contralateral M1 (CTB-647$^+$) (A), from contralateral striatum (CTB-555$^+$) (B) or from both regions (CTB-647$^+$/CTB-555$^+$) (C). (D-F) Quantification of laminar distribution of CTB-647$^+$ (D), CTB-555$^+$ (E) and double labelled CTB-647$^+$/CTB-555$^+$ (F) neurons. Ten equal-sized bins were drawn over each image. Data represent mean +/- SEM. Control: n= 6 mice, 23 sections; Plxnd1 cKO: n=4 mice, 16 sections. **, p<0.01; ***, p<0.001 with One-way ANOVA followed by the Sidak Multiple Comparisons test. Scale bar: 100 μm*

Since Sema3E is the main ligand for PlexinD1, we investigated the distribution of homotopic and heterotopic projecting CPNs in the motor cortex of *Sema3e⁻/⁻* mice, which exhibits normal distribution of the layer specific markers *Cux1* and *Er81* (Fig 2.12, panels A and B).
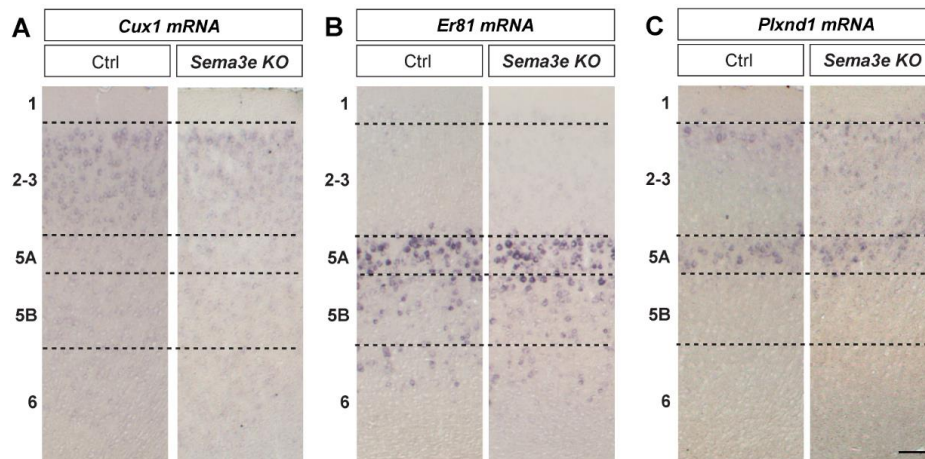
Figure 2.12 Laminar organization of the cortex of Sema3e mutant mice

ISH for the laminar markers Cux1 (A) and Er81 (B) in the motor cortex of adult Sema3e⁻/⁻ mice was indistinguishable from control mice. In contrast, Plxnd1 (C) seems to be expressed in a greater number of cells in layers 2/3 of the mutant cortex. Scale bar: 40 μm

Significant difference was observed in the distribution of heterotopically projecting CTB-555⁺ neurons, with ectopic cells in layers 2/3 (Fig. 2.13).
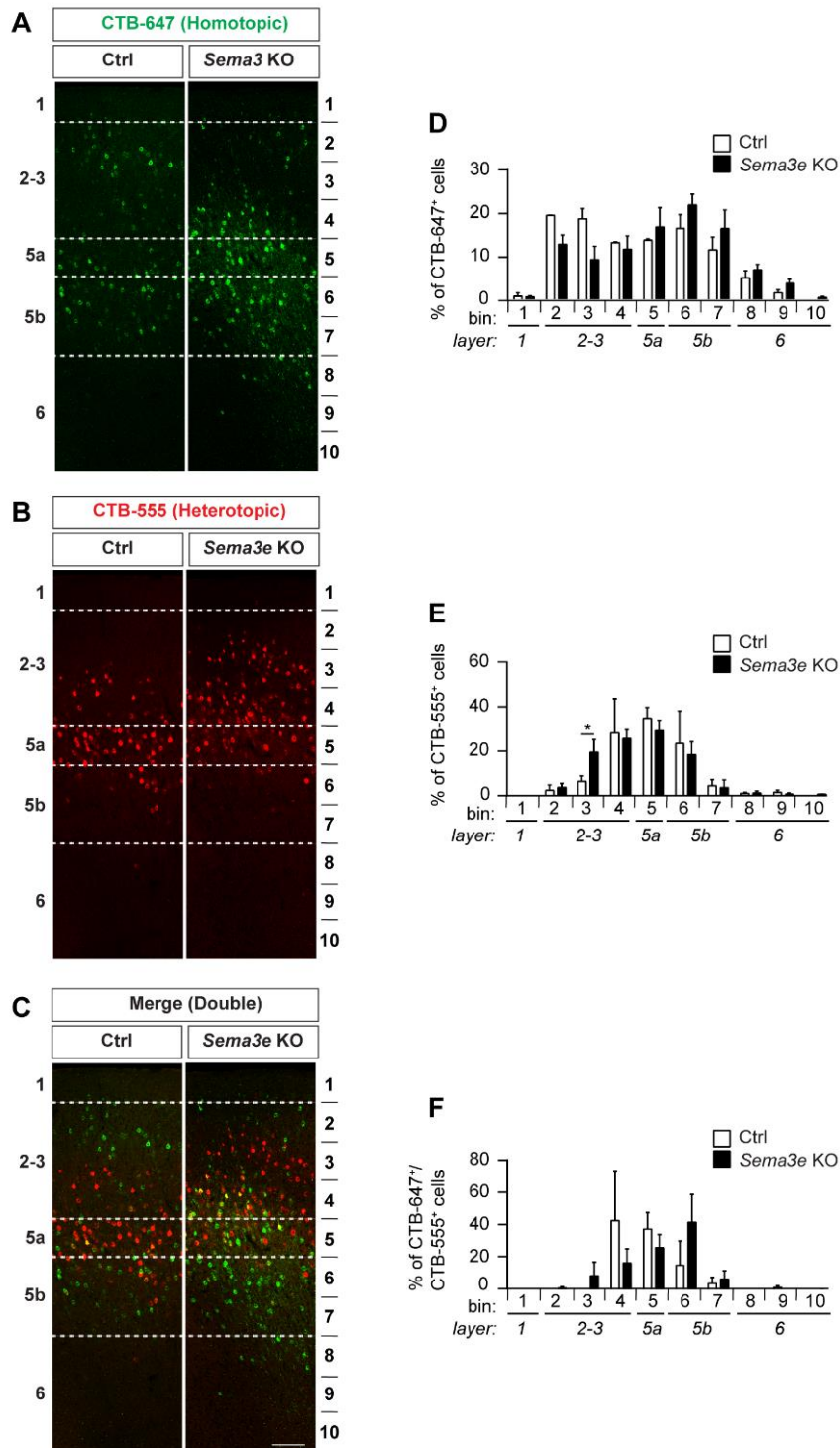
Figure 2.13 Mispositioning of heterotopically projecting CPNs in the cortex of Sema3e null mice

*Adult control and Sema3e$^{-/-}$ mice were subjected to dual injections of CTB-647 and CTB-555 in M1 and dorsolateral striatum, respectively. (A-C) Distribution of CPNs in M1 cortex with retrograde labelling from contralateral M1 (CTB-647$^+$) (A), from contralateral striatum (CTB-555$^+$) (B) or from both regions (CTB-647$^+$/CTB-555$^+$) (C). (D-F) Quantification of laminar distribution of CTB-647$^+$ (D), CTB-555$^+$ (E) and double labelled CTB-647$^+$/CTB-555$^+$ neurons. Ten equal sized bins were drawn over each image. Data represent mean +/- SEM. Control: 3 mice, 12 sections; Sema3e KO: n=3 mice, 12 sections. *, p=<0.05 with One-way ANOVA followed by the Sidak Multiple Comparisons test. Scale bars: 100 µm*

These results (summarized in Fig 2.14) suggest that PlexinD1 and Sema3E are required for the correct laminar positioning of heterotopically projecting CPNs in the neocortex.
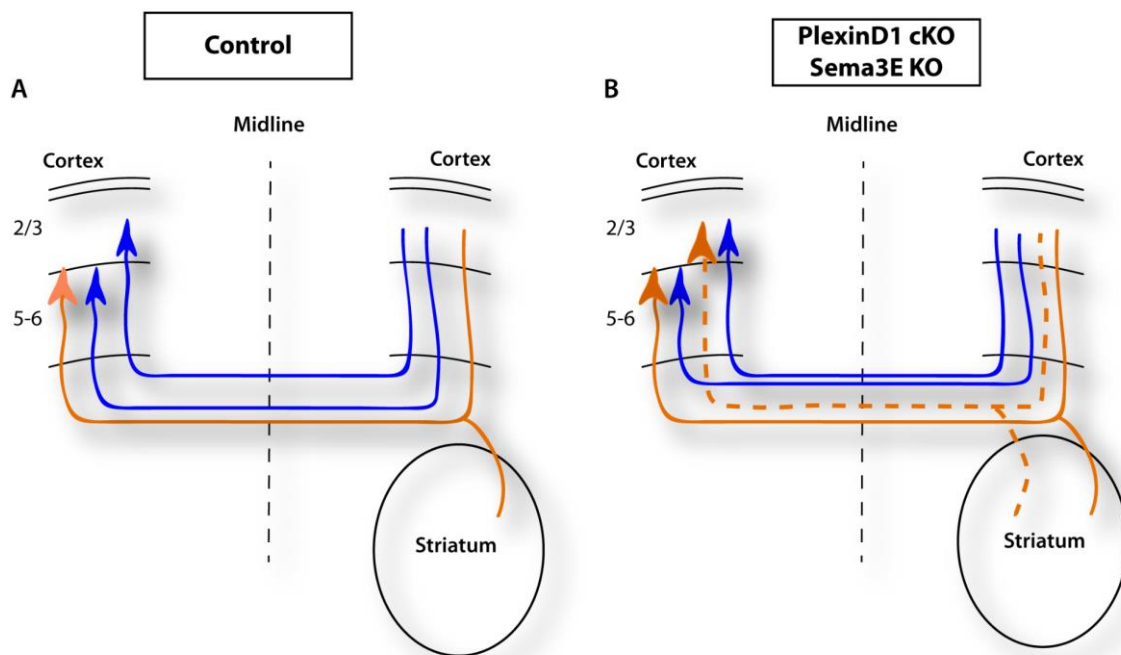
Figure 2.14 Mispositioning of heterotopically projecting CPNs in the cortex of Plxnd1 conditional knockout and Sema3e null mice

Schematic summary showing the laminar distribution of M1 CPNs projecting to the contralateral M1 cortex (homotopic) and/or to the striatum (heterotopic) in control (A), Plxnd1$^{lox/-}$; Emx1^{cre} (Plxnd1 cKO) and Sema3e KO mice (B). The distribution of homotopically projecting neurons does not differ between control and mutant mice, while some heterotopically projecting neurons are aberrantly located in superficial layers in mutant mice.

2.6   Effect of Sema3E/PlexinD1 signaling on neuronal migration during neocortical development

One interpretation of the above results is that knockdown of *Plxnd1* or *Sema3e* induces a mispositioning of layer 5A heterotopically projecting CPNs in upper cortical layers. No defects in the distribution of the layer 5 marker Er81 has been observed in the mutant cortices. However, in the rodent cortex, *Er81* is expressed in nearly all SCPNs and in only one third of the layer 5 CPNs (Yoneshima et al., 2006). Moreover, in P7 *Plxnd1*-eGFP mice,

Er81 is expressed by only 8.04 % of all layer 5A eGFP+ neurons (K. Harb, data not shown). Thus the normal distribution of Er81 does not exclude the possibility of mispositioning for some layer 5A CPNs. Consistent with this idea, ISH for *Plxnd1* in the cortex of *Sema3e^{-/-}* mice seems to reveal a higher number of labelled neurons in layers 2/3 than in controls (Fig 2.12, panel C).

We therefore tested whether Sema3E/PlexinD1 signaling regulates the migration of cortical neurons and their laminar distribution. To this aim, we first electroporated a Tomato-expressing vector into the lateral ventricle of *Sema3e^{-/-}* or control embryos at E13.5 to target layer 5 cortical neurons. At E17.5, most neurons have migrated into the CP, but in *Sema3e^{-/-}* embryos a higher proportion of neurons were found in the upper CP as compared to controls (Fig 2.15). This suggests that Sema3E restricts the radial migration of layer 5 cortical neurons.
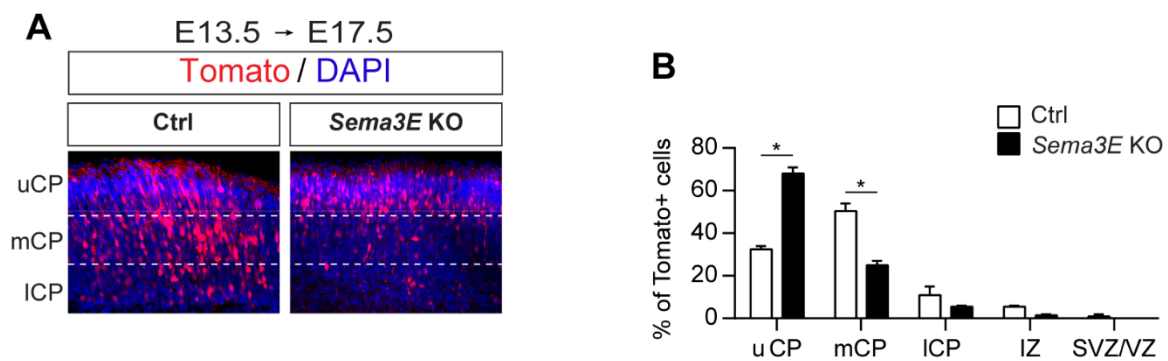
Figure 2.15 Sema3E regulates the migration of cortical neurons

(A) Control and Sema3e^{-/-} embryos were electroporated in utero at E13.5 using a Tomato-expressing plasmid and analyzed 3 days later. (B) Quantification graph showing the distribution of Tomato-positive cells in different zones of the cortex: upper, median and lower cortical plate (uCP, mCP and lCP), intermediate zone (IZ) and subventricular zone/ ventricular zone (SVZ/VZ). Data are presented as the mean ± s.e.m. Control: n= 1 embryo, 2 sections; Sema3e KO : n= 1 embryo, 2 sections., p<0.05 with One-way ANOVA followed by the Sidak Multiple Comparisons test. Scale bar, 200 μm.*

Next, we examined the role of PlexinD1 by loss and gain of function. A cre-expressing plasmid was electroporated at E13.5 in the brain of *Plxnd1*^{lox/lox} mouse embryos. The laminar position of the electroporated neurons was examined at P16. The results obtained in a single mouse suggest a possible shift in final positioning toward the upper layers and will need to be confirmed by analysis of other animals (Fig. 2.16).
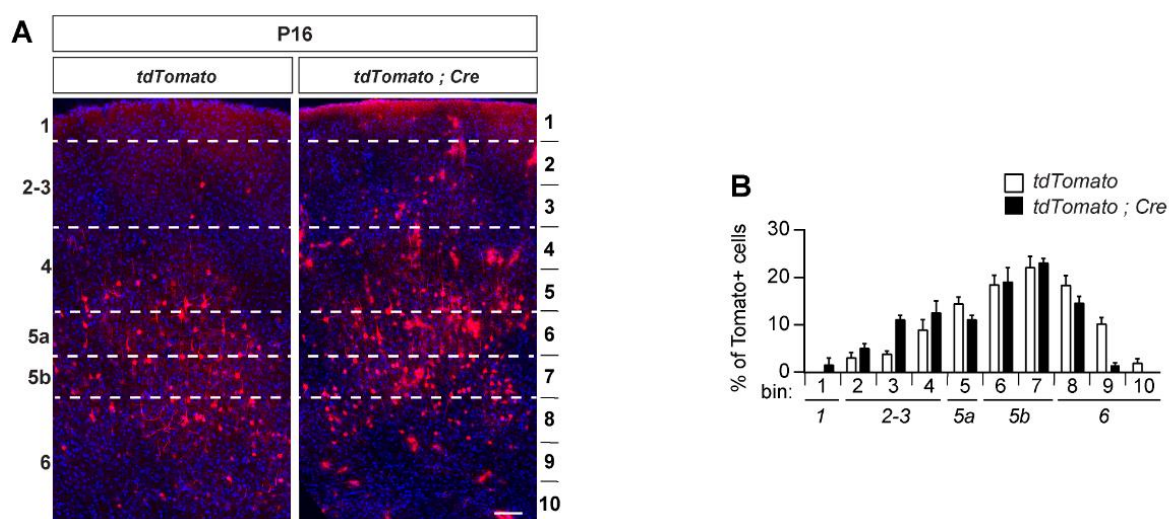
Figure 2.16 Mispositioning of neurons born at E13.5 after ablation of Plxnd1

(A) Plxnd1^{lox/lox} embryos were electroporated in utero at E13.5 using a Tomato-expressing plasmid with or without a Cre-expressing plasmid and analyzed at P16. (B) Quantification graph showing the distribution of Tomato-positive cells in the cortex. Data are presented as the mean ± s.e.m. tdTomato: n= 1 brain, 6 sections; tdTomato, Cre: n= 1 brain, 6 sections. No statistical difference was observed. Scale bar, 100 μm.

Finally, we electroporated a PlexinD1-expressing plasmid in the brain of wild-type E15.5 embryos, which results in overexpression in layer 2/3 neurons of the neocortex. The laminar position of the electroporated neurons was examined at P12-P16. Most neurons over-expressing PlexinD1 have settled into the upper layer 2/3, but we found some misplaced neurons in deeper cortical layers (Fig. 2.17).
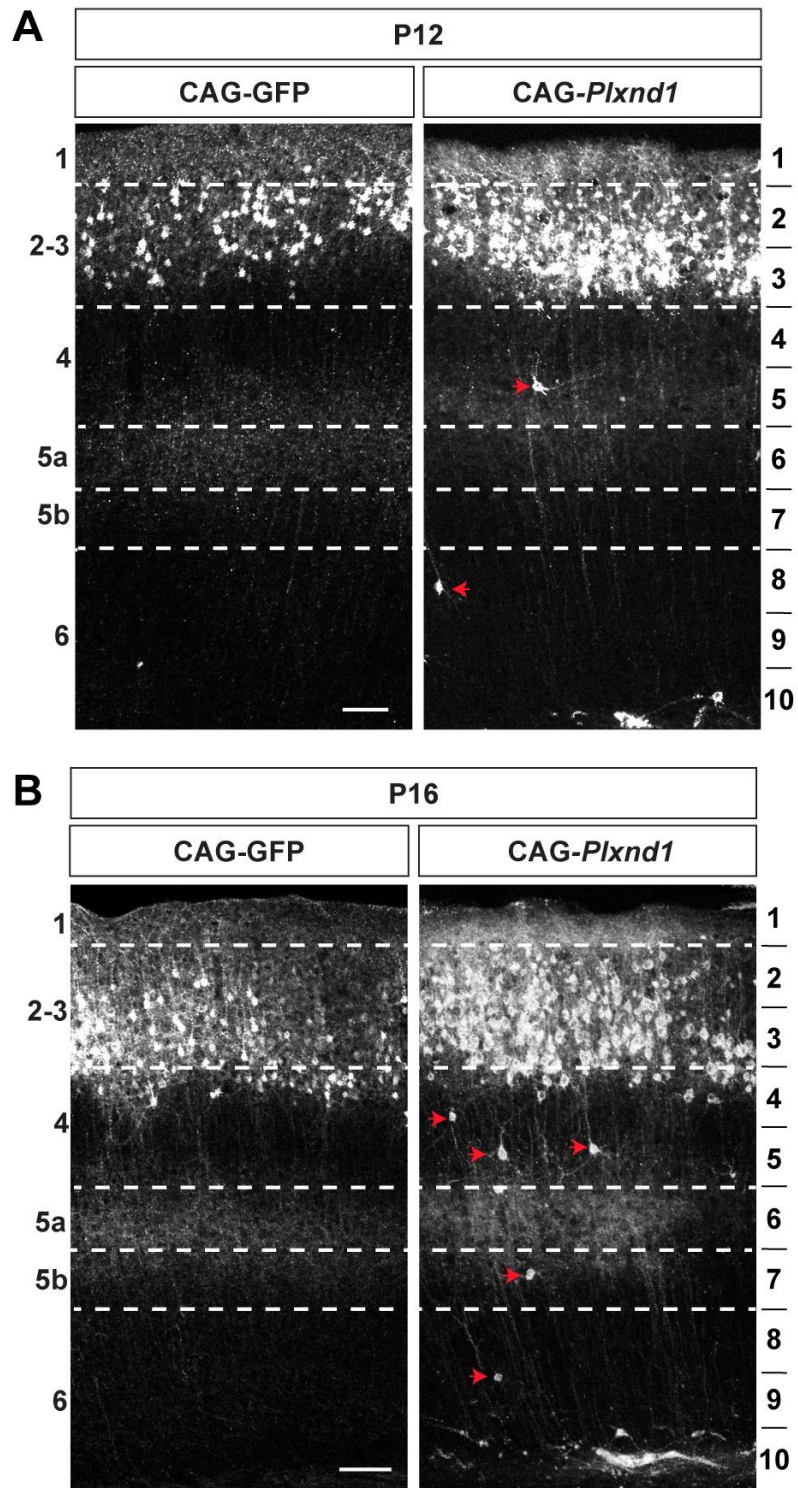
Figure 2.17 Mispositioning of neurons overexpressing PlexinD1 in the postnatal mouse brain.

(A-D) Embryos were electroporated in utero at E15.5 using a PlexinD1-expressing plasmid together with a GFP-expressing plasmid, whereas control embryos were electroporated only with a GFP-expressing plasmid. Mice were analysed at P12 and P16. (A-B) At both postnatal stages, the vast majority of neurons were positioned in upper layers 2/3 in control mice. (C-D) Red arrows show mispositioned cells in deeper layers (4, 5 and 6) in mice electroporated with the PlexinD1-expressing vector. Images acquired by Briz CG. Scale bar: 100 μm

3   MATERIALS AND METHODS

3.1   Mutant mice and genotyping

3.1.1   Mice

All animal procedures were conducted in accordance with the guidelines from the French Ministry of Agriculture (agreement number F1305521) and approved by the local ethics committee (C2EA-14 agreement 2015060510102024- V7 #1186).

Plxnd1;Emx1^{cre} and *Sema3e null* mice and were previously reported (Burk et al., 2017; Gu et al., 2005). To obtain mice with a cortex-specific deletion of *Plxnd1*, *Plxnd1$^{+/-}$;Emx1$^{cre/cre}$* males were crossed to *Plxnd1$^{lox/lox}$* (Zhang et al., 2009) females to generate *Plxnd1$^{lox/-}$;Emx1$^{cre/+}$* mutants and littermate controls (*Plxnd1$^{lox/+}$;Emx1^{cre}*). Adult heterozygous Sema3e$^{+/-}$ mice were mated to obtain Sema3e$^{-/-}$. Transgenic mice expressing eGFP under the control of the *Plxnd1* promoter [Tg(Plxnd1-EGFP)HF78Gsat/Mmucd] were purchased from the Mutant Mouse Resource Research Centers (MMRRC).

3.1.2   Genotyping protocols

Genotypes were identified by PCR on DNA extracted from the tail of each individual. Two different protocols were used, depending on their compatibility with each primer set.

3.1.2.1   Protocol 1

This protocol was used to genotype *Sema3e* and *Emx1^{cre}* mice.

DNA was extracted from fresh tail tissue using a lysis buffer containing 100 mM Tris HCl (Sigma, Cat# T3253-1KG) pH 8.5, 5 mM EDTA (EUROMEDEX, Cat# EU0007-C), 200 mM NaCl (Analar NORMAPUR, Cat# 27810) and 0.2% SDS diluted in distilled water (Life Technologies, Cat# 10977-035). Right before use, Proteinase K (Invitrogen, Cat# 100005393) was added to the buffer to obtain a final dilution of 0.5% (50 μl in 10 ml buffer). Each tail was incubated in 500 μl of this final solution, overnight (O/N) at 55°C. The day after, lysed tails

were centrifuged for 15 min at 15 000 rpm at 4°C. The supernatant was retrieved, and mixed with 500 μl of isopropanol (Analar NORMAPUR, Cat# 20842.312). The mixture was vortexed until the apparition of the white precipitate and centrifuged for 15 min at 15 000 rpm at 4°C. The supernatant was eliminated and the pellet was left to dry for a few minutes and resuspended in 100 μl of DNAase/RNAase free water (Life Technologies, Cat# 10977-035). The resuspension was incubated while shaking at 55°C for 1 hour and then kept at 4°C until use for PCR. The quantities for each reagent included in the PCR mix were different according to the primers. In all cases DNA was diluted at 1/20. Table 1 contains the reagent concentrations used for the different PCR reactions.

Table 3.1: Concentrations of reagents used for Taq Polymerase PCR reaction

Reagent\Line	$Emx1^+$	$Emx1^{cre}$	$Sema3e^+$, $Sema3e^-$
Tampon 10x (Invitrogen, Cat# Y02028)	1x	1x	1x
MgCl (Invitrogen, Cat#Y02016)	2 mM	2 mM	1 mM
dNTPs (Promega, Cat# U151A)	0.4 mM	0.4 mM	0.2 mM
Primer 1	0.8mM	0.4mM	0.2 mM
Primer 2	0.8mM	0.4mM	0.2 mM
Primer 3	-	-	0.2 mM
Taq Polymerase (Invitrogen, Cat# 100021274)	2 U/ reaction	2 U/ reaction	2 U/ reaction

3.1.2.2 Protocol 2

This protocol was used to genotype *Plxnd1*-eGFP, *Plxnd1* null and *Plxnd1^{lox}* mice. For DNA extraction and PCR a commercially available kit (ThermoFisher Scientific, Cat# F170L) was used and procedures were followed according to manufacturer instructions.

Table 3.2 reviews the primers that were used to identify each genotype, the annealing temperature for each set of primers and the size of the PCR product.

Table 3.2 Primer sequences and annealing temperatures for each allele

Allele	Primers		Annealing Temp
Plxnd1::egfp *Plxnd1KO*	Forward: CCTACGGCGTGCAGTGCTTCAGC		62°C
	Reverse: CGGCGAGCTGCACGCTGCGTCCTC		
Plxnd1 lox	Forward: ACAGGTGTGTGCTCAAGGCCACCTC		60°C
	Reverse: CAGCCCTATAGTTCTCCACCAAAGA		
Emx1::cre	P IMR1084 : GCG GTC TGG CAG TAA AAA CTA TC	mut	66°C
	P IMR 1085 : GTG AAA CAG CAT TGC TGT CAC TT		
	P IMR 4170 : AAG GTG TGG TTC CAG AAT CG	wt	
	P IMR 4171 : CTC TCC ACC AGA AGG CTG AG		
Sema3e	Sema 3E 1 : GACAGAAAGGCTTAGCGGATC		56°C
	Sema 3E 2 : GGTTCGCCGAGTGACCTG		
	Sema 3E 4 : CTTGCTCACCATGGTGCGTG		

3.2   Surgical procedures

3.2.1   Retrograde labelling with cholera toxin B subunit

Adult (8-10 weeks) mice were anaesthetised by intra-peritoneal injection of 100 mg/kg Ketamine (Merial, product name: Imalgene) and 10 mg/kg Xylazine (K/X) (Bayer, product name: Rompun), and their head was immobilised through ear-bars on a stereotaxic apparatus. Their eyes were covered with Ocrygel (TVM, Cat# *48026T613*/3) to prevent drying out during anaesthesia and a heating pad was placed under the mouse to prevent anaesthesia-related hypothermia. After shaving the head and sterilising with Betadine 10 % (Gifrer, Cat#

3400931499787), the skin of the skull was cut open along its rostrocaudal axis. The skin was held open with clamps (F.S.T., Cat# 18050-28). After drilling a hole in the scull, injections of Alexa 555-CTB (Life technologies, Cat# C34776) or Alexa 647-CTB (Life technologies, Cat# C34778) were performed at a concentration of 1 µg/µl, using the stereotaxic coordinates indicated in Table 3.3. The injections were delivered using a programmable nanoliter injector (Nanoject III, Drummond, Cat# 3-000-207) to control injection volumes, duration, number and time intervals (Table 3.4).

Table 3.3 Types of fluorophores, stereotaxic coordinates and quantities injected for each targeted area.

Target area	Alexa excitation wavelength (nm)	Stereotaxic Co-ordinates (mm)	Quantity (nl)
Motor Cortex	647	AP: +0.91 ML: +1.34 DV: -0.75	100
Striatum	555	AP: +0.01 ML: +2.28 DV: -2.6	100
Somatosensory Cortex	647	AP: -0.23, ML:+3, DV: -0.75	400
Pre-motor Cortex	555	AP: +2.77, ML:+1.875, DV: -1.2875	400

Table 3.4 Nanoject programs used for each targeted area.

Nanoject III program	Motor Cortex and Striatum	Somatosensory Cortex and Premotor Cortex
Volume (nl)	10	20
Speed (nl/sec)	10	10
Time between injections (sec)	20	15
Rounds	10	20

Capillaries suitable for the Nanoject (Drummond, Cat# 3-000-203-GX) were pulled with a Sutter P-97 micropipette puller. The capillary was backfilled with mineral oil (Sigma Cat#M8410-500ML) before being adapted to the Nanoject plunger. After surgery, the skin of the skull was sewed back using interrupted sutures (Ethicon, Cat# 4-0 786G). Mice were

injected with 5 mg/kg of Carprofen (Pfizer, product name : Rimadyl) to avoid post-operative inflammation and pain. Mice were left survive for 7 days after the injection.

3.2.2   Retrograde labelling with DiI

After post-fixation in 4 % PFA (in PBS) O/N, adult brains were washed briefly in PBS and embedded in 4 % molten agar in PBS. Once agar was solidified, brains were attached to a vibratome and trimmed by coronal sectioning, starting from caudal areas until the cerebral peduncle was revealed. Then agar was removed from the brain and a crystal of 1,1'-Dioctadecyl-3,3,3',3'-Tetramethylindocarbocyanine Perchlorate ('DiI'; $DiIC_{18}(3)$) (Thermo Fisher Scientific, Cat# D3911) was inserted in the cerebral peduncle. Brains were kept in PFA 4% at 37 °C for 4 weeks. DiI diffusion in the cortex was examined on 80 μm vibratome sections.

3.2.3   Retrograde labelling with rabies virus

The use of rabies virus was carried out in a biosafety level 2 laboratory and all the personnel involved had been previously vaccinated. The viral strain used was Challenge Virus Standard (CVS-11) which is commonly used in trans neuronal tracing experiments. In our experiments, we used a homemade recombinant rabies virus CVS N2C expressing mCherry (Gift from D. Blondel (I2BC, Gif sur Yvette)). The mice were anesthetized with K/X and placed in a stereotaxic frame (David Kopf). Rabies virus was pressure-injected (at the rate of 100 nl/min) as a cell culture supernatant in a final volume of 200 nl in minimal essential medium, titrated at 5×10^6 plaque forming units/ml at coordinates targeting the motor cortex (see Table 3.3). As reported previously (Salin et al., 2008), the post-injection survival time (40-42h) was adjusted to readily detect first-order infected neurons and to limit second-order infection to the weak labelling of neurons directly associated with primary infected neurons.

3.2.4   *In utero* electroporation

Plasmids for *in utero* electroporation (Table 3.5) were prepared using Qiagen EndoFree Maxiprep Kit (Macherey-Nagel, Cat# 74042250) according to manufacturer instructions. To prepare the solution injected, endotoxin-free plasmids were diluted to a final concentration of

1 µg/µl in sterile PBS and Fast Green (Sigma, Cat# F7252) was added to a dilution of 1/100 from an 1 % aliquot. Pipettes for the injection (Harvard Apparatus, Cat# 30-0057) were pulled with a Sutter P-97 micropipette puller. The pregnant mouse was injected subcutaneously with 0.1 mg/kg of Buprenorphine (Virbaq, product name : Bupaq), at least 20 min before the onset of the surgery, to minimise post-surgical pain. To anaesthetise the mouse, continuous flux of isofluorane was provided by anaesthesia workstation (Equipement Veterinaire Minerve). The mouse was placed in the anaesthetic induction chamber, and once the righting reflex was lost, it was transported to an isofluorane mask. The eyes were covered with Ocrygel so that they do not dry out during anaesthesia and a heating pad was placed under the mouse to prevent hypothermia throughout surgery. The belly was shaved and sterilised with Betadine 10 % (Gifrer, Cat# 3400931499787). After the pedal reflex of the mouse was lost, the skin of the belly was cut open vertically and a laparotomy was performed along the linea alba, to gain access to the abdominal cavity. The uterine horns were extracted with cotton swabs. All throughout the surgery, the uterus was kept hydrated using warm (37°C), sterile PBS. The micropipette was attached on a mouth tube and filled with plasmid solution. About 1 µl of solution was injected in the lateral ventricle of each embryo. The electroporated ventricle was coloured by the Fast-Green and was thus easily visible. Immediately after injection, the head of the embryo was held with forceps-type tweezer electrodes (Nepagene, CUY650P5) of 5 mm diameter and electric pulses were applied through an electroporator (Nepagene, CUY21). To target the somatosensory area, the positive paddle of the electrode was directed on top of the electroporated ventricle. For E13.5 embryos, 4 pulses of 30 V and 50 ms duration each were applied, with 950 ms interval and for E15.5 embryos, 4 pulses of 35 V and 50 ms duration each, with 950 ms interval. After this process, the uterine horns were relocated inside the abdominal cavity. PBS was poured into the cavity to help all organs "swim" gently back in place. The abdominal wall and skin were sewed back using appropriate surgical sutures. The muscle was sewed with a lock type suture (Surgical specialties, 3-0 781B) and the skin was sewed using internal interrupted sutures (Ethicon, 4-0 786G). The mouse was injected with 110 mg/g of Carprofen and kept on a warm heating pad until wake-up. Six hours later the mouse was examined for post-operative pain and if needed, Buprenorphine was administered as previously. Twenty-four hours after surgery, a second dose of Caprofen was administered to avoid inflammation.

Table 3.5 Plasmids used for in utero electroporation

Plasmid	Source	Reference
pCAG-IRES-Tomato	gift from Cecile Lebrand	(Minocha et al., 2015)
pCAG-CRE-IRES2-GFP	gift from Harold Cremer (M-C Tiveron)	(Woodhead et al., 2006)
pCAG-PlexinD1	Generated by GeneCust	(Burk et al., 2017)
pCAG-GFP	gift from Victor Borrell	(Martínez-Martínez et al., 2016)

3.3 Histological procedures

3.3.1 Tissue harvesting

Adult mice and P3 or older pups were anaesthetised with K/X. PBS and PFA 4% was passed through the vascular system by intracardial perfusion, in order to avoid red blood cell autofluorescence and to preserve the structure of the tissue. Table 3.6 shows the volumes of PBS and PFA 4% used in perfusion according to the developmental stage. Pups younger than P3 were anaesthetised by hypothermia and their brains were retrieved without perfusion. Brains were dissected and post-fixed in PFA (4% in PBS) at 4 ºC for 2-4 h if used for immunofluorescence or O/N if used for in situ hybridization.

Table 3.6 Volumes of buffers used for perfusion on each developmental stage

Stage	Volume
P3	5 ml PBS 1x/ 5 ml PFA 4%
P7	10 ml PBS 1x/ 5 ml PFA 4%
P15	10 ml PBS 1x / 10 ml PFA 4%
P21	10 ml PBS 1x/15 ml PFA 4%
Adult (over P56)	10 ml PBS 1x/20 ml PFA 4%

3.3.2 Immunohistochemistry

After post-fixation, brains were kept in PBS at 4°C. Brains were embedded in 4 % agar (Invitrogen, Cat# 30391-023) in PBS and sections were cut using a Leica Vibratome (Cat#VT1000S). Immunostainings were performed according to standard procedures. Sections were incubated in blocking buffer containing PBS with 0.3 % Triton X-100 (Acros Organics, Cat#AC215682500) and Goat Serum 10 % (Dutscher, Cat#S2000-100) for 1 hour at room temperature (RT). For staining with anti-PlexinD1 antibody, sections were incubated for 2 hours at RT in blocking buffer containing PBS with 0.25 % triton x-100 and 0.02 % gelatin (Sigma, Cat# G9382-500G). Then, sections were incubated with primary antibodies diluted in blocking buffer O/N at 4 °C. The following day, sections were washed and incubated with secondary antibodies diluted at 1:500 for 2 h at RT. Tables 3.7 and 3.8 provide information on the primary and secondary antibodies used during immunostainings.

Table 3.7 : Primary antibodies

1ary Antibody	Host animal	Dilution	Source	Identifier
anti-GFP	Chicken	1:500	Aves	Cat#GFP-1020, RRID:AB_10000240
anti-Satb2	Mouse	1:80	Abcam	Cat#ab51502, RRID:AB_882455
anti-Ctip2	Rat	1:500	Abcam	Cat#ab18465, RRID:AB_10015215
Anti-Cux1	Rabbit	1:200	Santa Cruz	Cat#sc-13024, RRID:AB_2261231
Anti-PlexinD1	Goat	1:150	R&D Systems	Cat# AF4160 RRID: AB_2237261
Anti-RV phosphoprotein 31G10	Mouse	1:10000	gift from P. Coulon (INT, Marseille)	

Table 3.8 : Secondary antibodies

2ary Antibody	Source	Identifier
Alexa 488 Donkey anti-Chicken IgY	Jackson ImmunoResearch	Cat#703 545 155, RRID: AB_2340375
Alexa 568 Donkey anti-Mouse IgG	Thermo Fisher Scientific	Cat# A10037, RRID:AB_2534013
Alexa 647 Donkey anti-Rat IgG	Jackson ImmunoResearch	Cat#712 605 153, RRID: AB_2340694
Alexa 568 Donkey anti-Rabbit IgG	Thermo Fisher Scientific	Cat#A10042, RRID:AB_2534017
Alexa 568 Donkey anti-Goat IgG	Thermo Fisher Scientific	Cat#A11057, RRID:AB_2534104

3.3.3 In situ hybridization

Post-fixed brains were immersed in progressively higher concentrations (15 % then 30 %) of sucrose (Analar NORMAPUR, Cat# 27480.294) in PBS for cryoprotection, until sinking of the tissue. Brains were then dipped in OCT (VWR Chemicals, Cat# 361603E) contained by plastic moulds (Polysciences, Cat# 18646A), which were placed inside smashed dry ice in order to rapidly freeze the tissue. Brains were then kept at -80 °C until cryosectioning.

3.3.3.1 RNA Probe synthesis

Plasmid amplification

DH5α electrocompetent *E.coli* (Invitrogen, Cat# 11319019) were used for plasmid amplification. 1 µl of vector (10-100 ng) was added in 50 µl of bacteria and the mix was transported in an electroporation cuvette (Eurogentec, Cat# CE-0002-50S) after 1 min in ice. The cells were electroporated using an electroporator (Eppendorf 2510) at 2500 V and transported directly in 950 µl of liquid bacteria growth medium (Sigma, Cat# L3022-1KG). The mix was incubated at 37 °C rocking for 1 h 30. 25 µl of the mix was plated by streaking on top of solid LB agar (Sigma, Cat# 05040-1KG) containing 100 µg/ml of Ampiciline (EUROMEDEX, Cat# EU0400-B) or 50 µg/ml of Kanamicin (Roth, Cat# T832.1) and bacteria

were left to grow at 37 °C O/N. The day after, a liquid culture was prepared by taking one colony from the solid agar with a clean tip and throwing the tip in a 250 ml flask containing 25 ml of liquid LB with the appropriate antibiotic. The culture was left to grow at 37 °C O/N. The following day, DNA was purified through midi prep, using a commercially available kit (Qiagen Cat#12243) according to the manufacturer instructions.

DNA linearization

DNA was linearized through digestion by the appropriate restriction enzymes (Table 3.9). For a final volume of 70 µl, 15 µg of DNA, 2 µl of the restriction enzyme and 7 µl of its specific buffer, were added in the appropriate volume of water. The reaction was developed for 3 h at 37 °C, after which a small aliquot (2 µl in 6 µl of water) was run in an agarose (Roth, Cat# 2267.4) gel to verify that the plasmid is completely linearized. DNA was then purified using a commercially available kit (Promega, Cat # A9281), according to manufacturer instructions.

Table 3.9 DNA templates for RNA probe synthesis

Gene	Plasmid reference	Restriction Enzyme	Restriction Enzyme Buffer ID	RNA polymerase
Cux1	Gift from M. Nieto lab	EcoRI (Promega, Cat# R601A)	Buffer H (Promega, Cat# R008A)	T7 (Promega, Cat# P207B)
Er81	(Arber et al., 2000)	SpeI (Promega, Cat# R659A)	Buffer J (Promega, Cat# R008A)	T7 (Promega, Cat# P207B)
Plxnd1	(Cheng et al., 2001)	Xba I (Promega, Cat# R618A)	Multicore (Promega, Cat# R999A)	Sp6 (Promega, Cat# P108B)
Sema3e	(Chauvet et al., 2007)	Not I (Promega, Cat# R643A)	Multicore (Promega, Cat# R999A)	T7 (Promega, Cat# P207B)

Probe synthesis reaction

In vitro transcription reaction was set up as follows: In a final volume of 50 µl were added 10 µl of Buffer 5X (Promega P118b), 5 µl of DIG RNA labelling mix (Roche, Cat# 11277073910), 2 µl of DTT (Promega, Cat # P117B), 1 µl of RNAsin (Promega, Cat # N261A), 3 µl of RNA polymerase and 2 µg of the DNA template. The mix was incubated at 37 $^{\circ}$C for 3 h. A small aliquot was run in 1 % agarose gel to verify that the probe was properly synthesized. Finally, template DNA was degraded by incubating with 2 µl of RNase-Free DNase (Promega, Cat # M610A) at 37 $^{\circ}$C for 15 min. RNA was purified using a commercially available RNA isolation kit (Qiagen, Cat#74104), according to manufacturer instructions.

3.3.3.2   Colorimetric ISH

Treatment and Hybridization: After a brief wash in PBS, sections were permeabilised with RIPA buffer containing 150 mM NaCl, 1 % NP-40 (Sigma, Cat# 74385-1L), 0.5 % Na deoxycholate (VWR Chemicals, Cat# 27836.135), 0.1 % SDS (EUROMEDEX, Cat# EU0660-B), 1 mM EDTA (EUROMEDEX, Cat# EU0007-C) and 50 mM Tris pH 8.0, twice for 10 min at RT. After post-fixation in PFA (4 % in PBS) at RT for 10 min, slides were washed 3 x 5 min with PBS. Treatment with triethanolamine buffer (100 mM Triethanolamine and 0.2 % acetic acid (CARLO ERBA Reagents, Cat# UN2789) in which acetic anhydride was added dropwise to a final concentration of 0.25 %, was performed for 15 min. After 3 washes with PBST (Tween 0.1 % in PBS) slides were blocked in Hybridization buffer at 65 °C for 2 h. Hybridization buffer contained 50 % Formamide, 5X SSC, 5X Denhardts, 500 µg/ml Salmon Sperm DNA and 250 µg/ml yeast RNA. RNA probes were diluted to 1 µg/ml in hybridization solution, denatured for 5 min at 85 °C and left to cool down in ice for 5 min. Sections were incubated with the mix in a humidified chamber at 65 °C O/N.

Post-hybridization washes and immunological detection: Slides were washed 2 x 1 h at 65 °C in post-hybridization solution containing 50 % Formamide, 2X SSC and 0.1 % Tween 20. Directly after, they were washed in buffer B1 containing 100 mM maleic acid (Panreac QUIMICA SAU, Cat# 141882.1211) pH 7.5, 150 mM NaCl and 0.1 % Tween 20 and blocked in buffer B2 (10 % Goat Serum in Buffer B1). Anti-DIG-AP (Roche, Cat# 11093274910, RRID: AB_514497) primary antibody was diluted 1:2000 in Buffer B2 and applied on sections for incubation O/N at 4 °C. Slides were washed with B1 buffer for 2 x 5min and then incubated in fresh Buffer B3 for 30 min at RT. Buffer B3 contained 100 mM Tris pH 9.5, 50 mM MgCl$_2$

(Analar NORMAPUR, Cat# 25108.260) 100 mM NaCl and 0.1 % Tween 20. AP substrate NBT-BCIP (Roche, Cat# 11681451001) was diluted in Buffer B3 at 20 µl/ml and applied on the sections to detect the DIG probe by means of a color reaction, which was left to develop in the dark at RT from 30 min to 1 day or O/N until apparition of the signal. Reaction was stopped with PBST once background noise started to develop. Sections were post-fixed with 4 % PFA in PBS for 10 min at RT, washed in PBS and mounted in aqueous mounting medium (Aqua Polymount, Polysciences, Cat#18606-20)

3.3.3.3 Fluorescent ISH followed by immunofluorescence

Hybridization: Cryostat sections of 20 µm were cut using a Leica (Cat# CM3050S) cryostat. All treatments before and during hybridization were conducted in RNAase-free conditions to avoid degradation of the RNA probes. Bench and tools were cleaned with RNAse Zap (Sigma, Cat# R2020-250ML) in order to minimise the presence of RNAases. Slides were left at RT to dry for at least 2h. Sections were treated with 0.008 mg/ml Protein Kinase (Invitrogen, Cat# 100005393) in 50 mM Tris-HCl (Sigma, Cat# T3253-1KG) at 37°C for 3 min. After 3 washes in PBS, sections were treated with acetylation solution containing 1 % triethanolamine (Sigma, Cat# T58300-500G) and 0.25 % acetic anhydride (Fluka, Cat#45830) at RT for 10 min. After two washes in PBS and one wash in 2X SSC pH 7.0 (EUROMEDEX, Cat#EU0300-C), slides were incubated in hybridization solution at RT for 2 h. Hybridization solution contained 5X Denhardt's solution (Sigma, Cat# D2532-5ML), 0.25 mg/mL baker yeast tRNA (Sigma, Cat# R6750), 0.2 mg/mL Salmon sperm DNA (Sigma, Cat# D7656-1ML), 5X SSC and 50 % Formamide (ACROS ORGANICS, Cat# 181090010). RNA probes were diluted in hybridization solution to obtain a final concentration of 4 µg/ ml (hybridization mix). The hybridization mix was then denatured for 5 min at 85 °C and cooled down for 5 min in ice. After the blocking step, sections were incubated with the hybridization mix at 65 °C O/N.

Post-Hybridization washes and Primary Antibody: After sequential washes with different buffers (5X SSC for 5 min at 65 °C, 2X SSC for 1 min at 65 °C, 0.2X SSC in 50 % formamide at 65 °C and 0.2X SSC for 5 min at RT), slides were equilibrated for 5 min in buffer 1 containing 100 mM Tris-HCl pH 7.5 and 150 mM NaCl (Analar NORMAPUR, Cat# 27810.295) and blocked in TNB blocking buffer containing 0.5 % blocking reagent (Perkin Elmer, Cat# FP1020) diluted in buffer 1. Sections were incubated with sheep anti-DiG-POD (Roche, Cat#

11207733910, RRID: AB_514500) antibody diluted up to 1:500 and chicken anti-GFP (Table 3.7) diluted up to 1:200 in TNB buffer O/N at 4 °C.

Detection: The following day, sections were washed in TNT containing 0.05 % Tween20 in buffer 1 for 3 times at RT. DIG probe was detected using Cy3 Tyramide (Perkin Elmer, Cat# NEL75) diluted up to 1:100 for 10 min at RT. Sections were again washed and incubated with secondary antibody (Alexa 488 Donkey anti-Chicken IgY, Table 3.8), diluted in TNT for 90 min at RT.

3.4   Imaging

All images of sections labelled with fluorescent markers, were taken using Zeiss confocal microscopes (LSM 780 and LSM 880). For cell counts and colocalization studies 20x magnification was used whereas for the analysis of dendrites and spines, images were taken at 40x magnification. Image processing was performed in Photoshop CS6 (Version 13.0.1) and ImageJ.

3D imaging of cleared brains was performed on a light sheet fluorescent microscope (LaVision BioTec Ultramicroscope II) using ImspectorPro software (LaVision BioTec). 3D volume images were generated using Imaris ×64 software (version 8.4.1, Bitplane). Segmentation of the distinct axonal tracts was performed manually using 'Isosurface'(imaris) by creating a mask around each volume and followed by second 'Isosurface' performed in automatic way on the first segmentation. 3D pictures were generated using the 'snapshot' tool.

3.5   Quantifications

To quantify the layer position of labelled cells, the cortical thickness was divided into 10 bins. The correspondence between bins and cortical layers was determined by overlaying with staining against Cux1 (layers 2/3), Ctip2 (layers 5B, 6) and Tbr1 (layer 6). In S1, bins 2-3 represent layers 2/3, bin 4-5 are layer 4, bin 6 is layer 5A, bin 7 is layer 5B and bins 8-10 are layer 6. In M1, bins 2-3 represent layers 2/3, bin 5 is layer 5A, bins 6-7 are layer 5B and bins 8-10 are layer 6. Cell counting was performed using the Photoshop count tool.

Analysis and quantification in electroporated embryos were performed as described in (Pacary et al., 2011). In brief, the VZ-SVZ was defined using nuclear staining, as the region around the

lateral ventricle with high cellular density. IZ was delineated from the CP as the area containing axons. Cells were counted in each zone and normalised to the total number of cells counted in each section. CP and IZ was divided in three equivalent domains: upper, medial and inferior CP and intermediate zone respectively. Cells counted in each domain were normalised to the total number in the zone.

Analysis of dendritic parameters was performed using ImageJ and Bitplane Imaris (Version 8.4.1). Dendrites were traced semi-manually using Neuro-filament plugin of Imaris and parameters were automatically quantified by the software statistics option. Spines were counted in Neuron Studio (Version 0.9.92) on maximum projections on segments of second order basal dendrites. Different types of spines were automatically assigned by the Spine Classifier option of the software, which classified the types of spines according to the following criteria. Neck Ratio: Spines with head to neck diameter ratio greater than 1.1 were considered Thin or Mushroom. Thin Ratio: Spines that did not meet the Neck Ratio value and have a length of spine to head diameter above 2.5 were classified as thin, otherwise as stubby. Mushroom Size: Spines that met the Neck Ratio value and had a head diameter equal or greater than 0.3 were labeled as mushroom, otherwise as stubby.

3.6 Statistics

Statistical analyses were performed using Graphpad Prism Version 6.05. (GraphPad Software, San Diego, CA, USA). For each experiment, the normal distribution of the data was examined using a D'Agostino–Pearson omnibus test for sample sizes of 6 or higher. The estimate of variance was determined by the standard deviation of each group. Since data were nonparametric, Mann–Whitney test was used to compare means of two groups of data, and Kruskal–Wallis test or with One-way ANOVA followed by the Sidak Multiple Comparisons test were used to compare differences between more than two groups. Statistical significance was set at $p < 0.05$. Statistical details (n, p value, statistical test used) can be found in the result section and figure legends.

4 DISCUSSION

Our results show that the absence of PlexinD1/Sema3E signalling leads to the appearance in layers 2/3 of the motor cortex of neurons heterotopically projecting in the contralateral striatum, while in control condition these neurons are mainly distributed in layer 5A. To explain this phenotype, we can make two different hypotheses.

Hypothesis 1: loss of PlexinD1/Sema3E signalling induces over-migration of some layer 5A neurons, which retain a heterotopic projection to the contralateral striatum.

Hypothesis 2: loss of PlexinD1/Sema3E signalling induce contralateral mis-projections of layer 2/3 neurons, which normally only target homotopic areas.

These two hypotheses are discussed in detail in the following chapters.

4.1 Hypothesis 1: Defective migration of layer 5A CPNs.

4.1.1 Identity of miss-projecting neurons

The appearance of heterotopically projecting neurons in more superficial layers than normal in the absence of PlexinD1/Sema3E signalling could result from mispositioning due to defects in migration of layer 5A neurons. Mispositioned layer 5A neurons may however retain their projection identity and therefore we are able to back-label them from the contralateral striatum. There is not a lot known about the molecular control of acquisition of projection identity by cCStrPNs. Sohur et al. (2014) reported that at P4, when cCStrPN axons are beginning to invade the contralateral striatum, all cCStrPNs express Satb2 and half of them also express Sox5, a transcription factor expressed by all CFuPNs. By P15, when they acquire their mature projection pattern, all cCStrPNs are positive for Sox5. The authors therefore proposed that cCStrPNs are a "hybrid" population of cortical projection neurons, with anatomic and molecular characteristics of both CFuPNs and CPNs. Whether this mixed molecular signature specifies the unique projection identity of these neurons has not been investigated yet. However, it would be interesting to determine whether the ectopic cCStrPNs observed in Sema3E and PlexinD1 mutant cortices express Sox5.

This analysis could be completed by studying the expression of Fezf2, which has been shown to label the majority of layer 5A cCStrPNs in the adult cortex (Nadarajah et al., 2001; Tantirigama et al., 2016) so its expression pattern may overlap with PlexinD1. Therefore, examination of the ectopic neurons for Fezf2 expression could give us interesting information about their identity. On the other hand, if these neurons are positive for markers restricted to upper layer CPNs, such as Cux1 and Cux2 (Molyneaux et al., 2009; Nieto et al., 2004), this would point to a mis-projection of layer 2/3 neurons (Hypothesis 2), and channel the study into this line of investigation.

Moreover, we may perform additional experiments in order to better characterise the ectopic neurons. We may use a tamoxifen-inducible *Nestin-Cre^{ERT2}* line (Imayoshi et al., 2006) in order to target neural progenitors in a tamoxifen-dependent manner. Early tamoxifen administration at E11.5 will induce recombination in progenitors of both deep and upper layer neurons (Miyata et al., 2001; Noctor et al., 2001). Late tamoxifen administration (after E14.5) will lead to recombination only in the late progenitor pool that gives rise to superficial layer neurons. We will administrate tamoxifen at E11.5 and E14.5 to *Nestin-Cre^{ERT2}; PlexinD1^{lox/lox}* embryos, retrogradely label cCStrPNs by CTB injections at adult stage and analyse their laminar distribution. In *Nestin-Cre^{ERT2}; PlexinD1^{lox/lox}* mice treated with tamoxifen at E11.5, we should observe the same phenotype as in *Plxnd1* cKO. In *Nestin-Cre^{ERT2}; PlexinD1^{loxlox}* mice treated with tamoxifen at E15.5, two different results may be obtained. 1) No defect: will indicate that the phenotype observed in *Plxnd1* cKO is due to mispositionning of *Plxnd1* deficient layer 5 neurons in layers 2/3, 2) presence of ectopic cCStrPNs: will indicate that loss of *Plxnd1* in layer 2/3 neurons induces contralateral misprojections to the striatum.

4.1.2 PlexinD1/Sema3E signalling may control migration of layer 5A neurons

We have hypothesized that PlexinD1/Sema3E signalling may control the migration and final positioning of a subset of layer 5A CPNs. Our preliminary data point towards this direction. More precisely, *in utero* electroporation of GFP-expressing vector at E13.5 to target layer 5 neurons in *Sema3e* KO embryos resulted in shift of electroporated neurons towards the upper part of the CP 4 days after electroporation. Furthermore, electroporation of a cre-expressing vector in *Plxnd1^{lox/lox}* embryos at E13.5 caused over-migration of cortical neurons to layer 2/3 at P16, whereas electroporation of a PlexinD1-expressing vector at E15.5 to target layer 2/3 neurons resulted in the mispositioning of some of the neurons in deeper cortical layers

at P12-16. These data suggest that PlexinD1/Sema3E signalling restrict neuronal migration in the developing mouse cortex (Figure 4.1). However, as experiments were carried out on 1 or 2 mice, these results will have to be confirmed. In addition, we are currently performing EdU (5-ethynyl-2'-deoxyuridine) labelling of dividing cells in E13.5 *Emx1-cre; Plxnd1* cKO embryos to examine the laminar distribution of labelled neurons in the postnatal cortex at P16 and compare with that of control littermates.
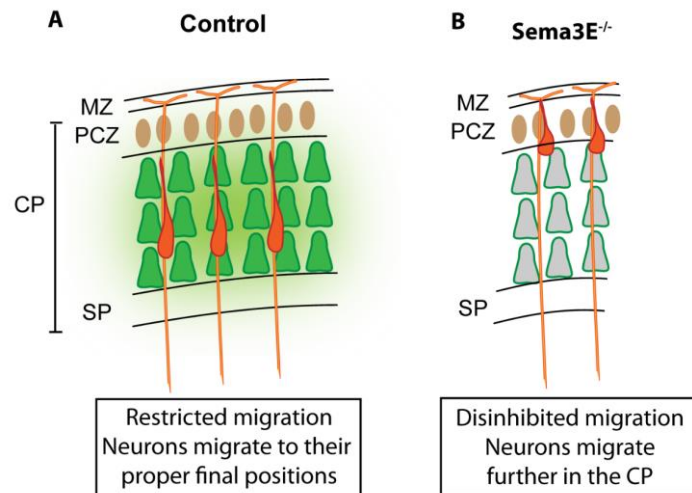
Figure 4.1 Proposed model for the effect of PlexinD1/Sema3E signalling in migration.

(A) In the control context, Sema3E/PlexinD1 signalling may restrict the motility of migrating neurons, thus ensuring their proper final positioning. (B) Absence of any component of this signalling causes over-migration of neurons and mispositioning in upper part of the cortical plate (CP).

A previous study reported that PlexinD1 signalling regulates neuronal migration in the rat cortex (Chen et al., 2008b). In that article, silencing of PlexinD1 resulted in accumulation of cells in deeper parts of the CP suggesting that in absence of PlexinD1 defective pyramidal neurons migrate less, which contrasts with our results. The study used only one shRNA and no control rescue experiments to verify whether this effect is specific for *Plxnd1* and not an off-target effect. Moreover, it is possible that different mechanisms regulate migration in mouse and rat. This is supported by the finding that in the rat brain *Plxnd1* is ubiquitously expressed in cortical neurons across all cortical layers, whereas in the mouse it is restricted to subpopulations of CPNs and cells in layer 4. For all these reasons, it is necessary to explore the potential role of PlexinD1 in the migration of pyramidal neurons in the mouse cortex.

4.1.3 Potential mechanisms of Sema3E/PlexinD1 action in neuronal migration

To understand how PlexinD1/Sema3E signalling may regulate migration of layer 5A neurons, the first task would be to describe the pattern of expression of these molecules at early developmental stages of corticogenesis, when migration happens. Layer 5 neurons are born around E13.5 (Greig et al., 2013). At this stage, *Plxnd1* is already expressed by deep layer neurons in the CP and subplate where it remains until E15.5, when it is downregulated in the CP (Deck et al., 2013). At E16, it is not present in the CP anymore, but its expression remains in the border between the subplate and IZ (Figure 4.2). This transient expression of *Plxnd1* in the CP is consistent with a possible role in migration of deep layer neurons. Our data reveal that *Sema3e* is present in the CP at E16 (Figure 4.2), but whether it is present at earlier stages it is not known. Further experiments will be necessary to describe the expression pattern of *Sema3e* at these stages in order to formulate hypotheses on the possible mechanisms of PlexinD1/Sema3E signalling in migration.
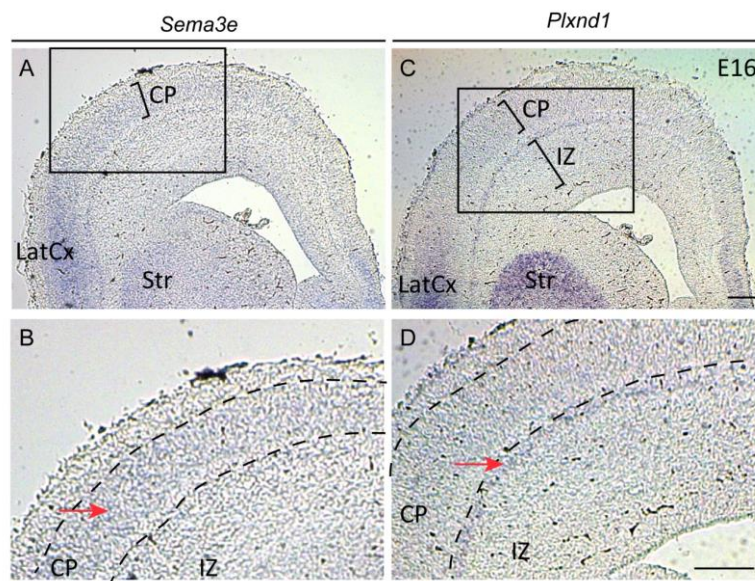
Figure 4.2 Expression of Plxnd1 and Sema3e in the embryonic mouse brain.

(A) Coronal section of E16.5 wild type brain showing strong mRNA expression of Sema3e in the lateral cortex and weaker in the CP. (B) Inset showing expression of Sema3e in the CP (arrow). (C) Coronal section of E16.5 wild type brain showing expression of Plxnd1 mRNA at the border between the IZ and the CP (arrow). Plxnd1 expression is also documented in the lateral cortex and the striatum. D) Inset showing expression of Plxnd1 at the border between the IZ and the CP (arrow). CP: Cortical plate, IZ: Intermediate zone. Scale bars: 200 μm

Early studies reported that neurons born between E12 and E14 mostly follow a mode of migration called somal translocation (Miyata et al., 2001; Nadarajah et al., 2001), while later born neurons go through a multi-step process that includes multipolar migration (Tabata and Nakajima, 2003), glia-guided locomotion (Nadarajah et al., 2001) and terminal translocation, which leads to the arrest of their migration and their final positioning (Sekine et al., 2011). The migratory mode of layer 5A PlexinD1-expressing neurons is not known. Given the fact that they reside in deep cortical layers, the majority of them may migrate in the CP using somal translocation. On the other hand, glia-guided locomotion cannot be excluded, as these neurons reside in the superficial layers of layer 5, and thus they cannot be considered strictly early-born. To verify the migratory mode of PlexinD1-positive neurons we should study their morphology and migration speed, which differ between somal translocation and locomotion (Nadarajah et al., 2001). If eGFP is expressed in *Plxnd1*-eGFP embryos at E13.5, time-lapse imaging of eGFP-expressing neurons migrating on acute cortical slices and examination of their morphology and properties of movement would provide a direct answer to this question.

4.2 Hypothesis 2: Mis-projection of layer 2/3 CPNs in the contralateral striatum

Expression of eGFP in the *Plxnd1*-eGFP mouse poorly recapitulates *Plxnd1* expression in layers 2/3. Nevertheless, retrograde tracing showed that layer 2/3 CPNs (including eGFP$^+$ CPNs) establish homotopic projections to the contralateral cortex. Thus, in layer 2/3, unlike in layer 5A, PlexinD1-positive CPNs may not project to the striatum at adult stage. Misprojection of layer 2/3 CPNs to the contralateral striatum in the absence of PlexinD1/Sema3E signalling may be mediated by i) *de novo* formation of a collateral innervating the striatum or ii) by the failure to retract a transient projection that normally is extended by these neurons into the striatum and later eliminated.

4.2.1 Mis-projection due to *de novo* branch formation in the striatum

Callosal axons sent by PlexinD1-positive neurons in layers 2/3 invade the contralateral M1, but not the striatum. This may be due to repulsive signalling from Sema3E secreted in the striatum at this timepoint. There are indications supporting this hypothesis. Indeed, in situ

hybridization data from the Allen brain atlas suggest that *Sema3e* expression is present in the striatum at P4 and maintained at P14 (Figure 4.3).
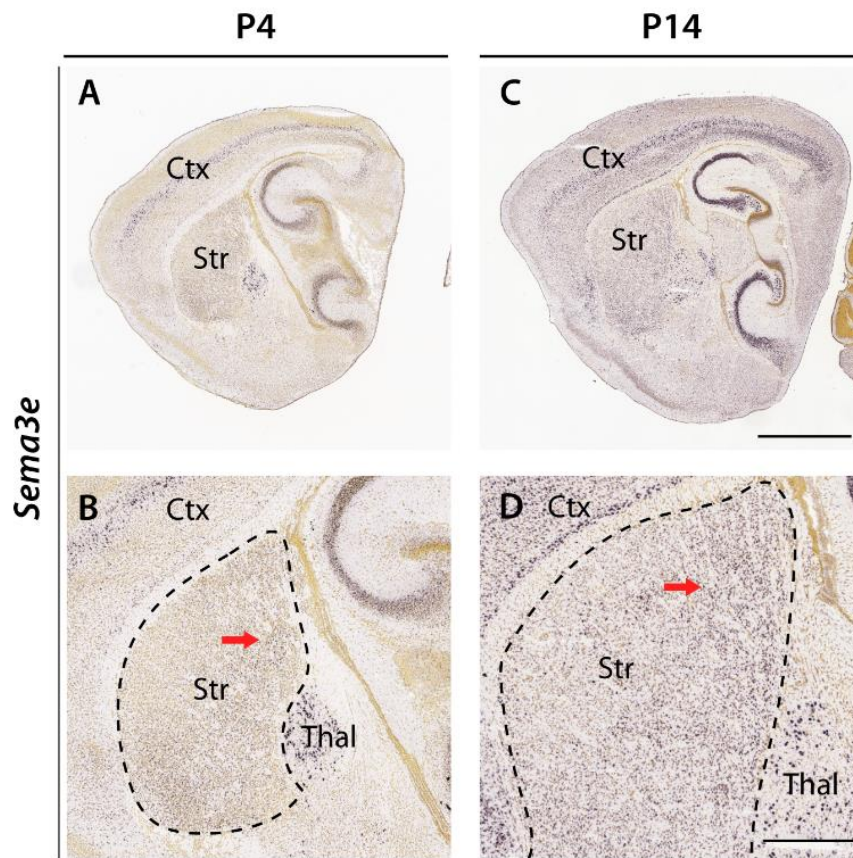
Figure 4.3 Expression of Sema3e in the early postnatal mouse brain

(A) Sagittal section of P4 wild type brain showing presence of weak expression of Sema3e in the striatum. (B) Inset showing expression of Sema3e in the striatum (arrow). (C) Sagittal section of P14 wild type brain showing stronger expression of Sema3e mRNA in the striatum (arrow). Sema3e expression is also documented in the deep layers of the cortex and the thalamus at these timepoints. D) Inset showing expression of Sema3e in the striatum (arrow). Ctx: Cortex, Str: Striatum, Thal: Thalamus. Scale bars: (A, C) 2000 μm, (B, D) 850 μm.

Furthermore, unpublished data from the team showed that Ctip2-positive SCPNs in cortical layer 5B express *Sema3e*. These neurons are known to send a collateral branch into the ipsilateral striatum. So, these data suggest that the intra-striatal projections of these neurons could be another source of secreted Sema3E in the striatum. In absence of Sema3E, PlexinD1-positive neurons of layer 2/3 may form heterotopic projections to the striatum. And in a PlexinD1 mutant background, heterotopic fibers may not be repelled anymore by striatal source of Sema3E and could be formed.

However, CPNs in layer 5A, which project to the contralateral striatum also express PlexinD1, so they should not be repelled by Sema3E in the striatum. PlexinD1-positive neurons of layer 2/3 and of layer 5A should respond differentially to Sema3E. My team has previously shown that Sema3E/PlexinD1 signalling has different effects on axon guidance, depending on the cell type. The expression of the co-receptor Npn1 can switch the response of a PlexinD1-positive axon to Sema3E from repulsion to attraction or switch off Sema3E signalling (Bellon et al., 2010; Chauvet et al., 2007). So, it would be interesting to see if expression of Npn1 differs between neurons in layers 2/3 and neurons in layer 5A between P4 and P15 which is the timing of establishment of the projections. Data from the Allen brain Atlas for Npn1 expression, reveal that at P4 *Npn1* is expressed faintly in some neurons of layer 5 in M1 and its expression raises in neurons of the layer 5 at P14 (Figure 4.4). In contrast, layer 2/3 neurons do not express Npn1 during these developmental stages. The two types of neurons may thus respond differentially to Sema3E.
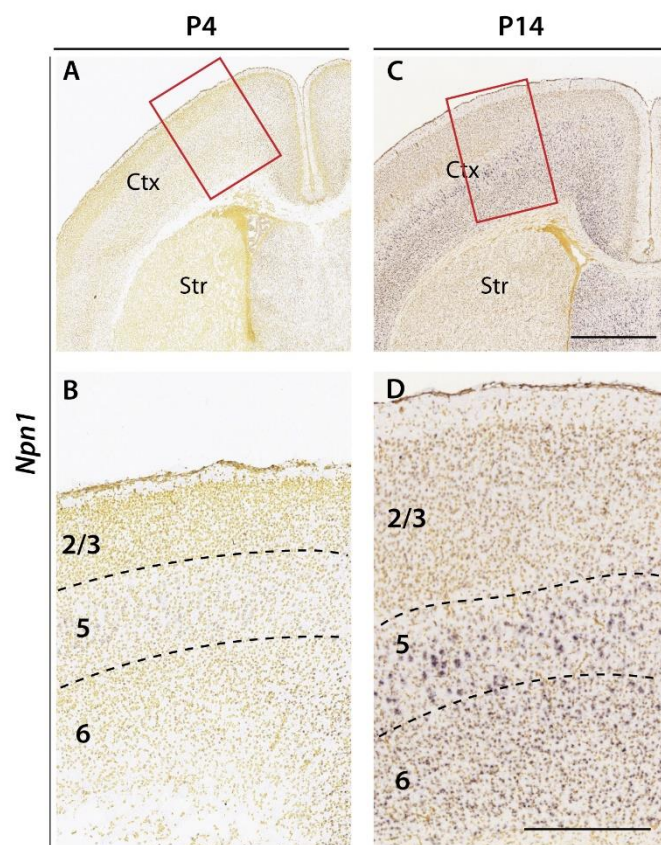
Figure 4.4 Expression of Npn1 in the early postnatal mouse brain

(A) Coronal section of P4 wild type brain showing presence of weak expression of Npn1 in the cortex. (B) Inset showing expression of Npn1 in layer 5 of the cortex. (C) Coronal section of P14 wild type brain showing stronger

expression of Npn1 mRNA in the cortex and the septum. D) Inset showing expression of Npn1 in layers 5 and 6 but not layers 2/3 of the cortex. Ctx: Cortex, Str: Striatum. Scale bars: (A, C) 1000 μm, (B, D) 400 μm.

Figure 4.5 summarised our proposed model.
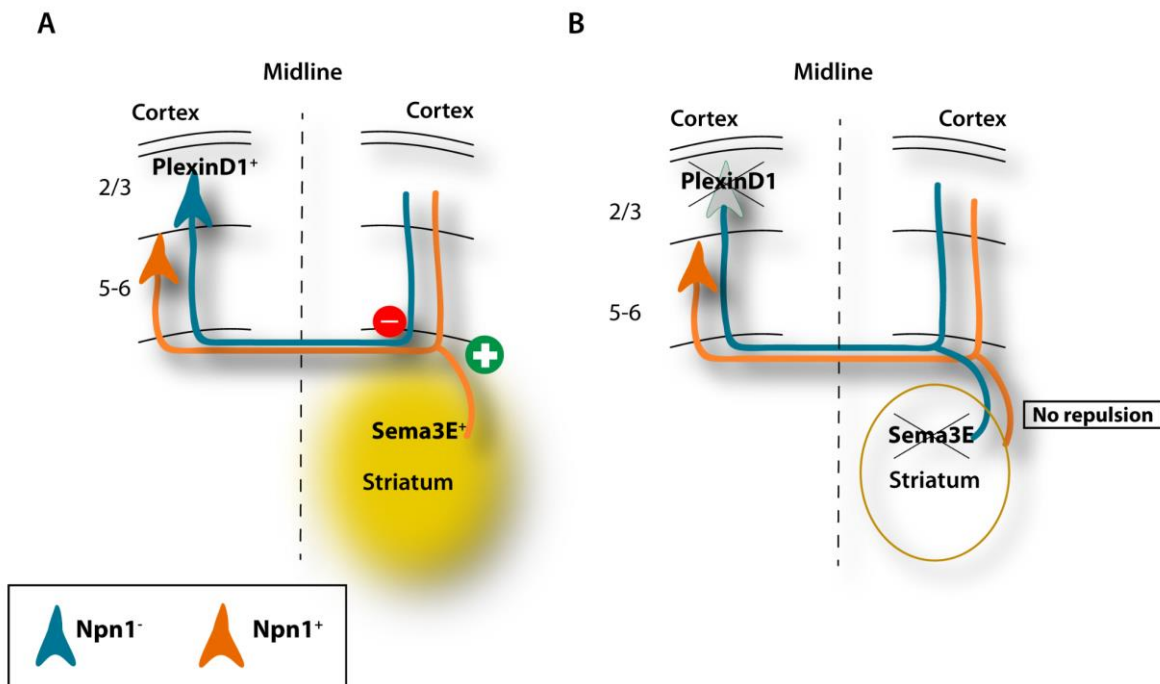
Figure 4.5*: De novo formation of aberrant projection in the striatum*

Schematic representation of the proposed model (Chapter 4.2.1) used to explain potential mis-projection of layer 2/3 CPNs in the contralateral striatum. (A) In the control context, PlexinD1⁺/Npn1⁻ axons from layer 2/3 CPNs are repelled by Sema3E secreted in the contralateral striatum, and do not form a projection in the striatum. On the other hand, layer 5A PlexinD1⁺/Npn1⁺ CPNs are not repelled by Sema3E and form a branch into the contralateral striatum. (B) In the absence of PlexinD1/Sema3E signalling, axons from layer 2/3 neurons are allowed to form collaterals into the striatum as there is not repulsive action of Sema3E.

4.2.2   Mis-projection due to maintenance of exuberant projection

The second scenario would be that during early postnatal stages PlexinD1-positive neurons in layers 2/3 send a transient projection in the contralateral striatum, which is later eliminated. We already know that during the formation of crossed corticostriatal projections there is extension and elimination of exuberant fibers. Specifically, Sohur et al (2014) showed

that around P4, all cortical areas send a fiber to the contralateral striatum, but by P14 fibers sent by neurons in the S1 are eliminated, restricting the population of cCStrPNs in the motor and premotor cortex. The same process could restrict cCStr projections in layer 5A, by eliminating exuberant fibers sent by layer 2/3 neurons in the M1. However, until now there is no study that shows exuberance and elimination of cCStr projections in layers 2/3 of the M1 between P4 and P14.

In order to test this hypothesis, we would need to prove that layer 2/3 neurons indeed project transiently to the contralateral striatum. This could be done using anterograde and retrograde tracing techniques. Retrograde approaches could involve the injection of tracers such as CTB in the striatum at different stages starting from P3, when invasion of transcallosal fibers into the contralateral striatum first happens (Sohur et al., 2014). Examination of the layers 2/3 in the contralateral M1 would answer whether these transient projections exist and when they are formed and later retract.

Such transient heterotopic projections from layer 2/3 neurons could be eliminated either by pruning or by cell death. I herein discuss these two possibilities.

4.2.2.1   Elimination of heterotopic projections by pruning

Exuberant heterotopic projections from layer 2/3 neurons could be eliminated by retraction through axon pruning, which could be regulated by repulsive signal from Sema3E expressed in the striatum. At P4, Sema3E levels of expression in the striatum should be low enough to permit axons from layer 2/3 and layer 5A CPNs to invade the striatum. Then, developmentally regulated increase in the quantity of secreted Sema3E may cause the pruning of fibers from layer 2/3 (Npn1$^-$), but not layer 5A (Np1$^+$), CPNs through selective repulsion. In situ data from Allen Brain atlas show a raise in *Sema3e* mRNA expression from P4 to P14 in the striatum (Figure 4.3), thus supporting this hypothesis. This model predicts that in the absence of PlexinD1, axons from both populations should be still able to invade the striatum at P4, but axons coming from layer 2/3 neurons are not sensitive to the increasing striatal Sema3E and thus are not pruned. On the other hand, in absence of Sema3E, PlexinD1 neurons from layer 2/3 do not receive repulsive signals from the striatum and thus remain (Figure 4.6). These scenarios are consistent with our results.
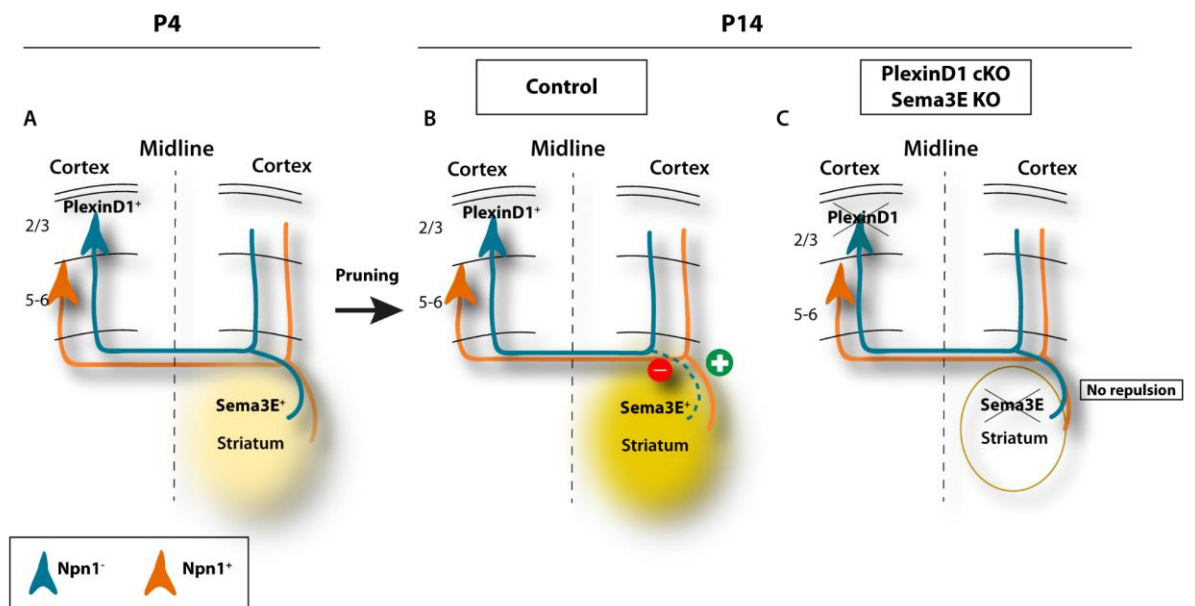
Figure 4.6 Maintenance of exuberant projections from layer 2/3 CPNs in the striatum, due to lack of pruning

Schematic representation of the proposed model (Chapter 4.2.2.1) used to explain potential misprojection of layer 2/3 CPNs in the contralateral striatum. In a first step happening around P4, PlexinD1+/Npn1- neurons in layers 2/3 send a transient projection in the contralateral striatum (A). This projection may be eliminated by P14 through pruning (B), caused by repulsive action of Sema3E in the striatum. PlexinD1+/Npn1+ neurons in layer 5A may also send an early projection in the contralateral striatum, which is retained due to lack of repulsion from Sema3E. (C) In absence of PlexinD1/Sema3E signalling repulsion is abolished and consequently exuberant axons from layer 2/3 neurons remain in the striatum

4.2.2.2 Elimination of heterotopic projections by neuronal cell death

Death due to PlexinD1 dependence receptor

Another mechanism that could mediate the elimination of heterotopic projections from layer 2/3 neurons could be PlexinD1-mediated cell death of the neurons themselves. Indeed, PlexinD1 has been shown to induce apoptosis by acting as a dependence receptor, which is active in both presence and absence of its ligand, but when the ligand is not there, its activation leads to cell death (Luchino et al., 2013). In the adult cortex, Sema3E-expressing neurons are localised in layers 5B and 6 (Watakabe et al., 2006), but *Sema3e* expression can be detected in deep cortical layers already at P4 (Figure 4.3). This suggests that Sema3E may exert a neuro-protective activity by inhibiting PlexinD1-induced cell death. PlexinD1-positive neurons of

layer 5A, which are positioned just above Sema3E-secreting cells, are thus subject to this neuro-protective effect, while PlexinD1-positive neurons in layers 2/3 are positioned further away and so some of them are prone to cell death as they may not receive enough Sema3E (Figure 4.7). However, there are still PlexinD1$^+$ neurons in layer 2/3 that survive. Most of them are eGFP-negative in *Plxnd1*-eGFP mice, perhaps due to a low level of *Plxnd1* expression.
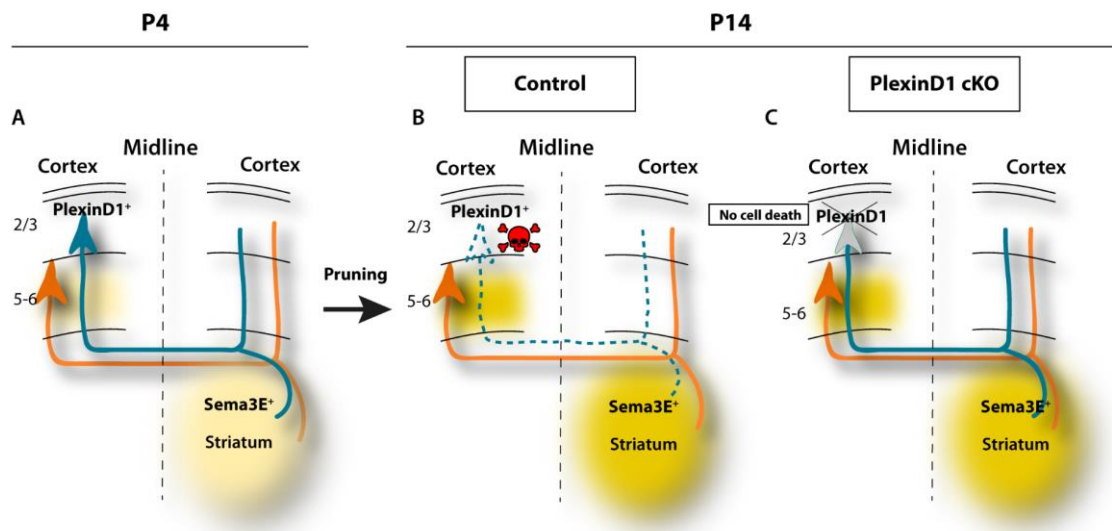
Figure 4.7 Maintenance of exuberant projections from layer 2/3 neurons in the striatum, due to lack of cell death

Schematic representation of proposed model (Chapter 4.2.2.2) used to explain potential misprojection of layer 2/3 CPNs in the contralateral striatum. As in the pruning hypothesis, in a first step happening around P4, both PlexinD1-positive neurons in layers 2/3 and PlexinD1-positive neurons in layer 5A send a projection in the contralateral striatum (A) Projections coming from layer 2/3 neurons may be eliminated by P14 through cell death, due to the action of PlexinD1 as a dependence receptor. In contrast to layer 5A neurons, PlexinD1+ neurons in layer 2/3 may be positioned too far from Sema3E-secreting cells in layers 5B and 6. In the control context, absence of sufficient concentration of Sema3E, may provoke the initiation of an apoptotic pathway by PlexinD1 in layer 2/3 neurons, while neurons in layer 5A receive enough Sema3E and are thus protected from apoptosis and maintain their projections in the contralateral striatum. In absence of PlexinD1 layer 2/3 neurons may survive aberrantly and the projections that they extend to the contralateral striatum are maintained.

This hypothesis allows to explain what happens in absence of PlexinD1, but not in absence of Sema3E. Indeed, if the phenotype is caused by a function of PlexinD1 as a dependence receptor, absence of its ligand should lead to increased cell death. In *Sema3e* knockout mice, the number of positive PlexinD1 neurons is expected to decrease, particularly heterotopic neurons, which is not observed in our results.

Death due to loss of PlexinD1 neurotrophic effect

In another study, it has been shown that PlexinD1/Sema3E signalling exert a cell survival effect. Indeed, in Gonadotropin Releasing Hormone (GnRH)-secreting neurons, PlexinD1 mediates Sema3E neuroprotective action. In that system, both the loss of PlexinD1 and Sema3E compromised the survival of GnRH neurons, indicating that Sema3E/PlexinD1 signalling promotes cell survival (Cariboni et al., 2015). However, in our model, both loss of ligand and receptor should promote survival of heterotopically projecting CPNs and not their loss.

So, the described phenotype does not seem compatible with the known functions of Sema3E/PlexinD1 in cell death/survival.

Overall, our data provide a characterisation of the molecular identity, morphology, and connectivity of a subpopulation of heterotopically projecting CPNs, defined by the expression of the axon guidance receptor PlexinD1. This characterisation contributes to the description of the diversity among the CPNs and can serve as a basis for the understanding of the function of heterotopic projections. Importantly, we have shown that PlexinD1 shapes the precise final positioning of heterotopically projecting CPN in layer 5A, through mechanisms that are yet to be unravelled.

4.3   Perspectives

4.3.1   Function of PlexinD1 in the adult brain

Our data show that PlexinD1 expression is maintained in the adult mouse cortex. This raises the question of the possible function of PlexinD1 in the adult brain. While in the mouse brain *Plxnd1* is expressed at both embryonic and postnatal stages, in the Macaque monkey brain, *Plxnd1* is only present in posmigratory and mature layer 5 neurons (Watakabe et al., 2006; Fame et al., 2017), suggesting a conserved function in the adult brain.

A possible function of PlexinD1 in the adult brain could be the regulation of synaptic plasticity. Up to now there is no documentation of an implication of PlexinD1/Sema3E signalling in synaptic plasticity. However, other semaphorins, such as Sema3F (Sahay, 2005) and Sema3A (Bouzioukh et al., 2006), have been shown to play a role in synaptic plasticity in the hippocampus.

4.3.2   Function of heterotopic projections

This study showed that PlexinD1 is expressed in different populations of heterotopically projecting CPNs in the motor and somatosensory cortex. As reviewed in the introduction, heterotopic projections have been described in many mammals from rodents to human. The conservation of heterotopic projections indicates that their function is important to the survival of the mammalian species and it would be interesting to study.

Nothing is known about the functions of the heterotopic projection from the S1 to the PMC of the mouse. However, several hypotheses have been made about the potential functions of the cCStrPNs, based on already known functions of the striatum, such as reward-based learning, habits and action selection, and the types of neurons targeted by cCStrPNs. Specifically, the glutamatergic projection neurons of the striatum, known as medium spiny neurons are divided into direct pathway (dMSNs) and indirect pathway (iMSNs), based on whether they target directly or indirectly the substantia nigra pars compacta and the internal part of the globus pallidus (Gerfen and Surmeier, 2011). The classical view is that dMSNs promote the initiation of actions while the iMSNs impede actions (Graybiel, 2005; Mink, 2003). Studies have suggested that cCStrPNs specifically target dMSNs and thus may promote the initiation of motor actions, however this specificity has been doubted by other studies

(Reviewed in Reiner et al., 2010). Our study opens a possibility to directly address the function of these projections using a mouse that expressed cre-recombinase under the control of the PlexinD1 promoter. Breeding of this line with mice expressing channelrhodopsin in a cre-dependent way would allow to target and modulate specifically the electrical activity of these neurons. Examination for performance in different motor tests would reveal their function.

5 REFERENCES

Aalto, S., Näätänen, P., Wallius, E., Metsähonkala, L., Stenman, H., Niem, P.M., and Karlsson, H. (2002). Neuroanatomical substrata of amusement and sadness: a PET activation study using film stimuli. Neuroreport *13*, 67–73.

Aboitiz, F., and Montiel, J. (2003). One hundred million years of interhemispheric communication: the history of the corpus callosum. Brazilian J. Med. Biol. Res. *36*, 409–420.

Akelaitis, A.J. (1944). A Study of Gnosis, Praxis and Language Following Section of the Corpus Callosum and Anterior Commissure. J. Neurosurg. *1*, 94–102.

Alcamo, E.A., Chirivella, L., Dautzenberg, M., Dobreva, G., Fariñas, I., Grosschedl, R., and McConnell, S.K. (2008). Satb2 Regulates Callosal Projection Neuron Identity in the Developing Cerebral Cortex. Neuron *57*, 364–377.

Alloway, K.D., Smith, J.B., Beauchemin, K.J., and Olson, M.L. (2009). Bilateral projections from rat MI whisker cortex to the Neostriatum, Thalamus, and Claustrum: Forebrain circuits for modulating whisking behavior. J. Comp. Neurol. *515*, 548–564.

Andrews, W., Liapi, A., Plachez, C., Camurri, L., Zhang, J., Mori, S., Murakami, F., Parnavelas, J.G., Sundaresan, V., and Richards, L.J. (2006). Robo1 regulates the development of major axon tracts and interneuron migration in the forebrain. Development *133*, 2243–2252.

Arber, S., Ladle, D.R., Lin, J.H., Frank, E., and Jessell, T.M. (2000). ETS gene Er81 controls the formation of functional connections between group Ia sensory afferents and motor neurons. Cell *101*, 485–498.

Arlotta, P., Molyneaux, B.J., Chen, J., Inoue, J., Kominami, R., and Macklis, J.D. (2005). Neuronal Subtype-Specific Genes that Control Corticospinal Motor Neuron Development In Vivo. Neuron *45*, 207–221.

Azzarelli, R., Pacary, E., Garg, R., Garcez, P., van den Berg, D., Riou, P., Ridley, A.J., Friedel, R.H., Parsons, M., and Guillemot, F. (2014). An antagonistic interaction between PlexinB2 and Rnd3 controls RhoA activity and cortical neuron migration. Nat. Commun. *5*, 3405.

Azzarelli, R., Guillemot, F., and Pacary, E. (2015). Function and regulation of Rnd proteins in cortical projection neuron migration. Front. Neurosci. *9*, 19.

Badaruddin, D.H., Andrews, G.L., Bölte, S., Schilmoeller, K.J., Schilmoeller, G., Paul, L.K., and Brown, W.S. (2007). Social and behavioral problems of children with agenesis of the corpus callosum. Child Psychiatry Hum. Dev. *38*, 287–302.

Bagri, A., Marín, O., Plump, A.S., Mak, J., Pleasure, S.J., Rubenstein, J.L.R., and Tessier-Lavigne, M. (2002). Slit Proteins Prevent Midline Crossing and Determine the Dorsoventral Position of Major Axonal Pathways in the Mammalian Forebrain. Neuron *33*, 233–248.

Baranek, C., Dittrich, M., Parthasarathy, S., Bonnon, C.G., Britanova, O., Lanshakov, D., Boukhtouche, F., Sommer, J.E., Colmenares, C., Tarabykin, V., et al. (2012). Protooncogene Ski cooperates with the chromatin-remodeling factor Satb2 in specifying callosal neurons. Proc. Natl. Acad. Sci. U. S. A. *109*, 3546–3551.

Bauswein, E., Fromm, C., and Preuss, A. (1989). Corticostriatal cells in comparison with pyramidal tract neurons: contrasting properties in the behaving monkey. Brain Res. *493*, 198–203.

Bellon, A., Luchino, J., Haigh, K., Rougon, G., Haigh, J., Chauvet, S., and Mann, F. (2010). VEGFR2 (KDR/Flk1) signaling mediates axon growth in response to semaphorin 3E in the developing brain. Neuron *66*, 205–219.

Beloozerova, I.N., Sirota, M.G., and Swadlow, H.A. (2003). Activity of different classes of neurons of the motor cortex during locomotion. J. Neurosci. *23*, 1087–1097.

De Benedictis, A., Petit, L., Descoteaux, M., Marras, C.E., Barbareschi, M., Corsini, F., Dallabona, M., Chioffi, F., and Sarubbo, S. (2016). New insights in the homotopic and heterotopic connectivity of the frontal portion of the human corpus callosum revealed by microdissection and diffusion tractography. Hum. Brain Mapp. *37*, 4718–4735.

Bodensteiner, J., Schaefer, G.B., Breeding, L., and Cowan, L. (1994). Hypoplasia of the corpus callosum: A study of 445 consecutive MRI scans. J. Child Neurol. *9*, 47–49.

Boussaoud, D., Tanné-Gariépy, J., Wannier, T., and Rouiller, E.M. (2005). Callosal connections of dorsal versus ventral premotor areas in the macaque monkey: a multiple retrograde tracing study. BMC Neurosci. *6*, 67.

Bouzioukh, F., Daoudal, G., Falk, J., Debanne, D., Rougon, G., and Castellani, V. (2006). Semaphorin3A regulates synaptic function of differentiated hippocampal neurons. Eur. J. Neurosci. *23*, 2247–2254.

Boyd, E.H., Pandya, D.N., and Bignall, K.E. (1971). Homotopic and nonhomotopic interhemispheric cortical projections in the squirrel monkey. Exp. Neurol. *32*, 256–274.

Bribián, A., Nocentini, S., Llorens, F., Gil, V., Mire, E., Reginensi, D., Yoshida, Y., Mann, F., and del Río, J.A. (2014). Sema3E/PlexinD1 regulates the migration of hem-derived Cajal-Retzius cells in developing cerebral cortex. Nat. Commun. *5*, 4265.

Britanova, O., de Juan Romero, C., Cheung, A., Kwan, K.Y., Schwark, M., Gyorgy, A., Vogel, T., Akopov, S., Mitkovski, M., Agoston, D., et al. (2008). Satb2 Is a Postmitotic Determinant for Upper-Layer Neuron Specification in the Neocortex. Neuron *57*, 378–392.

Brown, L.N., and Sainsbury, R.S. (2000). Hemispheric Equivalence and Age-Related Differences in Judgments of Simultaneity to Somatosensory Stimuli.

Brown, W.S., and Paul, L.K. (2000). Cognitive and psychosocial deficits in agenesis of the corpus callosum with normal intelligence. Cogn. Neuropsychiatry *5*, 135–157.

Burk, K., Mire, E., Bellon, A., Hocine, M., Guillot, J., Moraes, F., Yoshida, Y., Simons, M., Chauvet, S., and Mann, F. (2017). Post-endocytic sorting of Plexin-D1 controls signal transduction and development of axonal and vascular circuits. Nat. Commun. *8*, 14508.

Cariboni, A., André, V., Chauvet, S., Cassatella, D., Davidson, K., Caramello, A., Fantin, A., Bouloux, P., Mann, F., and Ruhrberg, C. (2015). Dysfunctional SEMA3E signaling underlies gonadotropin-releasing hormone neuron deficiency in Kallmann syndrome. J. Clin. Invest. *125*, 2413–2428.

Carman, J.B., Powell, T.P., and Webster, K.E. (1965). A bilateral cortico-striate projection. J. Neurol. Neurosurg. Psychiatry *28*, 71–77.

Catani, M., and ffytche, D.H. (2005). The rises and falls of disconnection syndromes. Brain *128*, 2224–2239.

Cauller, L.J., Clancy, B., and Connors, B.W. (1998). Backward cortical projections to primary somatosensory cortex in rats extend long horizontal axons in layer I. J. Comp. Neurol. *390*, 297–310.

Caviness, V.S. (1975). Architectonic map of neocortex of the normal mouse. J. Comp. Neurol. *164*, 247–263.

Chauvet, S., Cohen, S., Yoshida, Y., Fekrane, L., Livet, J., Gayet, O., Segu, L., Buhot, M.C., Jessell, T.M., Henderson, C.E., et al. (2007). Gating of Sema3E/PlexinD1 Signaling by Neuropilin-1 Switches Axonal Repulsion to Attraction during Brain Development. Neuron *56*, 807–822.

Chédotal, A. (2010). Further tales of the midline. Curr. Opin. Neurobiol. *21*, 68–75.

Chen, B., Wang, S.S., Hattox, A.M., Rayburn, H., Nelson, S.B., and McConnell, S.K. (2008a). The Fezf2-Ctip2 genetic pathway regulates the fate choice of subcortical projection neurons in the developing cerebral cortex. Proc. Natl. Acad. Sci. U. S. A. *105*, 11382–11387.

Chen, G., Sima, J., Jin, M., Wang, K., Xue, X., Zheng, W., Ding, Y., and Yuan, X. (2008b). Semaphorin-3A guides radial migration of cortical neurons during development. Nat. Neurosci. *11*, 36–44.

Cheng, H.J., Bagri, A., Yaron, A., Stein, E., Pleasure, S.J., and Tessier-Lavigne, M. (2001). Plexin-A3 mediates semaphorin signaling and regulates the development of hippocampal axonal projections. Neuron *32*, 249–263.

Chovsepian, A., Empl, L., Correa, D., and Bareyre, F.M. (2017). Heterotopic Transcallosal Projections Are Present throughout the Mouse Cortex. Front. Cell. Neurosci. *11*, 36.

Courchet, J., Lewis, T.L., Lee, S., Courchet, V., Liou, D.Y., Aizawa, S., and Polleux, F. (2013). Terminal axon branching is regulated by the LKB1-NUAK1 kinase pathway via presynaptic mitochondrial capture. Cell *153*, 1510–1525.

David, A.S., Wacharasindhu, A., and Lishman, W.A. (1993). Severe psychiatric disturbance and abnormalities of the corpus callosum: Review and case series. J. Neurol. Neurosurg. Psychiatry *56*, 85–93.

Deck, M., Lokmane, L., Chauvet, S., Mailhes, C., Keita, M., Niquille, M., Yoshida, M., Yoshida, Y., Lebrand, C., Mann, F., et al. (2013). Pathfinding of Corticothalamic Axons Relies on a Rendezvous with Thalamic Projections. Neuron *77*, 472–484.

Decosta-Fortune, T.M., Li, C.X., de Jongh Curry, A.L., and Waters, R.S. (2015). Differential Pattern of Interhemispheric Connections Between Homotopic Layer V Regions in the Forelimb Representation in Rat Barrel Field Cortex. Anat. Rec. *298*, 1885–1902.

Deloulme, J.-C., Gory-Fauré, S., Mauconduit, F., Chauvet, S., Jonckheere, J., Boulan, B., Mire, E., Xue, J., Jany, M., Maucler, C., et al. (2015). Microtubule-associated protein 6 mediates neuronal connectivity through Semaphorin 3E-dependent signalling for axonal growth. Nat. Commun. *6*, 7246.

Deng, Y., Lanciego, J., Goff, L.K.-L., Coulon, P., Salin, P., Kachidian, P., Lei, W., Del Mar, N., and Reiner, A. (2015). Differential organization of cortical inputs to striatal projection neurons of the matrix compartment in rats. Front. Syst. Neurosci. *9*, 51.

Dimond, S.J. (1976). Depletion of attentional capacity after total commissurotomy in man. Brain *99*, 347–356.

Ding, J.B., Oh, W.J., Sabatini, B.L., and Gu, C. (2012). Semaphorin 3Eg-Plexin-D1 signaling controls pathway-specific synapse formation in the striatum. Nat. Neurosci. *15*, 215–223.

Edwards, T.J., Sherr, E.H., Barkovich, A.J., and Richards, L.J. (2014). Clinical, genetic and imaging findings identify new causes for corpus callosum development syndromes. Brain *137*, 1579–1613.

Ellenberg, L., and Sperry, R.W. (1979). Capacity for Holding Sustained Attention Following Commissurotomy. Cortex *15*, 421–438.

En Ezit, A.B., Hertz-Pannier, L., Dehaene-Lambertz, G., Monzalvo, K., Germanaud, D., Duclap, D., Guevara, P., Mangin, J.-F., Poupon, C., Moutard, M.-L., et al. (2015). Organising white matter in a brain without corpus callosum fibres. Cortex *63*, 155–171.

Fame, R.M., MacDonald, J.L., and Macklis, J.D. (2011). Development, specification, and diversity of callosal projection neurons. Trends Neurosci. *34*, 41–50.

Fame, R.M., Dehay, C., Kennedy, H., and Macklis, J.D. (2017). Subtype-Specific Genes that Characterize Subpopulations of Callosal Projection Neurons in Mouse Identify Molecularly Homologous Populations in Macaque Cortex. Cereb. Cortex *27*, 1817–1830.

Fenlon, L.R., and Richards, L.J. (2015). Contralateral targeting of the corpus callosum in normal and pathological brain function. Trends Neurosci. *38*, 264–272.

Fischer, M., Ryan, S.B., and Dobyns, W.B. (1992). Mechanisms of Interhemispheric Transfer and Patterns of Cognitive Function in Acallosal Patients of Normal Intelligence. Arch. Neurol. *49*, 271–277.

Fothergill, T., Donahoo, A.-L.S., Douglass, A., Zalucki, O., Yuan, J., Shu, T., Goodhill, G.J., and Richards, L.J. (2014). Netrin-DCC Signaling Regulates Corpus Callosum Formation Through Attraction of Pioneering Axons and by Modulating Slit2-Mediated Repulsion. Cereb. Cortex *24*, 1138–1151.

Fukuhara, K., Imai, F., Ladle, D.R., Katayama, K., Leslie, J.R., Arber, S., Jessell, T.M., and Yoshida, Y. (2013). Specificity of Monosynaptic Sensory-Motor Connections Imposed by Repellent Sema3E-PlexinD1 Signaling. Cell Rep. *5*, 748–758.

Galazo, M.J., Emsley, J.G., and Macklis Correspondence, J.D. (2016). Corticothalamic Projection Neuron Development beyond Subtype Specification: Fog2 and Intersectional Controls Regulate Intraclass Neuronal Diversity. Neuron *91*, 90–106.

Garcez, P.P., Henrique, N.P., Furtado, D.A., Bolz, J., Lent, R., and Uziel, D. (2007). Axons of callosal neurons bifurcate transiently at the white matter before consolidating an interhemispheric projection. Eur. J. Neurosci. *25*, 1384–1394.

Gazzaniga, M.S. (2000). Cerebral specialization and interhemispheric communication. Does the corpus callosum enable the human condition? Brain *123*, 1293–1326.

Gazzaniga, M.S. (2005). Forty-five years of split-brain research and still going strong. Nat. Rev. Neurosci. *6*, 653–659.

Gerfen, C.R., and Surmeier, D.J. (2011). Modulation of Striatal Projection Systems by Dopamine. Annu. Rev. Neurosci. *34*, 441–466.

Gitler, A.D., Lu, M.M., and Epstein, J.A. (2004). PlexinD1 and Semaphorin Signaling Are Required in Endothelial Cells for Cardiovascular Development. Dev. Cell *7*, 107–116.

Gorski, J.A., Talley, T., Qiu, M., Puelles, L., Rubenstein, J.L.R., and Jones, K.R. (2002). Cortical excitatory neurons and glia, but not GABAergic neurons, are produced in the Emx1-expressing lineage. J. Neurosci. *22*, 6309–6314.

Graybiel, A.M. (2005). The basal ganglia: Learning new tricks and loving it. Curr. Opin. Neurobiol. *15*, 638–644.

Greig, L.C., Woodworth, M.B., Galazo, M.J., Padmanabhan, H., and Macklis, J.D. (2013). Molecular logic of neocortical projection neuron specification, development and diversity. Nat. Rev. Neurosci. *14*, 755–769.

Gu, C., Yoshida, Y., Livet, J., Reimert, D. V, Mann, F., Merte, J., Henderson, C.E., Jessell, T.M., Kolodkin, A.L., and Ginty, D.D. (2005). Semaphorin 3E and plexin-D1 control vascular pattern independently of neuropilins. Science *307*, 265–268.

Guillem, P., Fabre, B., Cans, C., Robert-Gnansia, E., and Jouk, P.S. (2003). Trends in elective terminations of pregnancy between 1989 and 2000 in a French county (the Isère). Prenat. Diagn. *23*, 877–883.

Hand, R., and Polleux, F. (2011). Neurogenin2 regulates the initial axon guidance of cortical pyramidal neurons projecting medially to the corpus callosum. Neural Dev. *6*, 30.

Harb, K., Magrinelli, E., Nicolas, C.S., Lukianets, N., Frangeul, L., Pietri, M., Sun, T., Sandoz, G., Grammont, F., Jabaudon, D., et al. (2016). Area-specific development of distinct projection neuron subclasses is regulated by postnatal epigenetic modifications. Elife *5*, e09531.

Hatanaka, Y., and Yamauchi, K. (2013). Excitatory Cortical Neurons with Multipolar Shape Establish Neuronal Polarity by Forming a Tangentially Oriented Axon in the Intermediate Zone. Cereb. Cortex *23*, 105–113.

Heng, J.I.-T., Nguyen, L., Castro, D.S., Zimmer, C., Wildner, H., Armant, O., Skowronska-

Krawczyk, D., Bedogni, F., Matter, J.-M., Hevner, R., et al. (2008). Neurogenin 2 controls cortical neuron migration through regulation of Rnd2. Nature *455*, 114–118.

Hetts, S.W., Sherr, E.H., Chao, S., Gobuty, S., and Barkovich, A.J. (2006). Anomalies of the corpus callosum: An MR analysis of the phenotypic spectrum of associated malformations. Am. J. Roentgenol. *187*, 1343–1348.

Hoppe, K.D., and Bogen, J.E. (1977). Alexithymia in twelve commissurotomized patients. Psychother. Psychosom. *28*, 148–155.

Hutchins, B.I., Li, L., and Kalil, K. (2011). Wnt/calcium signaling mediates axon growth and guidance in the developing corpus callosum. Dev. Neurobiol. *71*, 269–283.

Imamura, T., Yamadori, A., Shiga, Y., Sahara, M., and Abiko, H. (1994). Is disturbed transfer of learning in callosal agenesis due to a disconnection syndrome? Behav. Neurol. *7*, 43–48.

Imayoshi, I., Ohtsuka, T., Metzger, D., Chambon, P., and Kageyama, R. (2006). Temporal regulation of Cre recombinase activity in neural stem cells. Genesis *44*, 233–238.

Innocenti, G.M., Dyrby, T.B., Andersen, K.W., Rouiller, E.M., and Caminiti, R. (2017). The Crossed Projection to the Striatum in Two Species of Monkey and in Humans: Behavioral and Evolutionary Significance. Cereb. Cortex *27*, 3217–3230.

Jeeves, M.A., Silver, P.H., and Milne, A.B. (1988). Role of the corpus callosum in the development of a bimanual motor skill. Dev. Neuropsychol. *4*, 305–323.

Jeret, J.S., Serur, D., Wisniewski, K., and Fisch, C. (1985). Frequency of agenesis of the corpus callosum in the developmentally disabled population as determined by computerized tomography. Pediatr. Neurosci. *12*, 101–103.

Jones, E.G., Coulter, J.D., Burton, H., and Porter, R. (1977). Cells of origin and terminal distrubution of corticostriatal fibers arising in the sensory-motor cortex of monkeys. J. Comp. Neurol. *173*, 53–80.

Keeble, T.R., Halford, M.M., Seaman, C., Kee, N., Macheda, M., Anderson, R.B., Stacker, S.A., and Cooper, H.M. (2006). The Wnt receptor Ryk is required for Wnt5a-mediated axon guidance on the contralateral side of the corpus callosum. J. Neurosci. *26*, 5840–5848.

Kennedy, H., Dehay, C., and Bullier, J. (1986). Organization of the callosal connections of visual areas v1 and v2 in the macaque monkey. J. Comp. Neurol. *247*, 398–415.

Kim, E.J., Juavinett, A.L., Kyubwa, E.M., Jacobs, M.W., and Callaway, E.M. (2015). Three Types of Cortical Layer 5 Neurons That Differ in Brain-wide Connectivity and Function. Neuron *88*, 1253–1267.

Künzle, H. (1975). Bilateral projections from precentral motor cortex to the putamen and other parts of the basal ganglia. An autoradiographic study in Macaca fascicularis. Brain Res. *88*, 195–209.

Lanz, F., Moret, V., Ambett, R., Cappe, C., Rouiller, E.M., and Loquet, G. (2017). Distant heterotopic callosal connections to premotor cortex in non-human primates. Neuroscience *344*, 56–66.

Larsen, D.D., and Callaway, E.M. (2006). Development of layer-specific axonal arborizations in mouse primary somatosensory cortex. J. Comp. Neurol. *494*, 398–414.

Larsen, D.D., Wickersham, I.R., and Callaway, E.M. (2008). Retrograde tracing with recombinant rabies virus reveals correlations between projection targets and dendritic architecture in layer 5 of mouse barrel cortex. Front. Neural Circuits *1*, 1–7.

Lassonde, M., Sauerwein, H., Chicoine, A.-J., and Geoffroy, G. (1991). Absence of disconnexion syndrome in callosal agenesis and early callosotomy: Brain reorganization or lack of structural specificity during ontogeny? Neuropsychologia *29*, 481–495.

Leone, D.P., Heavner, W.E., Ferenczi, E.A., Dobreva, G., Huguenard, J.R., Grosschedl, R., and McConnell, S.K. (2015). Satb2 regulates the differentiation of both callosal and subcerebral projection neurons in the developing cerebral cortex. Cereb. Cortex *25*, 3406–3419.

Lodato, S., Shetty, A.S., and Arlotta, P. (2015). Cerebral cortex assembly: generating and reprogramming projection neuron diversity. Trends Neurosci. *38*, 117–125.

Luchino, J., Hocine, M., Amoureux, M.-C., Gibert, B., Bernet, A., Royet, A., Treilleux, I., Lécine, P., Borg, J.-P., Mehlen, P., et al. (2013). Semaphorin 3E Suppresses Tumor Cell Death Triggered by the Plexin D1 Dependence Receptor in Metastatic Breast Cancers. Cancer Cell *24*, 673–685.

MacDonald, J.L., Fame, R.M., Gillis-Buck, E.M., and Macklis, J.D. (2018). Caveolin1 Identifies a Specific Subpopulation of Cerebral Cortex Callosal Projection Neurons (CPN) Including Dual Projecting Cortical Callosal/Frontal Projection Neurons (CPN/FPN). Eneuro *5*, 1–17.

Martínez-Martínez, M.Á., De Juan Romero, C., Fernández, V., Cárdenas, A., Götz, M., and Borrell, V. (2016). A restricted period for formation of outer subventricular zone defined by Cdh1 and Trnp1 levels. Nat. Commun. *7*, 11812.

Mata, A., Gil, V., Pérez-Clausell, J., Dasilva, M., González-Calixto, M.C., Soriano, E., García-Verdugo, J.M., Sanchez-Vives, M. V., and del Río, J.A. (2018). New functions of Semaphorin 3E and its receptor PlexinD1 during developing and adult hippocampal formation. Sci. Rep. *8*, 1381.

McGuire, P.K., Bates, J.F., and Goldman-Rakic, P.S. (1991). Interhemispheric integration: II. Symmetry and convergence of the corticostriatal projections of the left and the right principal sulcus (PS) and the left and the right supplementary motor area (SMA) of the rhesus monkey. Cereb. Cortex *1*, 408–417.

McKenna, W.L., Betancourt, J., Larkin, K.A., Abrams, B., Guo, C., Rubenstein, J.L.R., and Chen, B. (2011). Tbr1 and Fezf2 regulate alternate corticofugal neuronal identities during neocortical development. J. Neurosci. *31*, 549–564.

Miller, M.W., and Vogt, B.A. (1984). Heterotopic and Homotopic Callosal Connections in Rat Visual Cortex. Brain Res. *297*, 75–89.

Mink, J.W. (2003). The Basal Ganglia and Involuntary Movements. Arch. Neurol. *60*, 1365.

Minocha, S., Valloton, D., Ypsilanti, A.R., Fiumelli, H., Allen, E.A., Yanagawa, Y., Marin, O., Chédotal, A., Hornung, J.-P., and Lebrand, C. (2015). Nkx2.1-derived astrocytes and neurons together with Slit2 are indispensable for anterior commissure formation. Nat. Commun. *6*, 6887.

Miré, E., Hocine, M., Bazellières, E., Jungas, T., Davy, A., Chauvet, S., and Mann, F. (2018). Developmental Upregulation of Ephrin-B1 Silences Sema3C/Neuropilin-1 Signaling during Post-crossing Navigation of Corpus Callosum Axons. Curr. Biol. 1768–1782.

Mitchell, B.D., and Macklis, J.D. (2005). Large-Scale Maintenance of Dual Projections by Callosal and Frontal Cortical Projection Neurons in Adult Mice. J. Comp. Neurol *482*, 17–32.

Miyata, T., Kawaguchi, A., Okano, H., and Ogawa, M. (2001). Asymmetric inheritance of radial glial fibers by cortical neurons. Neuron *31*, 727–741.

Mizuno, H., Hirano, T., and Tagawa, Y. (2007). Evidence for activity-dependent cortical wiring: formation of interhemispheric connections in neonatal mouse visual cortex requires projection neuron activity. J. Neurosci. *27*, 6760–6770.

Molyneaux, B.J., Arlotta, P., Menezes, J.R.L., and Macklis, J.D. (2007). Neuronal subtype specification in the cerebral cortex. Nat. Rev. Neurosci. *8*, 427–437.

Molyneaux, B.J., Arlotta, P., Fame, R.M., MacDonald, J.L., MacQuarrie, K.L., and Macklis, J.D. (2009). Novel Subtype-Specific Genes Identify Distinct Subpopulations of Callosal Projection Neurons. J. Neurosci. *29*, 12343–12354.

Mori, K. (1992). Giant interhemispheric cysts associated with agenesis of the corpus callosum. J. Neurosurg. *76*, 224–230.

Morishima, M., and Kawaguchi, Y. (2006). Recurrent Connection Patterns of Corticostriatal Pyramidal Cells in Frontal Cortex. J. Neurosci. *26*, 4394–4405.

Nadarajah, B., and Parnavelas, J.G. (2002). Modes of neuronal migration in the developing cerebral cortex. Nat. Rev. Neurosci. *3*, 423–432.

Nadarajah, B., Brunstrom, J.E., Grutzendler, J., Wong, R.O.L., and Pearlman, A.L. (2001). Two modes of radial migration in early development of the cerebral cortex. Nat. Neurosci. *4*, 143–150.

Nakamura, K., Yamashita, Y., Tamamaki, N., Katoh, H., Kaneko, T., and Negishi, M. (2005). Rapid communication In vivo function of Rnd2 in the development of neocortical pyramidal neurons.

Nieto, M., Monuki, E.S., Tang, H., Imitola, J., Haubst, N., Khoury, S.J., Cunningham, J., Gotz, M., and Walsh, C.A. (2004). Expression of Cux-1 and Cux-2 in the Subventricular Zone and Upper Layers II-IV of the Cerebral Cortex. J. Comp. Neurol *479*, 168–180.

Niquille, M., Garel, S., Mann, F., Hornung, J.P., Otsmane, B., Chevalley, S., Parras, C., Guillemot, F., Gaspar, P., Yanagawa, Y., et al. (2009). Transient neuronal populations are required to guide callosal axons: A role for semaphorin 3C. PLoS Biol. *7*, 1–20.

Niquille, M., Minocha, S., Hornung, J.P., Rufer, N., Valloton, D., Kessaris, N., Alfonsi, F.,

Vitalis, T., Yanagawa, Y., Devenoges, C., et al. (2013). Two specific populations of GABAergic neurons originating from the medial and the caudal ganglionic eminences aid in proper navigation of callosal axons. Dev. Neurobiol. *73*, 647–672.

Nishikimi, M., Oishi, K., Tabata, H., Hashimoto-Torii, K., and Nakajima, K. (2003). Segregation and Pathfinding ofCallosal Axons through EphA3 Signaling. J. Neurosci. *23*, 11523–11538.

Noctor, S.C., Flint, A.C., Weissman, T.A., Dammerman, R.S., and Kriegstein, A.R. (2001). Neurons derived from radial glial cells establish radial units in neocortex. Nature *409*, 714–720.

Nomura, T., Yamashita, W., Gotoh, H., Correspondence, K.O., and Ono, K. (2018). Species-Specific Mechanisms of Neuron Subtype Specification Reveal Evolutionary Plasticity of Amniote Brain Development. Cell Rep. *22*, 3142–3151.

Oh, J., and Gu, C. (2013). The role and mechanism-of-action of Sema3E and Plexin-D1 in vascular and neural development. Semin. Cell Dev. Biol. *24*, 156–162.

Ohtaka-Maruyama, C., and Okado, H. (2015). Molecular Pathways Underlying Projection Neuron Production and Migration during Cerebral Cortical Development. Front. Neurosci. *9*, 447.

Oswald, M.J., Tantirigama, M.L.S., Sonntag, I., Hughes, S.M., and Empson, R.M. (2013). Diversity of layer 5 projection neurons in the mouse motor cortex. Front. Cell. Neurosci. *7*, 174.

Otsuka, T., and Kawaguchi, Y. (2011). Cell diversity and connection specificity between callosal projection neurons in the frontal cortex. J. Neurosci. *31*, 3862–3870.

Pacary, E., Heng, J., Azzarelli, R., Riou, P., Castro, D., Lebel-Potter, M., Parras, C., Bell, D.M., Ridley, A.J., Parsons, M., et al. (2011). Proneural Transcription Factors Regulate Different Steps of Cortical Neuron Migration through Rnd-Mediated Inhibition of RhoA Signaling. Neuron *69*, 1069–1084.

Parent, M., and Parent, A. (2006). Single-Axon Tracing Study of Corticostriatal Projections Arising from Primary Motor Cortex in Primates. J. Comp. Neurol *496*, 202–213.

Paul, L.K., Brown, W.S., Adolphs, R., Tyszka, J.M., Richards, L.J., Mukherjee, P., and Sherr, E.H. (2007). Agenesis of the corpus callosum: Genetic, developmental and functional aspects of connectivity. Nat. Rev. Neurosci. 287–299.

Pecho-Vrieseling, E., Sigrist, M., Yoshida, Y., Jessell, T.M., and Arber, S. (2009). Specificity of sensory–motor connections encoded by Sema3e–Plxnd1 recognition. Nature *459*, 842–846.

Piper, M., Plachez, C., Zalucki, O., Fothergill, T., Goudreau, G., Erzurumlu, R., Gu, C., and Richards, L.J. (2009). Neuropilin 1-Sema Signaling Regulates Crossing of Cingulate Pioneering Axons during Development of the Corpus Callosum. Cereb. Cortex *19*, i11–i21.

Reiner, A., Jiao, Y., Del Mar, N., Laverghetta, A. V, and Lei, W.L. (2003). Differential morphology of pyramidal tract-type and intratelencephalically projecting-type corticostriatal neurons and their intrastriatal terminals in rats. J. Comp. Neurol. *457*, 420–440.

Reiner, A., Hart, N.M., Lei, W., and Deng, Y. (2010). Corticostriatal projection neurons – dichotomous types and dichotomous functions. Front. Neuroanat. *4*, 142.

Rodríguez-Tornos, F.M., Briz, C.G., Weiss, L.A., Sebastián-Serrano, A., Ares, S., Navarrete, M., Frangeul, L., Galazo, M., Jabaudon, D., Esteban, J.A., et al. (2016). Cux1 Enables Interhemispheric Connections of Layer II/III Neurons by Regulating Kv1-Dependent Firing. Neuron *89*, 494–506.

Rouiller, E.., Simm, G.., Villa, A.E.., de Ribaupierre, Y., and de Ribaupierre, F. (1991). Auditory corticocortical interconnections in the cat: evidence for parallel and hierarchical arrangement of the auditory cortical areas. Exp. Brain Res. *86*, 483–505.

Royce, G.J. (1982). Laminar origin of cortical neurons which project upon the caudate nucleus: A horseradish peroxidase investigation in the cat. J. Comp. Neurol. *205*, 8–29.

Sahay, A. (2005). Secreted Semaphorins Modulate Synaptic Transmission in the Adult Hippocampus. J. Neurosci. *25*, 3613–3620.

Salin, P., Castle, M., Kachidian, P., Barroso-Chinea, P., López, I.P., Rico, A.J., Kerkerian-Le Goff, L., Coulon, P., and Lanciego, J.L. (2008). High-resolution neuroanatomical tract-tracing for the analysis of striatal microcircuits. Brain Res. *1221*, 49–58.

Sanides, D. (1978). The Retinotopic Distribution of Visual Callosal Projections in the Suprasylvian Visual areas Compared to the Classical Visual Areas (17,18,19) in the Cat. In Exp Brain Res, pp. 435–443.

Sawada, M., Ohno, N., Kawaguchi, M., Huang, S.-H., Hikita, T., Sakurai, Y., Bang Nguyen, H., Quynh Thai, T., Ishido, Y., Yoshida, Y., et al. (2018). PlexinD1 signaling controls morphological changes and migration termination in newborn neurons. EMBO J. *37*, 1–16.

Segraves, M.A., and Innocenti, G.M. (1985). Comparison of the Distributions of lpsilaterally and Contralaterally Projecting Corticocortical Neurons in Cat Visual Cortex Using Two Fluorescent Tracers.

Sekine, K., Honda, T., Kawauchi, T., Kubo, K., and Nakajima, K. (2011). The outermost region of the developing cortical plate is crucial for both the switch of the radial migration mode and the Dab1-dependent "inside-out" lamination in the neocortex. J. Neurosci. *31*, 9426–9439.

Shu, T., and Richards, L.J. (2001). Cortical axon guidance by the glial wedge during the development of the corpus callosum. J. Neurosci. *21*, 2749–2758.

Sohur, U.S., Padmanabhan, H.K., Kotchetkov, I.S., Menezes, J.R.L., and Macklis, J.D. (2014). Feature article: Anatomic and molecular development of corticostriatal projection neurons in mice. Cereb. Cortex *24*, 293–303.

Solursh, L.P., Margulies, A.I., Ashem, B., and Stasiak, E.A. (1965). The relationships of agenesis of the corpus callosum to perception and learning. J. Nerv. Ment. Dis. *141*, 180–189.

Spatz Birgit Kunz, W., and Steffen, H. (1987). CA new heterotopic callosal projection of primary visual cortex in the monkey, Callithrix jacchus. Brain Res. *403*, 151–161.

Srivatsa, S., Parthasarathy, S., Britanova, O., Bormuth, I., Donahoo, A.-L., Ackerman, S.L., Richards, L.J., and Tarabykin, V. (2014). Unc5C and DCC act downstream of Ctip2 and Satb2 and contribute to corpus callosum formation. Nat. Commun. *5*, 3708.

Stickles, J.L., Schilmoeller, G.L., and Schilmoeller, K.J. (2002). A 23-year review of communication development in an individual with agenesis of the corpus callosum. Int. J. Disabil. Dev. Educ. *49*, 367–383.

Suárez, R., Gobius, I., and Richards, L.J. (2014a). Evolution and development of interhemispheric connections in the vertebrate forebrain. Front. Hum. Neurosci. *8*, 497.

Suárez, R., Fenlon, L.R., Marek, R., Avitan, L., Sah, P., Goodhill, G.J., and Richards, L.J. (2014b). Balanced Interhemispheric Cortical Activity Is Required for Correct Targeting of the Corpus Callosum. Neuron *82*, 1289–1298.

Tabata, H., and Nakajima, K. (2003). Multipolar migration: The third mode of radial neuronal migration in the developing cerebral cortex. J. Neurosci. *23*, 9996–10001.

Tantirigama, M.L.S., Oswald, M.J., Clare, A.J., Wicky, H.E., Day, R.C., Hughes, S.M., and Empson, R.M. (2016). Fezf2 expression in layer 5 projection neurons of mature mouse motor cortex. J. Comp. Neurol. *524*, 829–845.

Tovar-Moll, F., Moll, J., De Oliveira-Souza, R., Bramati, I., Andreiuolo, P.A., and Lent, R. (2007). Neuroplasticity in human callosal dysgenesis: A diffusion tensor imaging study. Cereb. Cortex *17*, 531–541.

Tovar-Moll, F., Monteiro, M., Andrade, J., Bramati, I.E., Vianna-Barbosa, R., Marins, T., Rodrigues, E., Dantas, N., Behrens, T.E.J., De Oliveira-Souza, R., et al. (2014). Structural and functional brain rewiring clarifies preserved interhemispheric transfer in humans born without the corpus callosum. PNAS *111*, 7843–7848.

Toyofuku, T., Yabuki, M., Kamei, J., Kamei, M., Makino, N., Kumanogoh, A., and Hori, M. (2007). Semaphorin-4A, an activator for T-cell-mediated immunity, suppresses angiogenesis via Plexin-D1. EMBO J. *26*, 1373–1384.

Trescher, J.H., and Ford, F.R. (1937). Colloid cyst of the third ventricle. Report of a case: operative removal with section of posterior half of corpus callosum. Arch. Neurol. Psychiatry *37*, 959.

Turner, R.S., and DeLong, M.R. (2000). Corticostriatal activity in primary motor cortex of the macaque. J. Neurosci. *20*, 7096–7108.

Di Virgilio, G., and Clarke, S. (1997). Direct interhemispheric visual input to human speech areas. Hum. Brain Mapp. *5*, 347–354.

Wang, C.-L., Zhang, L., Zhou, Y., Zhou, J., Yang, X.-J., Duan, S. -m., Xiong, Z.-Q., and Ding, Y.-Q. (2007). Activity-Dependent Development of Callosal Projections in the Somatosensory Cortex. J. Neurosci. *27*, 11334–11342.

Wang, F., Eagleson, K.L., and Levitt, P. (2015). Positive regulation of neocortical synapse formation by the Plexin-D1 receptor. Brain Res. *1616*, 157–165.

Watakabe, A., Ohsawa, S., Hashikawa, T., and Yamamori, T. (2006). Binding and complementary expression patterns of semaphorin 3E and plexin D1 in the mature neocortices of mice and monkeys. J. Comp. Neurol. *499*, 258–273.

Wichterle, H., Turnbull, D.H., Nery, S., Fishell, G., and Alvarez-buylla, A. (2001). In utero fate mapping reveals distinct migratory pathways and fates of neurons born in the mammalian basal forebrain. Development *128*, 3759–3771.

Wilson, C.J. (1986). Postsynaptic Potentials Evoked in Spiny Neostriatal Projection Neurons by Stimulation of Ipsilateral and Contralateral Neocortex. Brain Res. *367*, 201–213.

Wilson, C.J. (1987). Morphology and synaptic connections of crossed corticostriatal neurons in the rat. J. Comp. Neurol. *263*, 567–580.

Wise, S.., and Jones, E.. (1976). The Organization and Postnatal Development of the Commissural Projection of the Rat Somatic Sensory Cortex. J Comp Neurol *168*, 313–344.

Wolman, D. (2012). The split brain: A tale of two halves. Nature *483*, 260–263.

Woodhead, G.J., Mutch, C.A., Olson, E.C., and Chenn, A. (2006). Cell-autonomous beta-catenin signaling regulates cortical precursor proliferation. J. Neurosci. *26*, 12620–12630.

Wright, A.K., Ramanathan, S., and Arbuthnott, G.W. (2001). Identification of the source of the bilateral projection system from cortex to somatosensory neostriatum and an exploration of its physiological actions. Neuroscience *103*, 87–96.

Yeh, T.F., Wang, L.W., and Huang, C.C. (2004). Major brain lesions detected on sonographic screening of apparently normal term neonates. Neuroradiology *46*, 368–373.

Yoneshima, H., Yamasaki, S., Voelker, C.C.J., Molnár, Z., Christophe, E., Audinat, E., Takemoto, M., Nishiwaki, M., Tsuji, S., Fujita, I., et al. (2006). ER81 is expressed in a subpopulation of layer 5 neurons in rodent and primate neocortices. Neuroscience *137*, 401–412.

Yoshida, Y. (2012). Semaphorin Signaling in Vertebrate Neural Circuit Assembly. Front. Mol. Neurosci. *5*, 71.

Zaidel, D., and Sperry, R.W. (1977). Some long-term motor effects of cerebral commissurotomy in man. Neuropsychologia *15*, 193–204.

Zhang, Y., Singh, M.K., Degenhardt, K.R., Lu, M.M., Bennett, J., Yoshida, Y., and Epstein, J.A. (2009). Tie2Cre-mediated inactivation of plexinD1 results in congenital heart, vascular and skeletal defects. Dev. Biol. *325*, 82–93.

Zhou, J., Wen, Y., She, L., Sui, Y.-N., Liu, L., Richards, L.J., and Poo, M.-M. (2013). Axon position within the corpus callosum determines contralateral cortical projection. Proc. Natl. Acad. Sci. U. S. A. *110*, E2714-23.